TU Delft
Delft University of Technology

Experimental Research on Spatial Distribution of Overtopping

Anestis C. Lioutas

September 2010

COLOPHON

MSc Thesis report

Title: "Experimental research on spatial overtopping of overtopping"

Delft, 2010

Institutes

Delft University of Technology

Department of Hydraulic Engineering

Van Oord

Dredging and Marine Contractors

Author

Anestis C. Lioutas

email: a_lioutas@yahoo.com

Graduation committee master thesis

prof.dr.ir. M.J.F. Stive, *Hydraulic Engineering, TU Delft*

ir. H.J. Verhagen, *Hydraulic Engineering, TU Delft*

prof.dr.ir. W.S.J. Uijttewaal, *Environmental Fluid Mechanics, TU Delft*

ir. G. Smith, *Engineering Department, Van Oord*

PREFACE

The present report is the overview of a research which has been conducted in the framework of graduation thesis for the MSc in Hydraulic Engineering of TU Delft.

The topic of this project is the distribution of wave overtopping in the space behind the crest. For the investigation of this subject, a physical model was developed at the Laboratory of Fluid Mechanics of TU Delft. The research was performed in close cooperation with the Engineering Department of van Oord.

I would like to thank in the first place prof. H.J. Verhagen (from TU Delft) for his instrumental arrangements and thoughtful supervision. I am equally thankful to ir. G.Smith (from van Oord) for providing me this opportunity and sharing his knowledge. His insightful guidance and help was essential for the completion of this study. I am also grateful to professors M. Stive and W. Uijttewaal for their constructive interest and ir. S. de Vree for his daily technical support during tests.

Finally, special thanks to Z. Afridi, exchange MSc student from Imperial College, London, UK, who conducted a part of the experimental work and generally supported with his enthusiasm this research.

A. Lioutas

Delft, September 2010

SUMMARY

The overtopping empirical formulas calculate the discharge only at the top of the crest of a coastal protection structure. On the other hand, the tolerable overtopping discharges are defined at certain points behind the crest where the total overtopping is reduced. The scope of this thesis is to find an empirical formula to describe the distribution of overtopping at the space behind the crest.

This thesis comes as a further investigation on the work conducted by v.Kester [2009] for regular waves. In this research, a physical model was developed on which irregular waves are tested. Because of the duration of the tests and the amount of collected water (significant lose of water during the test), a completely new measuring system was designed.

Five influencing parameters (variables) are considered on this research: wave height, wave period/steepness, slope angle, crest freeboard and crest permeability.

The entire overtopping process is analysed separately for the total overtopping discharge, the overtopping discharge directly behind the crest and the distribution of overtopping behind the structure.

In the analysis of the data collected from the measurements, the impact of the varying parameters is investigated leading to useful conclusions and better understanding of the entire process. Additionally, the experimental findings are analysed and compared to the relative existing methods.

Based on the TAW [2002] method which is proposed by the EurOtop Manual [2007], a prediction formula is developed which defines the entire process of overtopping

$$\frac{Q}{\sqrt{gH_{m0}^3}} = (0.2 - 0.133 \cdot k) \cdot \left(\frac{\gamma_b \cdot \xi_0}{\sqrt{\tan a}} \right)^k \exp\left[-(2.6 - 2.15 \cdot k) \frac{R_c}{H_{m0}} \frac{1}{\gamma_f \cdot \gamma_b \cdot \gamma_\beta \cdot \gamma_v \cdot \xi_0^{\,k} \cdot \gamma_c} \right]$$

This formula is a generic version of TAW [2002] formula in which a new reduction factor γc is introduced in order to describe the decay of the overtopping and thus predict the discharge at any certain distance behind the crest:

$$\gamma_c = -0.164 \cdot \frac{x}{B} + 0.677$$

Other relevant methods are also analysed (Juul Jensen [1984], Steenaard [2002], Besley [1999] and v.Kester [2009]) and conclusions for their applicability are drawn leading to suggested improvements or corrections.

Apart from the distribution of overtopping, on this thesis the determination of crest freeboard (which is an ambiguous issue) is also investigated.

Finally, suggestions of further research on this topic are discussed.

The entire work has been performed in cooperation with van Oord.

TABLE OF CONTENTS

LIST OF FIGURES & TABLES

1. INTRODUCTION

1.1 General

One of the primal functions of coastal defence structures like dikes, breakwaters, seawalls etc. is to protect inland from the wave attack. The most prominent process that directly affects inland is overtopping and so it always is one of the main parameters that determine the whole design in the majority of coastal defence structures. Consequently, its prediction is a major issue for designers and constructors.

1.1.1.1 Overtopping definition

Overtopping is the amount water that passes over (and through) the structure and moves landwards. It can be "produced" mainly by three different processes.

The first comes from the original definition given above: the wave attacks the structure and certain amount of water is carried over the crest because of surge action or run-up. This way produces the largest amounts of overtopping.

The second way of overtopping occurs by wave breaking on the slope of the structure. When a wave breaks, significant volumes of splash are produced. Those droplets can be transported landwards by their own momentum and/or by wind. The amount produced this way is smaller that the previous one but under circumstances it can be significant.

The last way by which overtopping can created is in the form of spray generated by the action of wind on the wave crests. This type of overtopping does not lead to significant amounts of water. Additionally, it is very difficult to be simulated in laboratory environment and thus usually it is not taken into account.

Fig. 1.1: Overtopping on sea wall

1.1.1.2 Overtopping problems and tolerable discharges

Overtopping can cause several problems in the coastal zone. The most prominent and dangerous is flooding which can occur under severe wave condition on a not properly protected coast and

can cause serious problems to pedestrian or vehicles. Figure 1.2 shows the extent of such an incident.

Fig. 1.2: Flooding caused by overtopping

Other commonly created problems are direct hazards on the buildings and infrastructure or secondary damages like scouring or corrosion. Those problems can be caused even by smaller amounts of water but they may be hazardous in long-term.

Reclaimed areas can be vulnerable to overtopping and may face serious problems if special action is not taken into account.

For these reasons, guidelines have been developed which define the tolerable overtopping discharges in coastal zone depending on the land use. In that way, designers of coastal protection structures determine the dimensions of the structure in such a way that the maximum resulting overtopping at a certain point of interest is not exceeding some limits which ensure the safety and convenience at this location.

1.2 Problem definition

The main problem in this entire situation is that the existing design formulae predict overtopping only on the crest of the structure while as described above, the guidelines dictate discharge limits at certain locations behind (onshore) the crest. This means that the predicted overtopping (used in the design) does not correspond with the required tolerable discharge leading to underestimations which can result in an inadequate protection and thus hazards, or overestimations which can lead to uneconomical structures.

Overtopping discharge reduces with the distance behind the front of the crest since a part of the water is infiltrated and only the rest of it travels landwards. This process, the distribution of overtopping behind the crest, has not yet been investigated adequately and thus there is no

widely accepted design formula which can describe it properly and predict the discharge at certain inland point.

1.3 Research Objectives

A thorough experimental research on this specific topic has been performed by D.v.Kester in the Laboratory of Fluid Mechanics of TU Delft. In that research, mainly regular waves were tested and a distribution formula was formed. However further investigation of the issue was recommended for irregular waves and develop a generic prediction method.

The current thesis describes further experimental research on this topic in which ***irregular waves*** are considered. The main objective (as stated in the title) is to define a prediction method to calculate the overtopping discharge at certain point behind the crest. Since overtopping is a multi-parametric process, sensible to several factors, the problem is approached empirically and not analytically.

In figure 1.3 the research goal, the investigated discharges are depicted.

Secondarily and to achieve this goal, several minor issues of total overtopping which remain ambiguous despite the considerable amount of research performed on the topic, must be clarified.

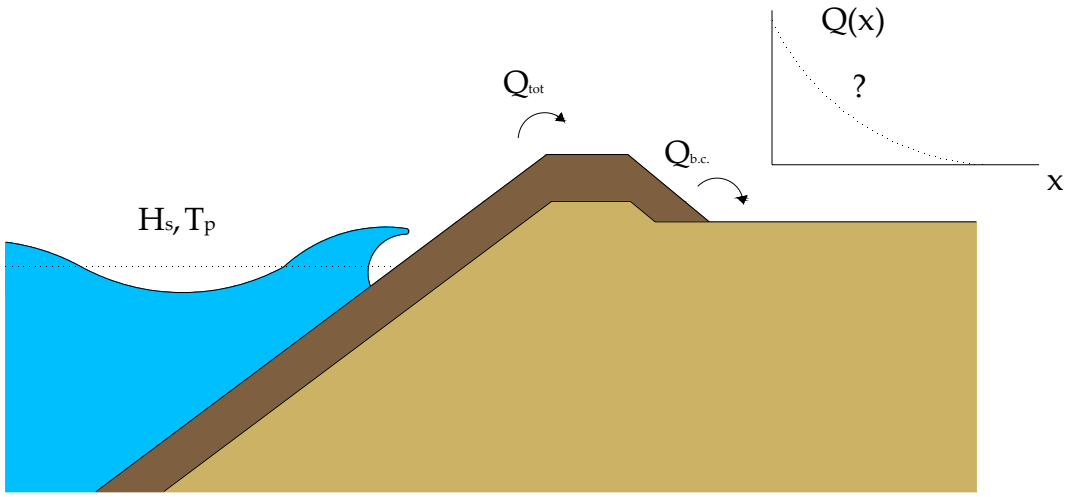

Fig. 1.3: Research objectives

1.4 Methodology

As stated in the title, the whole issue is approached experimentally. The steps followed in order to perform a complete research which will be able to draw safe conclusion are the following:

- First, a thorough study on the existing ***related literature*** is conducted in order to understand the basis of the problem and identify the critical parameters that should be taken into consideration.
- The second step is the design of a proper ***scale model*** which will simulate as realistic as possible the relevant physical processes. Depending on the available equipment, the model should be able to reproduce all the dominant parameters. The experimental set-up requires also an accurate and handy measuring system.
- Next, a practical test procedure is defined and the experiment is executed. During this step, apart from the continuous monitoring and inspection of all the devices, a regular evaluation of the results is performed. This evaluation may lead to adjustments of the experiment plan.
- The forth step consists of the result presentation. The influence of the dominant parameters on the process is investigated and through analysis of these data, the development of a prediction method (which is the main goal) is attempted. The measurements are also processed in such a way in order to be compared with the existing methods.
- Finally, the last stage is to draw conclusions, apply the proposed method and give some recommendations for further research.

1.5 Reader

The current report contains of three main chapters. Chapter 2 is the literature study where all the existing related methods are presented. Next, in Chapter 3, the experimental research is described including a detailed presentation of the scale model used in this research. The result presentation and analysis can be found in Chapter 4. In this chapter, the existing methods are investigated also. The report closes with Chapter 5 where the main conclusions and recommendations are presented.

2. LITERATURE STUDY

2.1 Physical and hydraulic parameters

2.1.1 Physical dimensions

2.1.1.1 Crest height

The crest height of the structure (relative to the water level) is defined by the crest freeboard R_c. The basic definition of the freeboard for a dike is the vertical distance between the horizontal part of the crest and the SWL (still water level). This is the most commonly used definition in the overtopping methods.

However, in the EurOtop Manual [06], it is suggested that for rubble mound structures (with crest structure), the upper limit is the top of an impermeable crest element and not the height of the rubble mound armour. The later distance is called armour freeboard A_c, and it can be higher, equal or sometimes lower than the crest freeboard R_c. Those distances are depicted in figure 2.1.

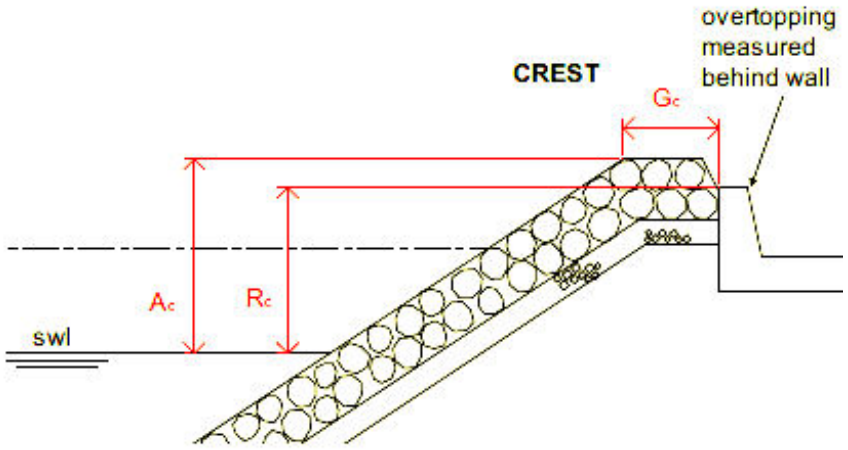

Fig. 2.1: Crest properties for rubble mound protection with crest element as defined in EurOtop [06]

In case of a structure without a crest element, it is proposed that the whole crest should be ignored and instead of the armour layer Ac, the crest freeboard should be considered (figure 2.2). The (crest) freeboard in this case is defined as the distance from SWL to upper non (or only slightly) water-permeable layer.

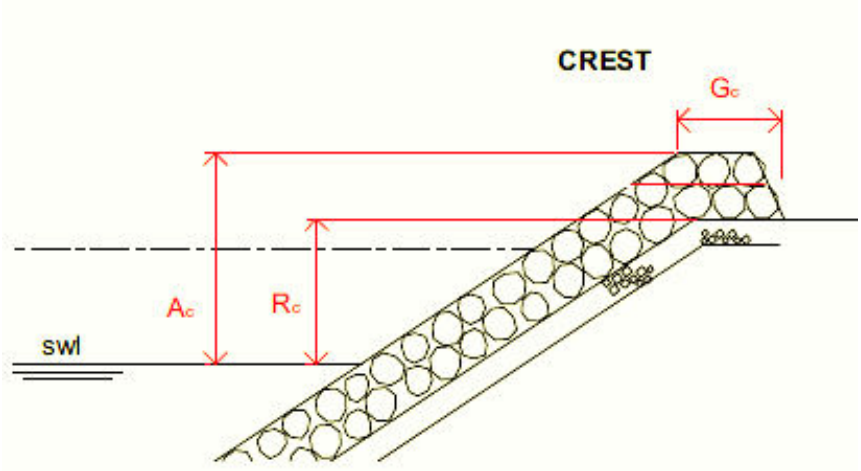

Fig. 2.2: Crest properties for rubble mound protection without crest element (from EurOtop [06])

When a crest is not completely horizontal but rounded in the middle, the seaward edge is considered as the upper limit and not the highest point.

2.1.1.2 Crest width

The crest width has no direct influence on the total wave overtopping at the front of the crest, but is important for the behaviour of the total overtopping discharge on top of the crest.

In the case of armour stone, the crest width should be sufficient to permit at least three to four stones to be placed on the crest (Rock Manual, 2007 [04]). This is a particularly important requirement if significant overtopping is expected to occur. The stones on the crest should be placed with maximum interlocking or packing density to ensure the greatest stability under wave action.

2.1.1.3 Slope

The angle of the slope in rubble mound structures commonly varies between 1:1 and 1:8. Often the slope is taken as steep as possible in order to reduce the total volume of the structure. The limits depend on the structural and hydraulic conditions.

In practice, the slope is generally not steeper than 1:1.5 and may be compared to the natural angle of repose of material dumped under water, which can be as steep as 1:1.2. If seismic activity is to be taken into account, the slopes should generally be gentle, to allow for the expected horizontal accelerations to be absorbed without damage.

2.1.1.4 Foreshore

The foreshore, the seabed section in front of the structure, is defined as having a minimum length of one wave length L_0 (EurOtop [06]). It can be horizontal or up to a maximum slope of 1:10. The depth of the foreshore varies according to the geomorphologic conditions. If the water is shallow then depth-induced phenomena should be considered also (such as breaking and shoaling).

2.1.1.5 Permeability and porosity

Porosity (n_v) is defined as the percentage of voids between units or particles. This parameter mainly depends on the shape, grading and method of placement of the armour stones on the slope. Loose materials always have some porosity. For rock and concrete armour the porosity may range roughly between 30-55%. Sand has also a comparable porosity. However, the wave behaviour is different on a sand beach and on a rubble mound slope.

The difference is caused by the difference in permeability. The permeability of a structure depends on the size of the rock layers. The permeability of a structure is generally given as a notional index that represents the global permeability of the structure, or as the ratio of diameters of core material and armour material. It is an important parameter with respect to the stability of armour layers under wave attack.

Generally, a rubble mound structure is considered permeable when up-rushing waves can penetrate through the armour layer into the under-layer and core.

2.1.1.5 Roughness

Roughness can decrease wave run-up and consequently overtopping as it can dissipate wave energy. Roughness is created by irregular shaped block revetments, artificial ribs or blocks on a smooth slope. In common overtopping design formulae, it is characterized by the roughness reduction factor γ_f.

Generally, rubble mount and concrete block structures have the highest roughness factors.

2.1.2 Hydraulic parameters

2.1.2.1 Wave height

The wave height used in the overtopping formulae is the incident significant wave height (H_{m0}) at the toe of the structure, called the spectral wave height, $H_{m0}=4(m_0)^{1/2}$ (m_n is the n^{th}-moment of the variance spectrum). Another definition of significant wave height is the average of the highest third of the waves, $H_{1/3}$. In deep water both definitions produce almost the same value, but situations in shallow water can lead to differences of 10-15%.

In many cases, a foreshore is present on which waves can break and by which the significant wave height can be reduced. There are numerical models that predict the reduction in energy from breaking of the waves and thereby the accompanying wave height at the toe of the structure. The wave height must be calculated over the total spectrum including any long-wave energy present.

Bases on the spectral significant wave height, it is reasonably simple to calculate a wave height distribution and accompanying significant wave height $H_{1/3}$ using the method of Battjes and Groenendijk (2000) [01].

2.1.2.2 Wave period

Various wave periods can be defined from a wave spectrum or wave record. The most commonly used wave periods are the peak period T_P (the period that gives the peak of the spectrum), the average period T_m (calculated from the spectrum or from the wave record) and the significant period $T_{1/3}$ (the average of the highest 1/3 of the waves). The relationship T_P/T_m usually lies between 1.1 and 1.25 while T_P and $T_{1/3}$ are almost the same.

The period used in some overtopping formulae is the spectral period $T_{m-1.0}$ ($=m_{-1}/m_0$). This period gives more weight to the longer periods of the spectrum than an average period and, independent of the type of the spectrum, gives similar overtopping for the same values of $T_{m-1.0}$ and the same wave heights. In this way, wave overtopping can be predicted for double-peaked and "flattened" spectra, without the need for the other difficult procedures.

For single peaked JONSWAP spectrum there is a fixed relationship between the spectral period $T_{m-1.0}$ and the peak period: $T_P=1.1T_{m-1.0}$ (EurOtop Manual [06]).

In this research, since JONSWAP spectra are mainly considered, the peak period T_P is calculated during the experiments and therefore used in the formulae.

2.1.2.3 Wave steepness

Wave steepness is defined as the ratio of wave height to wave length: $s_0=H_{m0}/L_0$. Depending on the used wave period (T_P, T_m, T_{-1}), different wave lengths can be calculated (see below in 2.1.2.4) resulting in different wave steepness: s_{0p}, s_{0m} and s_{-1}.

This number can give some information about the wave's generation and characteristics. Generally a steepness of $s_0=0.01$ indicates a typical swell wave and a steepness of 0.04 to 0.06 a typical wind wave. Swells will often be associated with long period waves where it is the period that becomes the main parameter that affects the overtopping.

Wind sea conditions can also lead to low steepness waves if the there is wave breaking on a gentle foreshore. When wave breaking occurs, the period does not change significantly (EurOtop [06]) but the wave height decreases resulting in lower steepness. Generally, low wave steepness in deep water means swells while for depth limited conditions it often means broken waves on a gentle foreshore. (For heavy breaking on shallow foreshore, things can be different since the wave period must be specially calculated.)

2.1.2.4 Wave length

The significant wave length (L_0) in deep water is equal to $L_0 = gT^2/2\pi$. The wave flume in this research is assumed as deep water, so this formula for the wave length can also be applied.

2.1.2.5 Breaker parameter

The beaker parameter is also known as surf similarity parameter (ξ) or Irribaren number. Originally it was introduced as an indicator for whether a wave would break on a plane slope. Apart from whether or not breaking will occur, it also describes the way a wave will break. It is

widely used for the modelling of many phenomena related to waves in shallow waters such as wave breaking, run-up and overtopping.

The breaker parameter is basically a ratio of the bed slope (angle *a*) and the wave steepness (s).

$$\xi = \frac{\tan a}{\sqrt{s}} = \frac{\tan a}{\sqrt{H/L}} = \frac{\tan a}{\sqrt{(2\pi \cdot \mathrm{H})/(g \cdot T^2)}} \qquad \text{eq.2.1-1}$$

Depending again on the used wave period (T_p, T_m or T_{-1}) and thus steepness (s_{0p}, s_{0m} or s_{-1}), different breaker parameters can be calculated (ξ_0,ξ_{0p} and ξ_{-1}).

The main types of breaking are surging, collapsing, plunging and spilling. Figure 2.3 shows those different types of breaking for characteristic values of ξ.

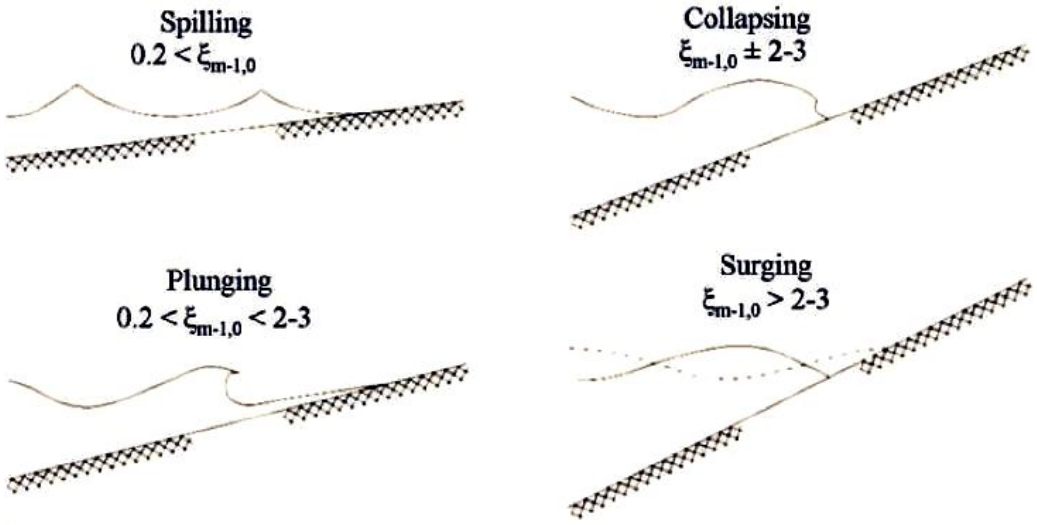

Fig. 2.3: Types of waves breaking

2.1.2.6 Wave spectrum

The wave spectrum is the most characteristic aspect of a sea state. A common type of spectrum is JONSWAP (JOint North Sea WAve Project) which is an empirical relationship that defines the distribution of wave energy with frequency for agrowing sea state. It derives from the Pierson-Moskowitz spectrum which is defined by the following formula:

$$E_{PM}(f) = \alpha_{PM} g^2 (2\pi)^{-4} f^{-5} \exp\left[-\frac{5}{4}\left(\frac{f}{f_{PM}}\right)^{-4}\right] \qquad \text{eq.2.1-2}$$

The difference of JONSAWP spectrum is that it is narrower and presents a sharper peak. The shape of the two spectra is basically the same but in JONSWAP, the peak is enhanced with use of peak enhancement factor:

$$G(f) = \gamma^{\exp\left[-\frac{1}{2}\left(\frac{f/f_{peak}-1}{\sigma}\right)^2\right]} \qquad \text{eq.2.1-3}$$

where:

f_{peak}	= peak frequency	(Hz)
γ	= peak-enhancement factor	(-)
σ	= peak-width parameter	(-)
σa	= peak-width parameter for $f<f_{peak}$	(-)
σb	= peak-width parameter for $f>f_{peak}$	(-)

This leads to the formula that describes the JONSWAP spectrum:

$$E_{JONSWAP}(f) = \alpha g^2 (2\pi)^{-4} f^{-5} \exp\left[-\frac{5}{4}\left(\frac{f}{f_{peak}}\right)^{-4}\right] \gamma^{\exp\left[-\frac{1}{2}\left(\frac{f/f_{peak}-1}{\sigma}\right)^2\right]} \qquad \text{eq.2.1-4}$$

where:

f	= frequency	(Hz)
α	= energy scale parameter	(-)

The average values of these parameters for normal wind waves are: $\gamma = 3.3$, $\sigma_a = 0.07$ and $\sigma_b = 0.09$. For swells which are much more uniform (sinusoidal) waves, the peak enhancement factor is higher. According to Goda [07] the proper value of γ is around 8-9.

Figure 2.4 shows how the JONSWAP spectrum is derived by the Pierson-Moskowitz (Holthuijsen [08]).

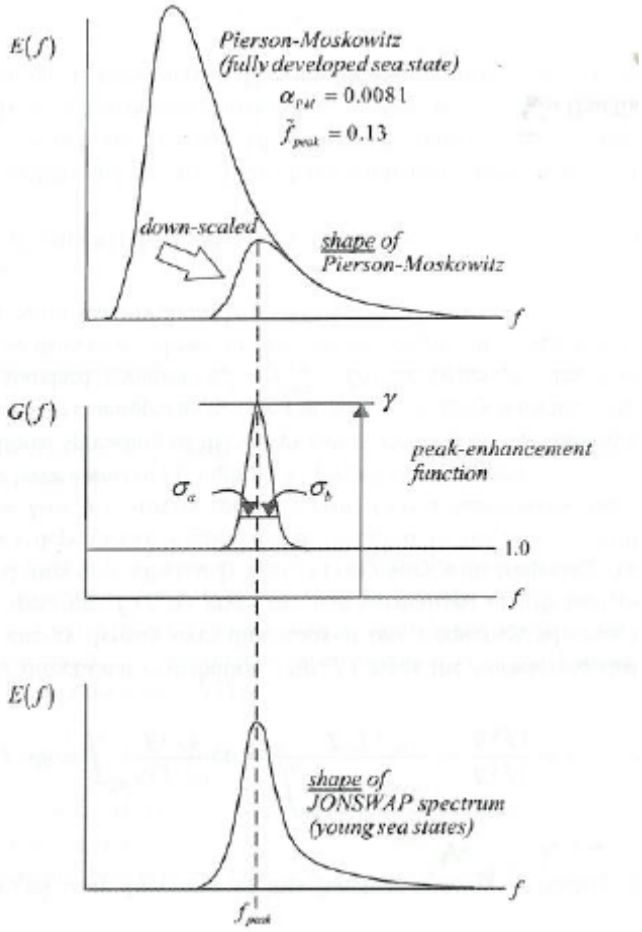

Fig. 2.4: Pierson-Moskowitz and JONSWAP spectrum

2.2 Total overtopping

Total overtopping is defined as the entire amount of water that passes the front side of the crest. This amount is measured at the seaward edge of the crest as it is depicted in figure 2.5.

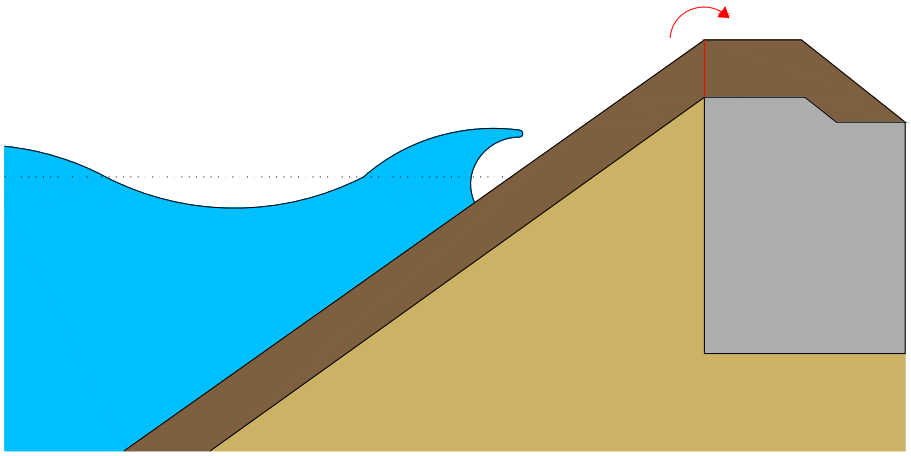

Fig. 2.5: Definition of overtopping

A number of different methods have been developed to predict overtopping of particular structures under given wave conditions and water levels. Theoretically an analytical approach can relate the waves and the structure through equations based on the knowledge of the physics of the phenomenon. However, it is hardly possible for the structure, the waves and the overtopping process to be all so simple and well-controlled that an analytical method on its own can give reliable predictions. Normally, the hydraulic properties can be well defined and controlled but this is the case not for the structural response. This is the reason why empirical methods are used instead of analytical approach.

Empirical methods are based on simplified representation of the physics of overtopping and relate (usually through dimensionless equations) the overtopping parameters (overtopping discharge, intensity etc.) to the main hydraulic and structural parameters. The form and the coefficients of the equations are adjusted to reproduce results from physical model (or field) measurements of waves and overtopping.

The majority of those empirical overtopping methods calculate the mean specific overtopping discharge Q (m^3/s per m) at the seaward edge of the crest (figure 2.5). They are based on exponential formulae of the following form:

$$Q = Ae^{B \cdot Rc} \qquad \text{eq.2.2-1}$$

or in dimensionless way of presentation, the principal formula is:

$$\frac{q}{\sqrt{g \cdot H_{m0}{}^3}} = a \exp(-bR_c / H_{m0}) \qquad \text{eq.2.2-2}$$

The coefficients *A* and *B* vary a lot depending on the method and normally they describe the hydraulic parameters (wave aspects) and physical dimensions (freeboard) of the phenomenon.

All structural aspects (permeability of the structure, roughness, armour material, oblique waves, shallow foreshore etc.) also are included in those formulae with the use of correction coefficients or explicit formulae. For special types of hydraulic structures (composite slopes, berms, toe structures, crest walls, caissons etc.) there have been developed special formulae to calculate the overtopping.

Since the total overtopping is not the main objective of this research, on this chapter only the two most updated and widely used methods will be presented. Both of them are proposed (and described in detail) in the EurOtop Manual in which the most important overtopping and wave run-up methods are reviewed.

2.2.1 Owen

Owen's method [15] was originally developed to calculate the overtopping discharge for smooth impermeable sloping structures. The method was based on measurements on a test model with 3 different slopes: 1:1, 1:2 and 1:4. The research was extended for several armour slopes also with the introduction of roughness factor γ_f (equation 2.2-5).

This method is based on two dimensionless parameters: the dimensionless freeboard R_c^* and the dimensionless discharge Q*. The definition of those parameters is the following:

$$R^* = \frac{R_c}{T_m \sqrt{g \cdot H_s}} = \frac{R_c}{H_s \sqrt{s_{0m} / 2\pi}} \qquad \text{eq.2.2-3}$$

$$Q^* = \frac{Q}{T_m \cdot g \cdot H_s} \qquad \text{eq.2.2-4}$$

where:

R_c = freeboard [m]

H_s = significant wave height [m]

T_m = mean wave period [sec]

s_{0m} = wave steepness [-]

The formula which combines those two parameters is:

$$Q^* = a \cdot \exp(-b \cdot R^* / \gamma_f) \qquad \text{eq.2.2-5}$$

where a and b are empirically derived coefficients that depend on the profile and γ_f is the correction factor for the influence of the slope roughness.

The influence of oblique waves is not taken into account on this method while the existence of a berm can be introduced by adapting the coefficients a and b. The influence of the permeable structures (such as breakwaters) is not also included. For straight smooth slopes, the values for a and b are given in table 2.1.

Slope	*a*	*b*	Slope	*a*	*b*
1:1	$7.94 \cdot 10^{-3}$	20.1	1:4.5	$1.20 \cdot 10^{-2}$	47.7
1:1.5	$8.84 \cdot 10^{-3}$	19.9	1: 5	$1.31 \cdot 10^{-2}$	55.6
1:2	$9.39 \cdot 10^{-3}$	21.6	1:6	$1.00 \cdot 10^{-2}$	65
1:2.5	$1.03 \cdot 10^{-2}$	24.5	1:8	$1.00 \cdot 10^{-2}$	86
1:3	$1.09 \cdot 10^{-2}$	28.7	1:10	$1.00 \cdot 10^{-2}$	108
1:3.5	$1.12 \cdot 10^{-2}$	34.1	1:15	$1.00 \cdot 10^{-2}$	162

Table 2.1: Values for coefficients a and b for straight smooth slopes

2.2.2 TAW (2002)

The TAW method (EurOtop Manual, [06], developed by van der Meer) makes a clear distinction between breaking and non-breaking wave conditions. In the case of breaking waves ($\gamma_b \cdot \xi_0 \le 2$) the overtopping increases for increasing beaker number ξ, while for non-breaking waves ($\gamma_b \cdot \xi_0 \ge 2$) the maximum overtopping occurs.

The overtopping formulae are given in the dimensionless form of eq.2.2-2. The coefficients a and b are functions of the wave height, breaker parameter and other influencing factors.

2.2.2.1 Breaking waves

For breaking wave conditions ($\gamma_b \cdot \xi_0 \le 2$), the average overtopping discharge can be calculated from the following formula:

$$\frac{Q}{\sqrt{gH_{m0}^3}} = \frac{A}{\sqrt{\tan a}} \cdot \gamma_b \cdot \xi_0 \exp(-B \frac{R_c}{H_{m0}} \frac{1}{\xi_0 \cdot \gamma_f \cdot \gamma_b \cdot \gamma_\beta \cdot \gamma_v}) \qquad \text{eq.2.2-6}$$

where γ_b,γ_f and γ_β are reduction factors to account for the effects of berm, slope roughness and angular wave attack respectively and tanα is the front slope of the structure.

Both the dimensionless overtopping discharge and the dimensionless wave height are related to the breaker number. Those two parameters are defined in equations 2.2-7 and 2.2-8.

$$\frac{Q}{\sqrt{gH_{m0}^3}}\frac{\sqrt{\tan a}}{\gamma_b \cdot \xi_0} \qquad \text{eq.2.2-7}$$

$$\frac{Q}{\sqrt{gH_{m0}^3}} \qquad \text{eq.2.2-8}$$

2.2.2.2 Non-breaking waves

For non-breaking wave conditions ($\gamma_b \cdot \xi_0 \geq 2$), the average overtopping discharge (per meter is described in eq.2.2-9.

$$\frac{Q}{\sqrt{gH_{m0}^3}} = C\exp(-D\frac{R_c}{H_{m0}}\frac{1}{\gamma_f \cdot \gamma_\beta}) \qquad \text{eq.2.2-9}$$

In this case the dimensionless parameters of overtopping discharge are independent of the breaker parameter. They are described in equations 2.2-10 and 2.2-11.

$$\frac{Q}{\sqrt{gH_{m0}^3}} \qquad \text{eq.2.2-10}$$

$$\frac{R_c}{H_{m0}}\frac{1}{\gamma_f \cdot \gamma_\beta} \qquad \text{eq.2.2-11}$$

2.2.2.3 Coefficients

In the equations 2.2-6 and 2.2-9, coefficients *A*, *B*, *C* and *D* have been introduced. For deterministic calculations different values for the parameters B and D are suggested including safety margin 1σ. For probabilistic calculations, the values for these coefficients have been derived representing the average trend through the user dataset. These values are presented in Table 2.3.

Coefficients	**Values for safety margin (μ-σ) – deterministic calculations**	**Values without safety margin/average trend - probabilistic calculations**

A	0.067	0.067
B	4.3	4.75
C	0.20	0.20
D	2.3	2.6

Table 3: Values for coefficients A, B, C and D in eq.2.2-6 and eq.2.2-9

2.2.2.4 Roughness factor

The values for the roughness factor γ_f are shown in the following table (Bruce et al [03]).

Structure type	γ_f
Concrete, asphalt and grass (smooth impermeable slope)	1
Pitched stone	0.80-0.95
Rocks - 1 layer on impermeable core	0.60
Rocks - 2 layers on impermeable base	0.55
Rocks - 1 layers on permeable base	0.45
Rocks - 2 layers on permeable base	0.40
Cubes - 1 layer random positioning	0.50
Cubes - 2 layers random positioning	0.47
Accropode	0.46
Xbloc	0.45
Tetrapods	0.38

Table 2.2: Values for roughness factor γ_f

According to the same research (Bruce et al. [03]), for rock armour layer(s) there is a dependency of γ_f and the slope angle. The roughness factor decreases for smaller slope angles.

Structure type	γ_f
1:1.3	1
1:1.5	0.80-0.95
1:2	0.60
1:3.5	0.55

Table 2.3: Roughness factor for difference slopes

2.3 Distribution of overtopping behind the crest

There are two different types of methods for the calculation of overtopping distribution. The first type examines the evolution of the overtopping process only till the point directly behind the crest ($Q_{b.c.}$ in figure 2.6). The second approach investigates the spatial distribution of overtopping behind the crest (noted as Q(x) in figure 2.6).

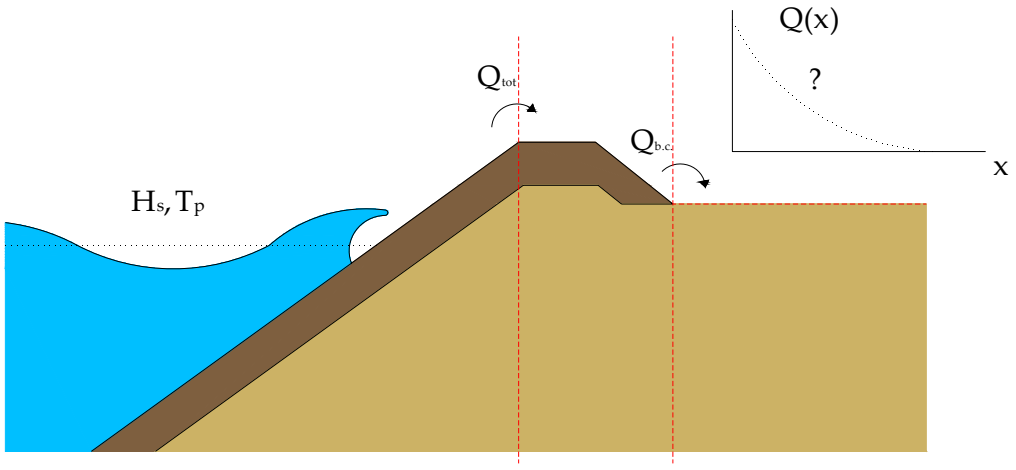

Fig. 2.6: Distribution of overtopping behind the crest

2.3.1 Overtopping discharge directly behind the crest

2.3.1.1 Steenaard (2002)

The overtopping discharge at the top of the crest can be divided in two parts: the overtopping discharge that infiltrates into the crest (infiltrating discharge) and the overtopping discharge that flows over the crest and is distributed in the area behind the crest (overtopping discharge directly behind the crest). Some research (based on physical model developed on the Fluid Mechanics Laboratory of TU Delft) has been performed on this topic by Steenaard (2002) [16] concluding to the equation 2.3-1. On that research, only regular waves were tested.

$$\frac{Q_{over}}{Q_{tot}} = \begin{cases} \dfrac{Q^*_{tot,S} - Q_d^*}{Q^*_{tot,S} + 7 \cdot 10^{-2}} & \text{for } Q^*_{tot,S} \geq Q_d^* \\ 0 & \text{for } Q^*_{tot,S} \leq Q_d^* \end{cases} \qquad \text{eq.2.3-1}$$

where:

$Q_{b.c.}$ = overtopping discharge directly behind the crest [m³/s/m]

Q_{tot} = total overtopping discharge (at the seaward edge of the crest) [m³/s/m]

$Q^*_{tot,S}$ = dimensionless total overtopping discharge (defined by Steenaard) [-]

$$= \frac{Q_{tot}}{\sqrt{g \cdot H_s^3}}$$

Q^*_d = threshold value for overtopping discharge directly behind the crest ($\approx 8.1 \cdot 10^{-3}$) [-]

2.3.1.2 D.v.Kester (2009)

D.v.Kester [12] performed further investigation on Steenaard's method based on different physical model (in with regular waves) and introduced more parameters on the formula.

$$\frac{Q^*_{over}}{Q^*_{tot}} = \begin{cases} \left(\frac{H^* - H_d^*}{H^* - 15} \right)^2 & \text{for } H^* \geq H_d^* \\ 0 & \text{for } H^* \leq H_d^* \end{cases} \qquad \text{eq.2.3-2}$$

where:

$Q^*_{b.c.}$ = dimensionless overtopping discharge directly behind the crest [-]

Q^*_{tot} = dimensionless total overtopping discharge [-]

H^*_d = threshold value for H* for overtopping discharge directly behind the crest(=26)

H^* = dimensionless factor for overtopping discharge directly behind the crest [-]

$$= \frac{H \cdot L}{B \cdot R_c}$$

B = crest width [m]

L = wave length [m]

2.3.2 Distribution of the overtopping behind the crest

2.3.2.1 P.Besley (1999)

Simple straight slopes including an armoured crest berm of about 3 nominal diameters ($B \approx 3D_n$) will reduce overtopping (behind the crest). This reduction can be larger with a wide crest as much more energy can be dissipated in a wider crest. Besley [02] describes in a simple and effective way the influence of a wide crest. First the wave overtopping discharge should be calculated for a simple slope, with a crest width up to $3D_n$. Then the following reduction factor on the overtopping discharge can be applied:

$$C_r = 3.06 \cdot \exp(-1.5 \cdot B / H_{m0}) \quad \text{with } C_r \leq 1 \qquad \text{eq.2.3-3}$$

where:

B = crest width

Equation 2.3-1 gives no reduction for a crest width smaller than about $0.75 \cdot H_{m0}$. This is fairly close to about $3 \cdot D_n$ in many cases and is, therefore consistent. A crest width of 1 H_{m0} reduces the overtopping discharge to 68%, a crest width of 2 H_{m0} gives a reduction to 15% and for a wide crest of 3 H_{m0} the overtopping reduces to only 3.4%. In all cases the crest wall has the same height as the armour crest: $R_c = A_c$.

2.3.2.2 Juul Jensen (1984)

Juul Jensen's [11] overtopping method is based on data from both laboratory tests and actual projects of Danish Hydraulic Institute (DHI). Irregular waves were considered and the impact of wind was also taken into account ("spray overtopping"). Several typical breakwater profiles were analyzed in order to include different structural aspect (mainly crest walls). The profile A (simple breakwater without crest wall) is comparable to the profile used in this thesis.

The main parameters of the physical model are presented in figure 2.7.

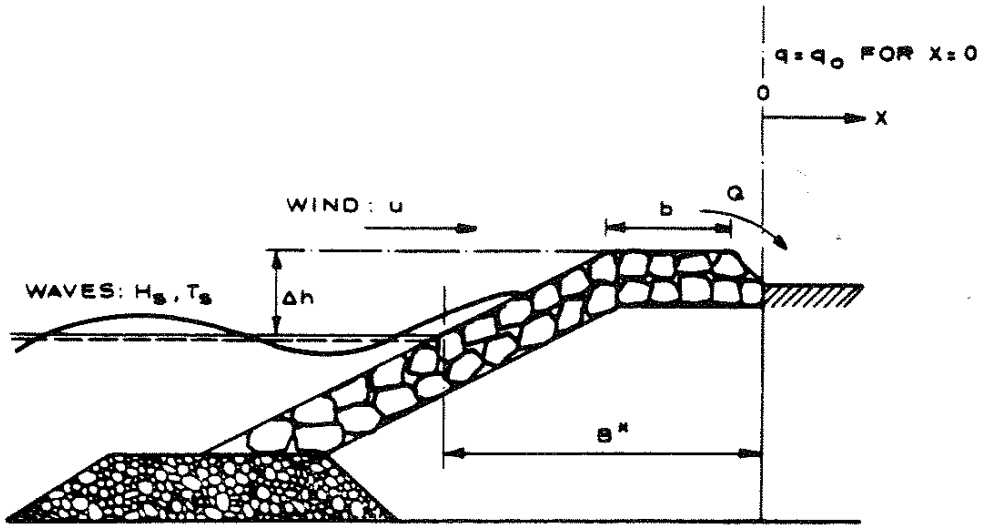

Fig. 2.7: Parameters for Juul Jensen's method

An important note for this method is that the overtopping discharge is made dimensionless with the use of wave period T_z (=mean zero-crossing period) and B* (the horizontal distance from the intersection of the SWL and the seaward slope of the breakwater to the rearmost extend of the crest).

$$Q_J^* = \frac{Q \cdot T_z}{B^{*2}} \qquad \text{eq.2.3-4}$$

For the horizontal distribution of overtopping, the method introduces the use of overtopping intensity $q(x)$ (m^3/s per meter width, per meter length) instead of overtopping discharge (m^3/s per meter width).

$$q(x) = q_0 \cdot 10^{-(x/\beta)} \qquad \text{eq.2.3-5}$$

where:

q_0 = overtopping discharge at x=0 (fig. 2.7) [m^3/sec/m]

β =constant

The parameter β is a constant and equal to the distance for which the overspill intensity decreases by factor of 10.

The total amount of overtopping (Q) may be calculated by integration:

$$Q = \int_0^\infty q_0 \cdot 10^{-(x/\beta)} \mathrm{d}x \qquad \text{eq.2.3-6}$$

resulting in the following formula:

$$Q = q_0 \cdot \beta / \ln 10 \qquad \text{eq.2.3-7}$$

Knowing Q and β, the intensity (q_0) for x=0 can be calculated and thus the intensity $q(x)$ for any distance x is known.

In all tests performed, β remained nearly constant, independent of both wave and wind conditions. For profile A which is identical to the profile used in this research, the approximate value of the dimensionless factor β/B^* is 0.40-0.55.

Figure 2.8 shows the exponential distribution from test on profile A.

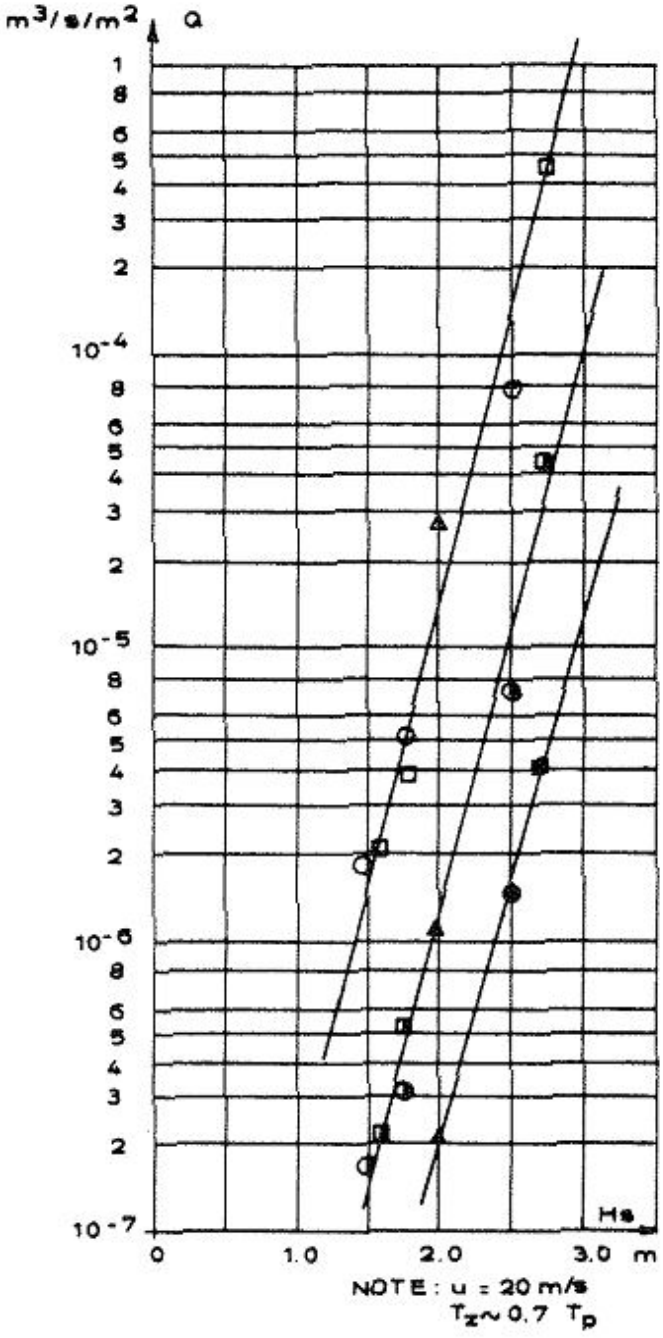

Fig. 2.8: Results for test on profile A

Generally, the results of this research show that the overtopping varies from structure to structure but some overall conclusions may be derived:

- The amount of overtopping increases rapidly with the parameter H_s/R_c. The logarithm of Q^*_J ($=\frac{Q \cdot T_z}{B^{*2}}$, dimensionless overtopping parameter according to the method) is normally a linearly function of H_s/R_c.
- The influence of the wave period differs per structure. However, there is a tendency that longer periods cause greater overtopping.
- No sharp limit exists between wind-carries spray and mass-overtopping where solid masses of water are passing the crest of the breakwater.
- The wind effect is most pronounced for small values of H_s/R_c, while for high sea states and/or high water levels (large values of H_s/R_c) where mass-overtopping occurs the wind has no influence on the amount of overtopping.

2.3.2.3 Lykke Andersen – Burcharth (2006)

Lykke Andersen and Burcharth [13] (Aalborg University) investigated the spatial distribution of wave overtopping only at breakwaters with crest wall. This distribution was measured by various trays behind the crest wall. Figure 2.9 gives different cross-sections with a set-up of three arrays.

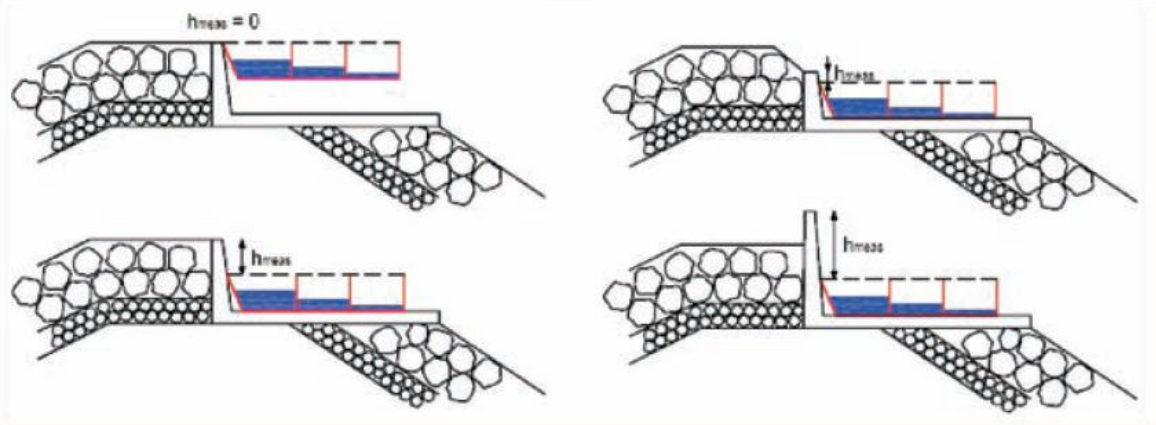

Fig. 2.9: Definition of y for various cross-sections

The distribution depends on the level with respect to the rear side of the crest wall and the distance from this rear wall, see figure 2.10. The coordinate system (x,y) starts at the rear side and at the top of the crest, with the positive y-axis downward.

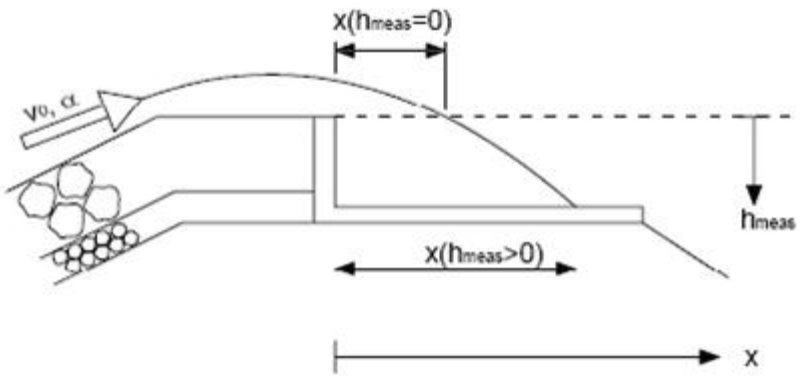

Fig. 2.10: Definition of x- and y-coordinate system

The exceedance probability (F) of the travel distance is defined as the volume of overtopping water passing a given *x*- and *y*-coordinate, divided by the total overtopping volume. The probability, therefore, lies between 0 and 1, with 1 at the crest wall. The probability at a certain location can be described with

$$F(x,y) = \exp\left(\frac{-1.3}{H_{m0}}\left\{\max\left(\frac{x}{\cos\beta} - 2.7\cdot y\cdot s_{0p}^{0.15}, 0\right)\right\}\right) \qquad \text{eq.2.3-8}$$

Equation 2.3-8 rewritten to calculate the travel distance *x* (at a certain level *y*) as:

$$\frac{x}{\cos\beta} = -0.77\cdot H_{m0}\cdot\ln(F) + 2.7\cdot y\cdot s_{0p}^{0.15} \qquad \text{eq.2.3-9}$$

Suppose cosβ=0, then we get:

F=1 x=0

F=0.1 x=1.77H_s

F=0.01 x=3.55H_s

It means that 10% of the volume of water travels almost two wave heights through the air and 1% of the volume travels more than 3.5 times the wave height. These percentages will be higher if $y \neq 0$, which is often the case with a crest unit.

The validity of equation 2.3-7 and 2.3-8 is for rubble mound slopes of approximately 1:2 and for angles of wave attack between $0^\circ \le |\beta| \le 45^\circ$. It should be noted that the equation is valid for the spatial distribution of the water through the air behind the crest wall. All water falling on the basement of the crest unit will of course travel on and will fall into the water behind and/or on the slope behind.

2.3.2.4 D.v.Kester

v.Kester [12] performed an experimental research on spatial distribution of wave overtopping at simple breakwaters without crest wall. The whole research was based on physical model (developed at the Fluid Mechanics Laboratory of TU Delft) where mainly regular waves were considered. The analysis of his results was based on Besley method (described at 2.3.2.1). The wave period and the freeboard R_c of the structure were introduced as parameters in the formula with the use of the dimensionless parameter H_0T_0, defined in equation 2.3.-10:

$$H_0T_0 = \frac{H_s}{R_c} \cdot T_s \cdot \sqrt{\frac{g}{R_c}} \qquad \text{eq.2.3-10}$$

A clear distinction is also made between permeable and impermeable backfill resulting in two different formulae. The analysis includes both deterministic and probabilistic approach.

Impermeable backfill

The spatial distribution of overtopping discharge can be approached with equation

2.3-11 (for ***probabilistic*** design).

$$\frac{Q^*(x)}{Q^*_{b.c}} = e^{-4\cdot10^8 \cdot \left(\frac{x}{H_s} \cdot \frac{1}{(H_0T_0)^6}\right)} \qquad \text{eq.2.3-11}$$

where:

$Q^*(x)$ = dimensionless overtopping discharge at a certain distance x behind the crest

$Q^*_{b.c.}$ = dimensionless overtopping discharge directly behind the crest (x=0)

For the deterministic design, the maximum value for the overtopping discharge at a certain point x behind can be calculated with equation 2.3-12 (***deterministic*** design or safety assessment).

$$\frac{Q^*(x)}{Q^*_{b.c}} = 1.1 \cdot e^{-3.4\cdot10^8 \cdot \left(\frac{x}{H_s} \cdot \frac{1}{(H_0T_0)^6}\right)} \qquad \text{eq.2.3-12}$$

Permeable backfill

Similarly to the previous case, for ***probabilistic*** design, the distribution of overtopping behind the crest is described by the equation 2.3-13:

$$\frac{Q^*(x)}{Q^*_{b.c}} = e^{-163793 \cdot \left(\frac{x}{H_s} \cdot \frac{1}{\left(H_0 T_0 \right)^3} \right)} \qquad \text{eq.2.3-13}$$

For a ***deterministic*** approach, the maximum overtopping discharge at a certain point x behind the crest can be calculated with equation 2.3-14.

$$\frac{Q^*(x)}{Q^*_{b.c}} = e^{-129874 \cdot \left(\frac{x}{H_s} \cdot \frac{1}{\left(H_0 T_0 \right)^3} \right)} \qquad \text{eq.2.3-14}$$

Irregular wave conditions

As mentioned in the beginning, all this research is based on regular waves. Based on very few tests with irregular waves, v.Kester suggests that the defined relation for wave overtopping discharge over impermeable backfill behind the crest (equations 2.3-12 & 13) can also be applied for actual sea states (irregular wave spectra) by using $H_{1/1000}$ instead of H_s.

2.4 Conclusions

The main conclusions that can be drawn from the above literature presentation are the following:

2.4.1 Total Overtopping

Total overtopping has been investigated extensively and many prediction formulas have been developed. EurOtop Manual summarises the majority of this research replacing older guidelines (such as Owen and TAW) and ends up in the TAW prediction formulae (developed by van der Meer). This method considers all the major hydraulic properties (wave height, period/steepness, oblique waves) and structural physical parameters (freeboard/crest height, slope angle, berm).

The parameters of the method are generally well defined which means that no major assumptions have to be made. For this reason, that formula is commonly used for the design of coastal structures.

In Rock Manual [04] Owen's formula is also proposed (together with TAW). The main differences of those two methods are described in detail in this guideline [04].

2.4.2 Overtopping directly behind the crest

The two methods have the same approach but v.Kester introduces 3 more parameters. Both of them are empirical formulae based on tests with *regular* waves. Thus their applicability for real sea state conditions is questionable. A disadvantage of v.Kester's method also is that different tests were performed for total overtopping and for overtopping-directly-behind-the-crest.

2.4.3 Distribution behind the crest

All formulae are again empirical and they are based on experiments. Besley's method was initially derived to predict overtopping-directly-behind-the-crest so its applicability is under question.

V.Kester used this idea to develop a prediction formula. More influencing parameters where taken into account (wave height, period, freeboard and backfill permeability). The entire research was based on regular waves so the applicability of the method is again under consideration.

Juul Jensen's method was developed to describe this problem and it is based also on measurements from actual projects (not only laboratory tests). Generally, it is the only method which based on real sea state conditions and gives a physical insight on the process. Despite this fact, the method is not included in EurOtop Manual [06] or Rock Manual [04]. An ambiguous issue of this method is the calculation of overtopping which is used as an input.

3. LABORATORY RESEARCH – PHYSICAL MODEL SET-UP

In this chapter, the experimental part of this research is described. First, a prototype structure is defined. Next, through the scaling process, the final dimensions of the physical model are calculated. Then, the laboratory equipment, the measurement setup, the measurement process and the special characteristics of this experimental system are described in detail. Finally, the initial test plan is presented.

3.1 Introduction

3.1.1 Approach

3.1.1.1 General

The desirable outcome this study is mainly the deduction of an empirical formula that can be applied rather than the theoretical description of the process itself. This is the common practice for research of multi-parametric processes which are not considered themselves as physical phenomena but as an interaction of known basic physical phenomena (for example gravity, viscosity or wave phenomena like shoaling, reflection, set-up etc.). Of course this does not exclude the physics (and mathematics) from the whole investigation; in fact these are the base on which the physical model is structured.

The main step in this research is to design and construct an appropriate physical model that will express clearly the overtopping process. Since overtopping is an interaction of several fundamental phenomena, an issue of critical importance is the selection of parameters that can be introduced properly. The physical model has to able to simulate in the best possible way the selected parameters and at the same time to provide to the user a direct control of them.

Finally, the last important aspect of the experiment set-up is its measuring system. Its importance on the final outcome is apparent and so it can be critical in the design of the physical model.

The final step before start running the experiments is to set-up a flexible test plan. Since the evolution of the tests is not known in advance, an advantage of the test plan is to be easily adjustable to changes.

3.1.1.2 Comparison with v.Kester's approach

As already mentioned in the introduction, the whole idea of this thesis was to continue and expand for irregular waves the work conducted by v.Kester (2009) [12]. This difference creates many particularities and leads inevitably to a different consideration of many practical issues.

Since this research comes as a further investigation of this work, the same general concept was followed (with mainly minor differences) for the formation of the physical model (prototype, scaling process and final dimensions). The difference with most significant impact is the

permeability of the backfill. v.Kester used two different sets of models, one with impermeable and one with very permeable backfill.

In this research, the case of impermeable surface is not examined since in that condition, the inclination of the surface affects directly the distribution; the water may have an initial distribution but immediately it will flow according to the slope of the surface and finally it will be collected into the lower point. Therefore, only the case with permeable backfill was considered (but with a more realistic value for the permeability).

As far as it concerns the measurement system, the whole concept (setup and process) is totally different. The importance of those differences and the problems solved by them will be presented extensively later on this chapter.

The test plan is also totally different firstly because different parameters were selected and secondly because different measuring system was used.

3.1.2 Parameters

One of the most important difficulties of modelling and predicting wave overtopping is the fact that it is very sensitive to many parameters. Its distribution behind the crest is even more complex process since more variables are introduced.

The first main problem is that it is not easy to distinguish and isolate one or two dominant parameters; the most of the factors are correlated to each other and are able to affect indirectly but still significantly the phenomenon. The second basic problem is the difficulty to introduce and simulate properly some of them on the physical model.

The selection of the parameters for this research is based on past research projects and on literature presented in the chapter 2.

Besley (1999) [02] expresses the process relatively only to wave height. Juul Jensen's (1984) [11] formula uses only one parameter, β, which is related to other parameters that are not defined by the method. On v.Kester's research, four main variables are used: wave height, wave steepness (wave period) and freeboard, plus the permeability of the backfill.

For this research, the basic parameters which will be considered are four:

- wave height, Hs
- wave period Tp (wave steepness 1/s0)
- freeboard Rc
- slope

Amongst the previously mentioned physical models, there are some details that are not clarified or are defined under very unique conditions, creating confusion on the applicability of their methods.

The main condition whose influence is not clear is the permeability of the crest. All the existing overtopping methods are based on physical models with impermeable crest as shown in figure 3.1. This is reasonable since the definition of overtopping is the discharge which flows over the seaward edge of the crest. However, when the distribution of overtopping is considered, the permeability of the crest has significant influence.

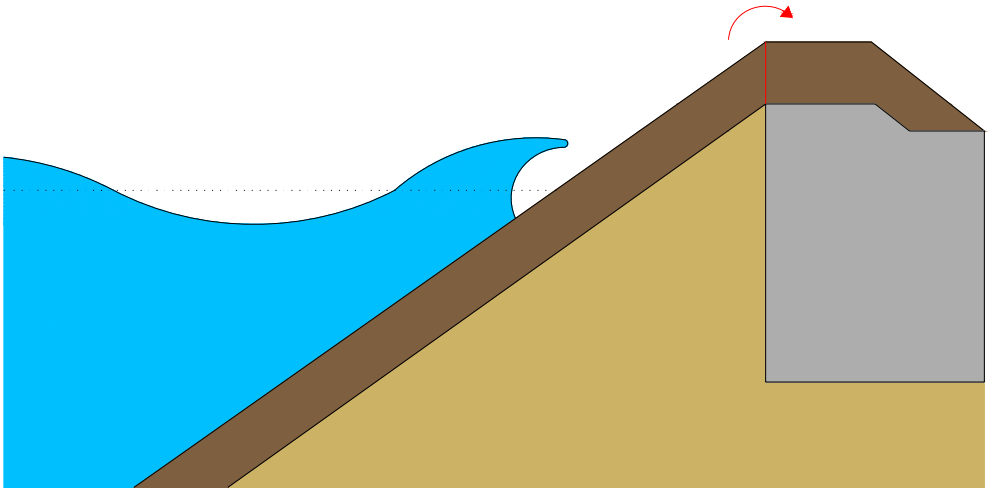

Fig. 3.1: Definition of overtopping

The second issue concerns the swells and generally waves for which different type of the wave spectrum is considered. The methods on which irregular waves were tested use the significant wave height H_s of JONSWAP spectra with the peak enhancement factor γ equal to 3.3. According to Goda [07], swells are better described by a more "peaked" JONSWAP spectrum with γ =8-9. Other sea states (rarely at coastal waters) are characterized by double-peaked spectra.

The influence of such differences is not investigated in any of the existing models. So the applicability of those methods for different types of waves is questionable.

For those reasons, two more factors are considered, not as parameters but mainly in order to better define the limits of application of the findings and relate them to existing method. Those two factors are:

- wave spectrum
- permeability of the crest

There are other parameters that influence the overtopping process but for several reasons (lack of appropriate equipment, time limitations etc.) it was not possible to be included. Such parameters are:

- toe structure/berm
- wind effect
- oblique waves
- shallow foreshore
- backfill permeability

3.2 Prototype

3.2.1 Dimensions

The first main issue in the set-up process of a physical model is the assumption of a proper prototype. The prototype should be a rather simple structure with characteristics that commonly apply in the majority of the cases. Several characteristics though can be excluded in order to express more clearly the phenomenon and more important, the influence of the most dominant parameters.

For this research, the prototype consists of a simplified rock protection structure. Several aspects have been excluded like a berm, toe structure and underlayers. Concerning the hydraulic conditions, as already mentioned above, the influence of the wind and the existence of oblique waves are not taken into account due to lack of proper simulation equipment.

The prototype which will be assumed is the almost the same that D.v.Kester used in his research.

The dimensions of this typical coastal structure are:

3.2.1.1 Structural dimensions

Total height:	h=14m
Crest freeboard:	R_c= 4m
Crest width:	B=3.4m
Slope:	tan(a)=1:2 (a= $\tan^{-1}(1/2)=26.6^o$)
Armor layer:	stone class 3-6 tons
	M_{15}=3.27 T, M_{50}=4.43 T, M_{85}=6.00 T
	D_{n15}=1.07m, D_{n50}=1.19m, D_{n85}=1.31m
	D_{15}=1.28m, D_{50}=1.41m, D_{85}=1.56m

3.2.1.2 Hydraulic parameters

Water depth:	d=10m
Wave height:	H_s= 3.2m (H_s= H_{m0})
Wave steepness:	s=1/30
Wave length:	L=96m
Wave period:	T_s= 7.84s
Breaking parameter:	ξ= 2.74
	for ξ_0<0.5, spilling
	for 0.5<ξ_0<3.3, plunging
	for ξ_0>3.3, collapsing or surging

An important assumption for the whole research is that the waves will not break before their interaction with the structure.

Thus, the following rules must be applied:

- s>1/7 or H>0.15L
- H>0.75d

The previously mentioned dimensions are shown in the following figure.

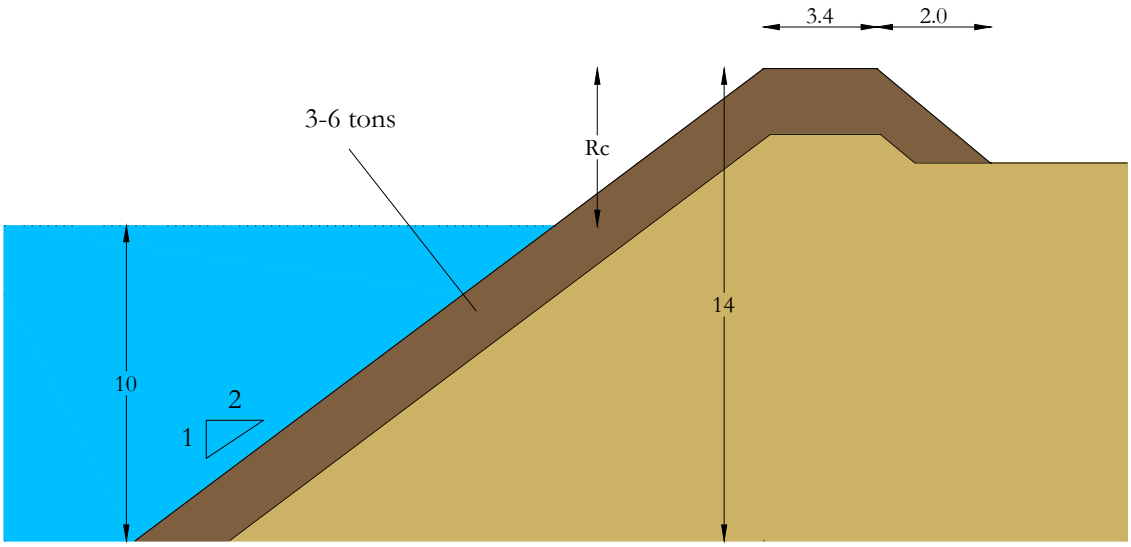

Fig. 3.2: Prototype

3.2.2 Stability armour layer

The research objective of this thesis is the overtopping and not the stability. Thus the only structural requirement is that the armour layer should be sufficiently strong (no stone movement) to withstand the wave action.

In order to ensure the stability, the van der Meer method [17] is used. The method consists of two formulae, one for plunging ($0.5<\xi_0<3.3$) and one for surging waves.

For ***plunging*** waves ($0.5<\xi_0<3.3$) the formula is:

$$\frac{H_s}{\Delta \cdot D_{n50}} = c_{pl} \cdot P^{0.18} \cdot \left(\frac{S_d}{\sqrt{N}} \right)^{0.2} \cdot \xi^{-0.5} \qquad \text{eq.3.2-1}$$

For ***surging*** waves (ξ_0>3.3) the formula is:

$$\frac{H_s}{\Delta \cdot D_{n50}} = c_s \cdot P^{-0.13} \cdot \left(\frac{S_d}{\sqrt{N}} \right)^{0.2} \cdot \sqrt{\cot \alpha} \cdot \xi^P \qquad \text{eq.3.2-2}$$

where:

N = number of incident waves at the toe (-), which depends on the duration of the wave conditions (1000 in the scale model experiments)

P = characteristic value of the damage level parameter (=2 for start of damage for a slope with cot(α)=2)

S_d = coefficient for plunging waves (-) (≈6.2)

c_{pl} = wave steepness

c_s = coefficient for surging waves (-) (≈1.0)

The breaker parameter for the prototype case is ξ= 2.74, so the plunging formula is used. The required D_{n50} for the described conditions is:

$$D_{n50} = \frac{H_s}{\Delta \cdot c_{pl} \cdot P^{0.18} \cdot \left(\frac{S_d}{\sqrt{N}} \right)^{0.2} \cdot \xi^{-0.5}} = \frac{3.2}{1.65 \cdot 6.2 \cdot 0.5^{0.18} \cdot \left(\frac{2}{\sqrt{1000}} \right)^{0.2} \cdot 2.74^{-0.5}} = 1.01\text{m}$$

The rock diameter of the armour layer is D_{n50}=1.187m and so it is sufficient to meet the requirement of v.d.Meer method. Consequently, the stability is ensured.

With the use of equation 3.2-2, the maximum significant wave height under which the stability is ensured can be calculated.

$$H_s = \Delta \cdot D_{n50} \cdot c_{pl} P^{0.18} \left(\frac{S_d}{\sqrt{N}} \right)^{0.2} \xi^{-0.5} = 1.65 \cdot 1.187 \cdot 6.2 \cdot 0.5^{0.18} \left(\frac{2}{\sqrt{1000}} \right)^{0.2} 2.74^{-0.5} = 3.65\text{m}$$

3.3 Scaling process

The extensive description and explanation of the scaling process of this physical model can be found in the research of v.Kester [12]. In this chapter, only a short overview of the general rules and conclusions will be presented.

3.3.1 Similitude

For coastal structures, three general conditions must be met to achieve model similitude:

- **Geometrical similarity**

Two objects or systems are geometrically similar if the ratios of all corresponding linear dimensions are equal. This means that the model represents a geometrical reproduction of the prototype.

Geometrically similar models are also called geometrically undistorted models.

- **Kinematic similarity**

Kinematic similarity indicates a similarity of motion between particles in model and prototype. Kinematic similarity is achieved when the ratio between the components of all vectorial motions for the prototype and model is the same for all particles at all times.

- **Dynamic similarity**

Dynamic similarity means that there must be constant prototype-to-model ratios of all masses and forces acting on the system. The forces exerted by the wave motion on an object or boundary are similitude when the dynamic similarity is maintained.

Hydraulic similitude requirements for coastal hydrodynamic models can be derived (Hughes [10]) from continuity and Navier-Stokes equations governing incompressible, free-surface flows. Those criteria are:

- **Froude**

The Froude number which is the ratio of inertia to gravity forces must be the same in the model as in the prototype.

$$\left(\frac{V}{\sqrt{gL}}\right)_p = \left(\frac{V}{\sqrt{gL}}\right)_m \quad \text{or} \quad \frac{N_V}{\sqrt{N_g N_L}} = 1 \qquad \text{eq.3.3-1}$$

This criterion applies for flow situations that inertial and gravity forces are considered to be the only dominant forces, which is the case in the most flows with free surface. Therefore the Froude law is the most important criterion for the design of a coastal scale model.

- **Reynolds**

The Reynolds number, which is the ratio of inertia to viscous forces, must be the same in prototype and in model.

$$\left(\frac{\rho LV}{\mu}\right)_p = \left(\frac{\rho LV}{\mu}\right)_m \quad \text{or} \quad \frac{N_\rho N_L N_V}{N_\mu} = 1 \qquad \text{eq.3.3-2}$$

The Reynolds law applies mainly in flows where viscous forces. In scale model conditions, this criterion does not correspond with the Froude law. This means that viscous forces can not be modelled with gravity forces in the same scale model.

- **Strouhal**

Strouhal number is the ratio of temporal to convective inertial forces and it must be kept the same in prototype and model.

$$\left(\frac{L}{Vt}\right)_p = \left(\frac{L}{Vt}\right)_m \quad \text{or} \quad \frac{N_L}{N_V N_t} = 1 \qquad \text{eq.3.3-3}$$

where:

V = characteristic velocity

L = characteristic length

t = time

g = gravitational acceleration

ϱ = fluid density

μ = dynamic viscosity

This criterion simply stated that the velocity scale ratio is equal to the length scale ratio divided by the time scale ratio. This is the same definition for velocity scale that arises from considerations of the fundamental dimensions of velocity.

3.3.2 Conclusions

In fluid models two types of forces are the most important: the gravity and the viscous forces. Forces related to surface tension and elastic compression are relatively small for practical coastal engineering issues and thus can be neglected. As already mentioned, in cases of free-surface flows, the dominant forces are the gravitational which correspond with the Froude law.

A process like overtopping on a rubble mount breakwater can be mainly considered as free surface flow and so the Froude criterion is the base for the scaling process. However, apart from the free surface flow, there is also infiltration into the breakwater and the backfill which has to be taken into account since it is an important part of the whole overtopping process. v.Kester investigated the influence of the viscous forces in this scale model.

3.4 Scale model

The final scale factor which was selected for the model was determined by the equipment limits. Practically this means that since the scale model should fit in a wave flume with certain depth, the height of the model will be the basic criterion in order to define a proper scale factor.

3.4.1 Dimensions

After the scaling process briefly described in the previous chapter, the final dimension of the scale model are:

Structural

Total height:	h= 0.73m
Crest freeboard:	R_c= 0.15m
Crest width:	B= 0.18m
Slope:	tan(a)= 1:2 (a= $\tan^{-1}(1/2)=26.6^o$)

Hydraulic conditions

Water depth:	d= 0.58m
Wave height	H_s= 0.15m
Wave steepness:	s= 1/30
Wave length:	L=4.8m
Wave period:	T_s= 1.75sec
Breaker parameter:	ξ= 2.74

3.4.2 Material

3.4.2.1 Armour layer

The hydraulic similitude results in the following material properties of the armour layer of the scale model:

Grading : 64-78mm

M_{15}=0.41kg, M_{50}=0.56kg, M_{85}=0.68kg

D_{n15}=53.7mm, D_{n50}=59.4mm, D_{n85}=65.7mm

D_{15}=63.9mm, D_{50}=70.7mm, D_{85}=78.2mm

Since there was not material sorted in such grading in the laboratory, a manual selection from material with very large grading was made. This inevitably led to a slightly narrower actual

grading, resulting in a (slightly) more permeable structure. Figure 3.3 shows the grading line from which the characteristic nominal diameters are calculated.

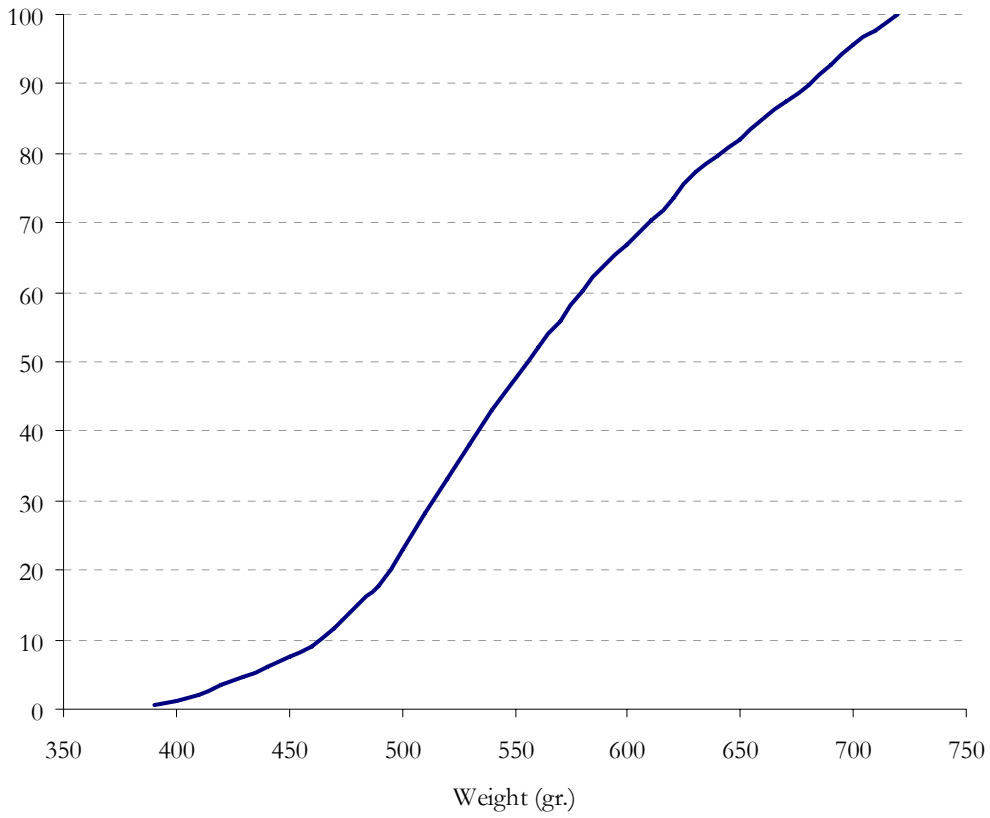

Fig. 3.3: Grading line of the armour layer

Grading: 66-76mm

M_{15}=0.48kg, M_{50}=0.56kg, M_{85}=0.67kg

D_{n15}=57mm, D_{n50}=60mm, D_{n85}=64mm

D_{15}=68mm, D_{50}=71mm, D_{85}=76mm

The specific density of the material was found ϱ_r=2625kg/m^3.

3.4.2.2 Core

According to Rock Manual [04], the mass ratio of subsequent layers of quarry should be kept between 1/10 and 1/15. Since in this model there is only one armour layer (while in reality it is highly recommended the application of a second one between the core and the main armour layer), the 1/10 ratio was selected in order to avoid under-pressure phenomena. Thus, the resulting grading for the core is the following.

Grading: 30-36mm

M_{15}=0.041kg, M_{50}=0.056kg, M_{85}=0.068kg

D_{n15}=24.9mm, D_{n50}=27.6mm, D_{n85}=30.5mm

D_{15}=29.6mm, D_{50}=32.9mm, D_{85}=36.3mm

No material with such grading was available in the laboratory and therefore a different material had to be selected. The material with the closest characteristics was the "Yellow Sun extra split 20-40mm". The characteristic nominal diameters for this material are:

D_{n15}=19mm, D_{n50}=22mm, D_{n85}=25mm

D_{15}=23mm, D_{50}=26mm, D_{85}=29.5mm

Its specific density is ϱ_r=2685kg/m^3.

3.4.2.3 Backfill

As mentioned in the beginning of the chapter, the backfill of the model used in this thesis is different than the one used by v.Kester. v.Kester's permeable backfill consisted of two layers of armour rock at the top and core material below. This construction leads to an extremely permeable surface which does not correspond to any kind of ground. For this reason in this model, only core material was used as backfill.

With this material, according to v.Kester's analysis for the infiltration of the core, the surface can be considered sufficiently permeable (corresponds to permeable gravel soil).

3.4.3 Stability check

3.4.3.1 Armour layer

In order to check the correctness of the scaling process (and particularly the dynamic similarity rule), the van der Meer [17] formula will be applied for the scaled dimensions of the model.

$$D_{n50} = \frac{H_s}{\Delta \cdot c_{pl} \cdot P^{0.18} \cdot \left(\frac{S_d}{\sqrt{N}}\right)^{0.2} \cdot \xi^{-0.5}} = \frac{0.15}{1.65 \cdot 6.2 \cdot 0.5^{0.18} \cdot \left(\frac{2}{\sqrt{1000}}\right)^{0.2} \cdot 2.74^{-0.5}} = 0.047\text{m}$$

The nominal diameter of the rock used in the model is 60mm, so the armour layer can be considered safe under wave attack.

The maximum wave that this armour layer can withstand is:

$$H_s = \Delta \cdot D_{n50} c_{pl} P^{0.18} \left(\frac{S_d}{\sqrt{N}} \right)^{0.2} \xi^{-0.5} = 1.65 \cdot 0.060 \cdot 6.2 \cdot 0.5^{0.18} \left(\frac{2}{\sqrt{1000}} \right)^{0.2} 2.74^{-0.5} = 0.19\text{m}$$

3.4.3.2 Filter stability

The rock protection apart from the direct wave attack can also fail internally due to processes mainly caused by the pressure developed between the armour layer and the core. For geometrically closed granular filters, two requirements are considered.

The application of the first requirement prevents movements of larger grains from the base layer (core). The free space in the filter area (armour layer) is determined by the smaller grains (D_{15F}) of it and when this space is not smaller than the larger grains (D_{85B}) of the base, then this core material can move to the armour layer making it less permeable.

The formula of the stability rule is:

$$\frac{D_{15F}}{D_{85B}} \leq 5 \quad \Rightarrow \quad \frac{0.068}{0.028} = 2.4 \leq 5$$

The stability requirement is met fir this case.

The second rule is applied to prevent pressure built-up in the interface between the filter and the base. This requirement is met when the permeability of the filter is larger than the permeability of the base. Since the permeability is determined by the smaller grains, the rule is:

$$\frac{D_{15F}}{D_{15B}} \geq 5 \quad \Rightarrow \quad \frac{0.068}{0.022} = 3.1$$

The requirement is not met. This happens mainly due to the large grading used in the core. However, in this case, both the armour layer and the core are considerably permeable which means that there is no large gradient perpendicular to the interface. Consequently, the permeability rule is not critical for this design.

3.4.4 Infiltration

Complete analysis for the infiltration of the scale model is performed by v.Kester [12]. The main conclusions of this analysis are only presented in this chapter.

The Reynolds numbers of the armour layer and the core in the scale model are lower than the minimum criterion defined by Hughes ($Re=3 \cdot 10^4$). Actually, this means that viscous forces can not be excluded. However, certain remarks can be made in relation to this subject:

The filter velocities are relatively large in comparison with the wave period (1.75s). The infiltrating water will be infiltrated deep enough before the next wave comes. In that way, viscous forces will not cause significant problems and the core will not get saturated.

The infiltrating water regarded in these calculations has no horizontal velocity. However, during the experiments, this water does have horizontal velocity, which causes turbulence. Because of this, viscosity will be of less importance.

Based on the calculations and remarks described above, scale effects in the overtopping discharge as a result of viscous forces will be excluded.

3.4.5 Final overview

The final overview of the model used in this research is presented in the figure 3.5. In this figure, the final dimensions along with the hydraulic condition and material properties are shown. Figure 3.5 is a picture of the real model as it was constructed in the Fluid Mechanics Laboratory of TU Delft. More photos of the model can be found in the appendix.

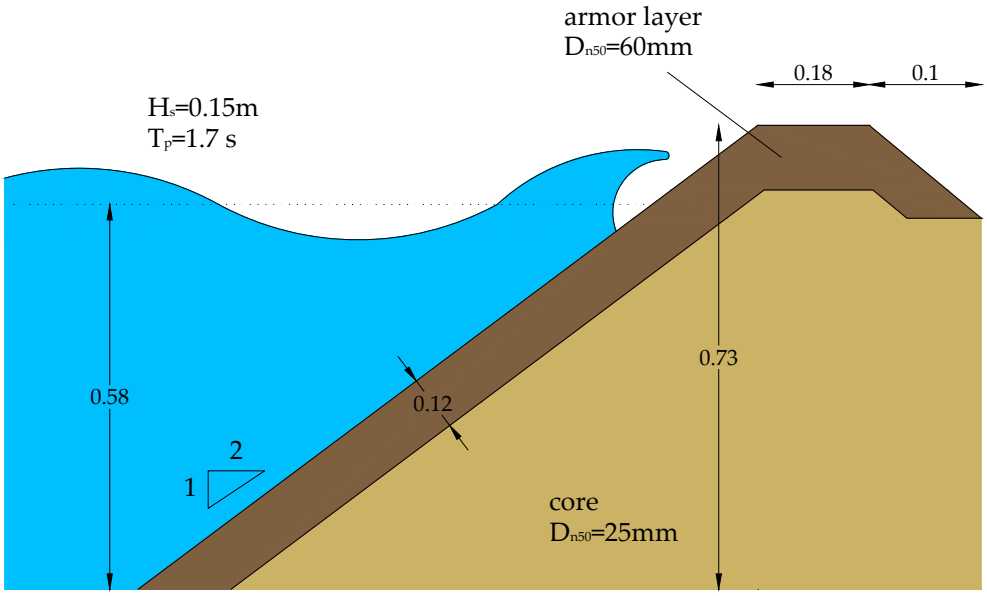

Fig. 3.4: Physical model properties

Fig. 3.5: Physical model cross-section

3.5 Measuring system

3.5.1 Important issues

As mentioned in the beginning of this chapter, the measuring system for this research was completely different from the one used in v.Kester's investigation. The main reason that a new set-up had to be considered is the consideration of irregular waves instead of regular waves.

In this chapter the innovations introduced to solve those practical problems will be presented in contradiction to v.Kester's model which is a typical overtopping model for regular waves.

3.5.1.1 Longer test duration

The most prominent difference between regular and irregular conditions is the duration of the test: for regular waves only few waves are sufficient (2-3 minutes) while for irregular conditions, approximately 1000 waves had to be tested for an acceptable development of a JONSWAP spectrum (around 30 minutes depending the wave period). Obviously, this leads to significantly larger amounts of overtopping water.

This means that during one test, the data gathered should be as much as possible. For example, v.Kester ran separate tests in order to find the total overtopping, the overtopping-directly-behind-the-crest and the overtopping discharge for each distance behind the crest. Given that the minimum distances for which the overtopping should be tested is 4-5, this leads to 6-7 tests for the same hydraulic conditions. Obviously, such an approach would not be feasibly for 30-minute tests.

Solution

In order to measure the overtopping discharge for several points simultaneously and find an acceptably accurate distribution, the backfill (the area behind the crest) was separated into 6

sectors as shown in figure 3.6. The water was collected and measured separately for each sector. Since from literature study it is expected an exponential decay, the width of those sectors was not the same; in this way a more accurate representation of the distribution can be found. The six sectors (splitting tanks) were finally constructed with the following widths:

- 2 first sectors: 5cm (1m in real scale)
- 2 next sectors: 10cm (2m in real scale)
- 2 last sectors: 20cm (4m in real scale)

This set-up covers a distance of 14m behind the crest.

Additionally, a separation tank (sector) was placed in the core of the model structure in order to collect also the water infiltrated in the crest. In that way, the total overtopping was also measured. An additional advantage of this solution is that for a certain distribution, all the data are collected in the same test under exactly the same conditions. Obviously, this corresponds to the real situation.

The final overview of this design is depicted in figure 3.6.

3.5.1.2 Water loss

The overtopping discharge, in order to be measured has to be separated from the flume. Pumping water out of the flume means that there is loss of water from the wave flume which is translated to decrease of the mean water level (and increase of the freeboard R_c) during the experiment. The alteration of the initial conditions during the test is a major problem and it essential to be avoided.

v.Kester solved this problem numerically by introducing a correction factor. This can be possible for regular waves where water loss is also regular and significantly smaller but for irregular waves, such solution is not applicable.

Solution

The solution on this very important problem was to store the collected overtopping water in tanks that float inside the flume. In that way, the water which is initially collected into these splitting tanks (sectors) is pumped out on the floating tanks (seven in total, one for each sector). The floating tanks, as they receive water, sink equalizing the expected decrease of the water level in the flume. In fact, the water stays inside the flume; it is only separated from the rest of the water. Since there is no water loss, the amount of the water stays exactly the same while the test is running. Thus, the water level remains intact during the whole procedure.

The theoretical explanation of this solution lies on the Archimedes' Principle of buoyancy.

Remark: Since those tanks are placed behind the model structure, it is necessary for the structure to be permeable (not watertight). In any case, the water of both sides should be sufficiently connected (communicating vessels).

3.5.1.3 Permeability of the backfill

This issue is not related to the difference between regular and irregular wave conditions; it is a practical problem which concerns the permeability of the backfill. This aspect of the model was not considered as a varying parameter in this research due to lack of time. However, its influence on the final distribution of the overtopping water is apparent.

The distribution of the overtopping behind the crest is formed by two processes-movements of the water. When the water flows over the crest, a part of the water "splashes" on the backfill moving further, while another part is infiltrated directly. When the (instant) discharge reaches a certain value, the ground becomes instantly impermeable and all the water flows further on the backfill. Obviously this phenomenon affects significantly the distribution.

Solution

In this model, the surface behind the crest consists of extra permeable material (same as the core). However and even the permeability is not a parameter of this analysis, a solution for introducing this also in the model is proposed. The infiltration (and consequently the permeability of this surface) can be adjusted by changing the power of the pumps (which pump out the water into the floating tanks) creating from very permeable to totally impermeable conditions. In that way, no additional constructions are needed to vary the permeability of the whole backfill (or a sector).

3.5.2 Final measurement set-up

The final measurement system with scale model is shown in the figure 3.6.

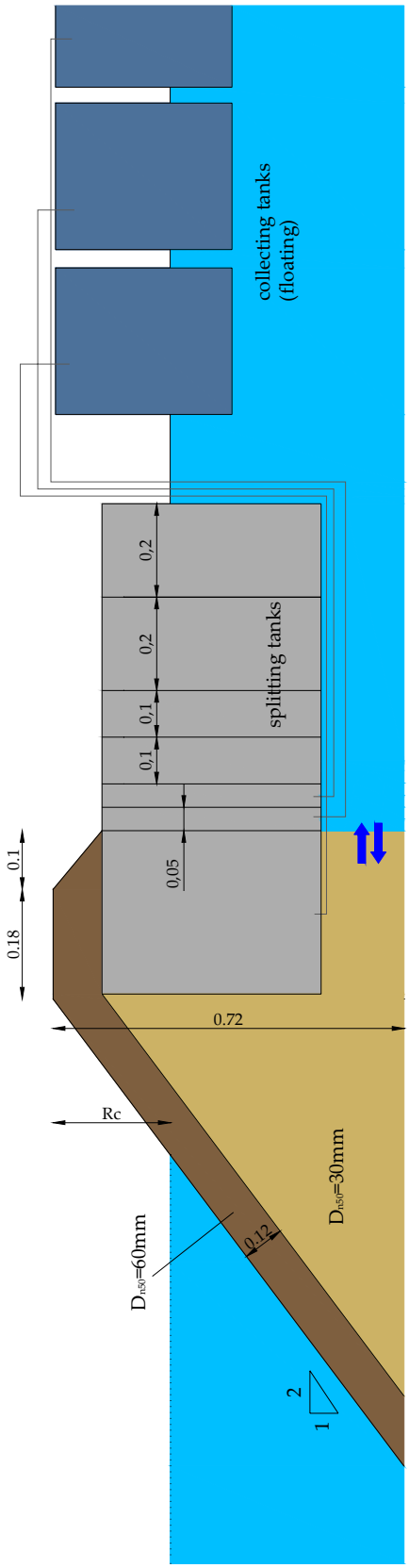

Fig. 3.6: Measuring system set-up

3.5.3 Test procedure

The typical process of a test consists of three main phases: a preparation phase before the generation of waves, the phase of the actual test where waves are generated and finally the phase after the completion of wave record where measurements, data collection and analysis are conducted.

Before the test

The main preparatory step is to create the appropriate input file with the correct wave characteristics. With this file, a steering file which controls the wave generator is created (see later on 3.6.1.2).

Of course, before starting the test, the whole equipment is checked; especially the floating tanks have to be totally empty.

Wave generation - Overtopping

The pumps are switched on so that the overtopping water is pumped out and collected in the floating tanks. The steering file is run activating the wave generator and the actual test begins. The wave data (from the gauges) start getting recorded.

After the wave generation

After the full generation of the wave record, the wave generator and the pumps are turned off. The wave data are gathered and analyzed by Matlab. From this step, the actual wave spectrum is found and from that, the significant wave height and period are calculated.

The final step is to measure the weight of the floating tanks on which the overtopping water is collected. With the use of an electronic balance and a crane, the tare weight is measured.

3.6 Laboratory equipment

3.6.1 Hydraulic equipment

3.6.1.1 Wave flume

This experimental research was performed at the wave flume "Lange Speurwerk Goot" at the Fluid Mechanics Laboratory of TU Delft. The characteristics of this fume are:

- Length: 40m
- Width: 0.80m
- Height: 0.80m

The walls consist of glass allowing the full observation process. The flume can be filled and emptied with pump valves which exist on both sides.

3.6.1.2 Wave generator

The wave generator which is installed in this flume operates with mechanical pressure machine. The wave generator of this flume is a second order wave generator which means that the second-order effects of the first higher and first lower harmonics of the wave field are taken into account in the wave generator motion. It is also equipped with Active Reflection Compensator (ACR) which reduces (even neutralizes) the wave reflection coming from the model structure.

Those aspects improve significantly the performance of the wave generator but still, its accuracy can not meet the one achieved with an electrical generator. The accuracy was an important issue and affected the evolution of the test planning since the requested wave characteristics were not obtained easily.

The wave generator is controlled with the use of DASYLab, software developed by *National Instruments*®. The function of the generator is determined by a steering file which contains all the wave information: the requested wave height and period, the type of the spectrum (JONSWAP, Pierson/Moscowitz, simple sinusoidal etc.), its characteristics (peak-enhancement factor, peak-width factor) and the duration. This steering file is created with the help of software developed by *Deltares* and basically consists of an electrical wave records which controls the movement of the pedal.

A picture with part of the flume and the generator is presented in the figure 3.7.

Fig. 3.7: Wave flume and generator

3.6.2 Measurement instruments

3.6.2.1 Wave gauges

The wave gauges were used in order to acquire all the actual wave information. The function of a wave gauge is based on the measurement the difference in voltage between the two poles of the gauge. This difference is converted into difference of the water level and this way the actual wave record is obtained.

A set of three gauges (with specific distance between them) was installed in front of the toe of the structure. The wave data recorded by a gauge consists of information of both the incoming and the reflecting wave. This is the reason that one or two wages are not sufficient. The records of both the three gauges are analyzed with the help of a Matlab script which decomposes the incoming and the reflecting wave and gives the (incoming) significant wave height H_s and significant wave period $T_{m-1,0}$.

3.6.2.2 Balance

The overtopping water was collected in floating tanks behind the structure (see figure 3.6). The weight of those tanks was measured with an electronic balance attached to a crane. The type of the balance is BOSCHE KHW.

Fig. 3.8: Balance

3.6.3 Measuring accuracy

The measuring error mainly depends on the measurement system as well as the accuracy of instruments used. The measured parameters in this research were six: the overtopping volume, the duration of the test, the wave height and period, the water depth (and freeboard) and finally the angle of the slope.

3.6.3.1 Volume

The volume is measured with the use of the electronic balance; its accuracy is ±2gr. Since the order of magnitude of the overtopping water (for the further sectors) was 1-10kg, the chosen accuracy was 50gr (=0.05kg).

3.6.3.2 Time (duration)

The duration of the test was measured from the wave data recorder. The start and finish of recording was manual but was quite accurate since in a wave record the time limits are easily noticeable.

An average short test lasted for about 1400sec, thus the selected accuracy was 10sec.

3.6.3.3 Wave height and period

The wave height and period are calculated by analyzing the actual wave spectrum with the use of Matlab. The error for those parameters is negligible.

3.6.3.4 Water depth and freeboard R_c

The water depth was easily controlled with the pump valves and since there was no water loss (see 3.5.1.2) the error was marginal.

As far as it concerns the freeboard, the critical dimension was the crest height. Since the crest is made of rock with $D_{n50} \approx 70$mm, the determination of the crest level was not clear. The expected error was around 1cm.

3.6.3.5 Slope

In this research, the slope was constructed by placing every stone manually, in empty flume, under easily manageable conditions contrary to real conditions. Thus, the deviation of the angle is beyond consideration.

3.6.3.6 Overall measuring error

With a conservative approach, the errors (in percentage) of the above mentioned aspects are assumed:

- Volume: 1%
- Wave height: 1%
- Wave period: 2% (steepness: 4%)
- Water depth/freeboard: 0.5%
- Slope angle 0.5%

These deviations result in a maximum total error of 2.5% which is insignificant compared to model errors especially in cases where small quantities of water were measured.

3.7 Test program

3.7.1. Varying parameter range

The main varying parameters of the model are four: the wave height, the wave steepness, the freeboard and the slope angle. These range of each parameter was specified firstly by possibilities of the available equipment and secondly by the time limitation. Within those limits, the maximum of the possible tests were attempted in order to acquire as much as possible data and increase the reliability of the final outcome.

Next, the range of each parameter is presented.

3.7.1.1 Wave height

The wave height was limited mainly by the wave generator and secondarily by the flume. The wave generator used in this experiment could create in practise waves up to 19-20cm. Four different wave heights were selected to be tested:

- Hs_1=12cm
- Hs_2=14cm
- Hs_3=16cm
- Hs_4=18cm

Additionally, few swells were also tested (Hs≈8-10cm).

3.7.1.2 Wave steepness

Wave steepness is an alternative parameter of wave period. Again, the range was limited by wave generator (limited pedal movement). For a wave in the order of 15cm, the maximum wave period was around 2.5sec. For smaller wave heights, longer periods could be achieved. For this experiment, four different wave steepness groups were created:

- s_1= 1/20 = 0.05
- s_2= 1/35 ≈ 0.03
- s_3= 1/50 = 0.02
- s_4= 1/200 = 0.005

The last steepness corresponds to swells.

3.7.1.3 Crest freeboard

The crest freeboard is structural dimension which is defined by the water level though. Since crest height is constant in this model, in many occasions it is referred according to water depth.

Normally, it is expressed relatively to wave height. In this test set, two different were selected within the range of 1·Hs and 1.5·Hs.

For the swell the corresponding value was higher (around 2·Hs).

3.7.1.4 Slope angle

Three different slope angles were tested in this research:

- $\tan\alpha_1$= 1:1.5
- $\tan\alpha_2$= 1:2
- $\tan\alpha_3$= 1:3

3.7.1.5 Other parameters

Other secondary parameters which varied during the experiment were the spectrum type and the permeability of the crest.

As mentioned above, several swells were tested. For them, the spectrum characteristics are different (peak enhancement factor γ=9 instead of 3.3 which corresponds to normal JONSWAP spectra).

As far as it concerns the crest permeability, initially the crest was "open" permeable crest (see figure 3.5). However, in order to clarify an important issue concerning the definition of crest freeboard, the whole test record was repeated (by Z.Afridi) for "closed"-impermeable crest (figure 3.9).

Fig. 3.9: "Close" – impermeable crest

3.7.2 Test code

In order to identify immediately the characteristics of each test, a code was tagged to each test name. The experiment code contains all the above mentioned parameters:

[T(open crest) or Z(closed)] – [wave height] – [wave steepness^{-1}] – [freeboard] – [slope (tan^{-1})]

For example T-0.14-35-0.21-2 is a test on open crest, with incident wave height Hs=14cm and steepness 1/35 (≈0.03). The crest freeboard is 21cm and the angle of the slope is 1:2.

3.7.3 Test program

Based on the above presentation and analysis of the varying range, the initial test set for each slope was:

Test name	Hs (m)	Tp (s)	s	Rc (m)	input Rc (m)	water depth	slope (1/)
T - 12 - 20 - 0.12 - 2	0.120	1.24	20.00	0.12	0.14	0.58	2
T - 12 - 35 - 0.12 - 2	0.120	1.64	35.00	0.12	0.14	0.58	2
T - 12 - 50 - 0.12 - 2	0.120	1.96	50.00	0.12	0.14	0.58	2
T - 14 - 20 - 0.14 - 2	0.140	1.34	20.00	0.14	0.14	0.58	2
T - 14 - 35 - 0.14 - 2	0.140	1.77	35.00	0.14	0.14	0.58	2
T - 14 - 50 - 0.14 - 2	0.140	2.12	50.00	0.14	0.14	0.58	2
T - 16 - 20 - 0.16 - 2	0.160	1.43	20.00	0.16	0.18	0.54	2
T - 16 - 35 - 0.16 - 2	0.160	1.89	35.00	0.16	0.18	0.54	2
T - 16 - 50 - 0.16 - 2	0.160	2.26	50.00	0.16	0.18	0.54	2
T - 12 - 20 - 0.18 - 2	0.120	1.24	20.00	0.18	0.18	0.54	2
T - 12 - 35 - 0.18 - 2	0.120	1.64	35.00	0.18	0.18	0.54	2
T - 12 - 50 - 0.18 - 2	0.120	1.96	50.00	0.18	0.18	0.54	2
T - 18 - 20 - 0.18 - 2	0.180	1.52	20.00	0.18	0.18	0.54	2
T - 18 - 35 - 0.18 - 2	0.180	2.01	35.00	0.18	0.18	0.54	2
T - 18 - 50 - 0.18 - 2	0.180	2.40	50.00	0.18	0.18	0.54	2
T - 14 - 20 - 0.21 - 2	0.140	1.34	20.00	0.21	0.20	0.52	2
T - 14 - 35 - 0.21 - 2	0.140	1.77	35.00	0.21	0.20	0.52	2
T - 14 - 50 - 0.21 - 2	0.140	2.12	50.00	0.21	0.20	0.52	2
T - 16 - 20 - 0.24 - 2	0.160	1.43	20.00	0.24	0.20	0.52	2
T - 16 - 35 - 0.24 - 2	0.160	1.89	35.00	0.24	0.20	0.52	2
T - 16 - 50 - 0.24 - 2	0.160	2.26	50.00	0.24	0.20	0.52	2
T - 18 - 20 - 0.27 - 2	0.180	1.52	20.00	0.27	0.30	0.42	2
T - 18 - 35 - 0.27 - 2	0.180	2.01	35.00	0.27	0.30	0.42	2
T - 18 - 50 - 0.27 - 2	0.180	2.40	50.00	0.27	0.30	0.42	2

This test set was repeated for slope 1:1.5 and 1:3. Additionally, the entire test record was executed again by Z.Afridi for "closed"-impermeable crest.

4. RESULT ANALYSIS

4.1 Introduction

4.1.1 General approach

The existing related literature which will be compared with the findings of this experimental data set, uses always as an input the total overtopping at certain point of the crest (depending on the method). However, the behaviour of the overtopping along the crest is not clear and so the final outcome can deviate significantly if the proper total overtopping is not used. For this reason, before any attempt to estimate the overtopping distribution behind the crest, it is important firstly to determine how the total overtopping can be calculated properly.

Thus, in this research, separate analysis will be performed for:

- total overtopping [Q_{tot}]
- overtopping-directly-behind-the-crest [$Q_{b.c.}$]
- distribution behind the crest [Q(x)]

The points where those dimensions apply are shown in the following figure.

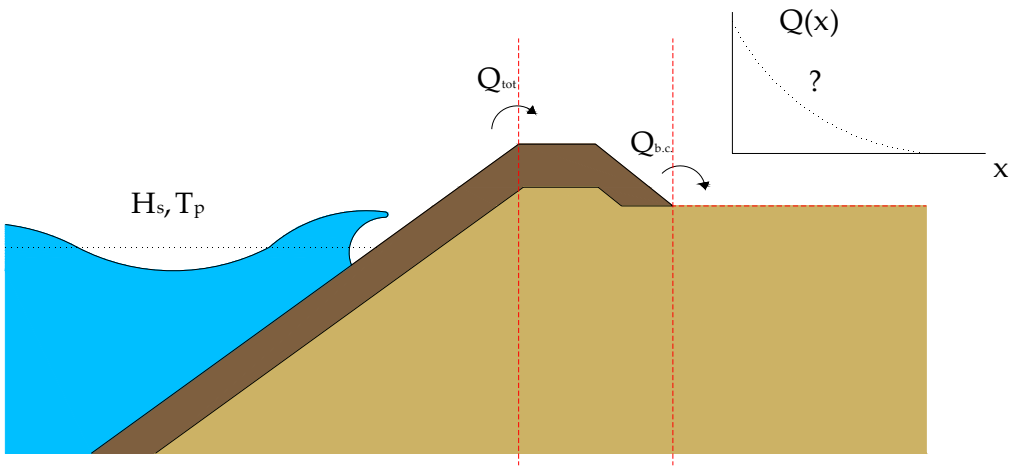

Fig. 4.1: Points of interest

4.1.2 Result presentation

Overtopping is a complex process which is sensitive to many different factors and thus, the results of this experimental research should be presented in such a way, that the influence of the several dominating parameters should be clear. The proper determination of these parameters can lead to a prediction formula that may describe the whole process.

Moreover, since some research has already been done on the topic, the existing formulae will be analysed based on the measurements of this experiment. The evaluation of those methods can lead to validation of the methods or adjustment/improvement in order to apply better.

Briefly, the way of result presentation which will be followed in this analysis is:

- investigation of the impact of several parameters
- comparison with existing methods (described in Chapter 2)
- evaluation of the existing methods
- conclusions

For better understanding, in the beginning of each subchapter, a brief review of the related literature is given. In the end of each analysis, the main conclusions will be collected.

4.2 Total Overtopping

4.2.1 General

4.2.1.1 TAW/EurOtop

As already mentioned in the literature part, EurOtop [06] (also referred as Overtopping Manual) is the most up-to-date and complete report which recapitulated and replaced the main existing overtopping methods. Thus it will serve as a guide in this analysis and it will be considered the most reliable literature.

Concerning the total overtopping, EurOtop proposes the TAW formula for overtopping prediction. TAW makes distinction between breaking and non-breaking wave conditions. The formula for breaking waves (ξ<2) is given in equation 2.2-6 and for the necessity of this analysis will be referred as ***"extended" TAW*** formula :

$$\frac{Q}{\sqrt{gH_{m0}^3}} = \frac{A}{\sqrt{\tan a}} \cdot \gamma_b \cdot \xi_0 \exp(-B \frac{R_c}{H_{m0}} \frac{1}{\xi_0 \cdot \gamma_f \cdot \gamma_b \cdot \gamma_\beta \cdot \gamma_v}) \qquad \text{eq.2.2-6}$$

According to the method, for non-breaking waves (ξ>2), there is a maximum limit which is defined in equation 2.2-9 and again for better understanding it will referred as ***"limited" TAW*** formula:

$$\frac{Q}{\sqrt{gH_{m0}^3}} = C \exp(-D \frac{R_c}{H_{m0}} \frac{1}{\gamma_f \cdot \gamma_\beta}) \qquad \text{eq.2.2-9}$$

The primal parameters that determine the whole process according to the method are:

- wave height Hs
- wave period Tp/steepness s0
- crest freeboard
- slope angle
- roughness
- angle of incident wave

The main difference of those two formulae is that the limited, by excluding the breaker number, is not taking into account the wave steepness/period and the slope angle.

4.2.2 Determination of the crest freeboard

The determination of the crest height (and consequently of the freeboard) is a major issue for structures with permeable crest (rubble mount protections). According to the two main definitions (described in the Chapter 2, 2.1.1.1) the crest height (the distance from the bottom of the structure) for this model case is:

- 0,72m (classical definition, the permeable crest is taken into account)
- 0,58m (TAW/EurOtop suggestion, the permeable crest is not considered)

The figure 4.2 presents the data collected for slope 1:2 using both definitions. In this graph, the data from tests with impermeable crest are also shown. (In this case there is no doubt about the freeboard: the whole crest height is taken into account). The line shown in the figure is the theoretical overtopping prediction using the TAW formula.

Those two series of data can serve as a basis in order to have a better insight and draw a conclusion on which definition is the most appropriate.

All these data are plotted using the dimensionless parameters proposed by TAW/EurOtop (see 2.2.2): Q*, dimensionless overtopping discharge and Rc*, dimensionless freeboard.

The impact of the different definitions is apparent: depending on the definition, the observations are shifted parallel to horizontal x-axis (red arrow).

If the EurOtop definition is considered and the data are compared with the TAW predictions, it seems that there the experimental findings do not follow the theoretical method; TAW theory tends to overestimate significantly the overtopping discharge. This is expected since EurOtop rule implies that the (permeable) crest does not exist and thus the prediction model calculates more overtopping.

Contrarily, the theoretical calculations with TAW formula seem to coincide in general with the test findings when that crest is taken into account (classical definition). Additionally, if the observations from the tests with the impermeable crest are taken into account, it can be noticed a very similar attitude between the two experimental conditions (permeable/impermeable crest). They both follow the same trend which coincides with the TAW method. The different position of the data along the TAW line (green arrow) can be explained by the amount of water which flows *through* the crest (in the case of permeable crest).

This remark serves also as a hint that this amount of water has similar attitude with the total overtopping (and thus the TAW method). Since the above mentioned shift is along the TAW line, it means that this difference is determined by the same parameters (Q^*_{tot}, R_c^*).

It is very important to note that the above observations for the classical definition are achieved if the crest height is slightly decreased (0.68m instead of 0.72m). This is reasonable since the upper part of the crest extremely permeable because of the dissimilarity of this layer (large stones). In case of rubble mount structures (like the test model of this research), this difference is prominent and thus a crest height reduction in the order of $0.5 \cdot D_{n50}$ is a reasonable estimation.

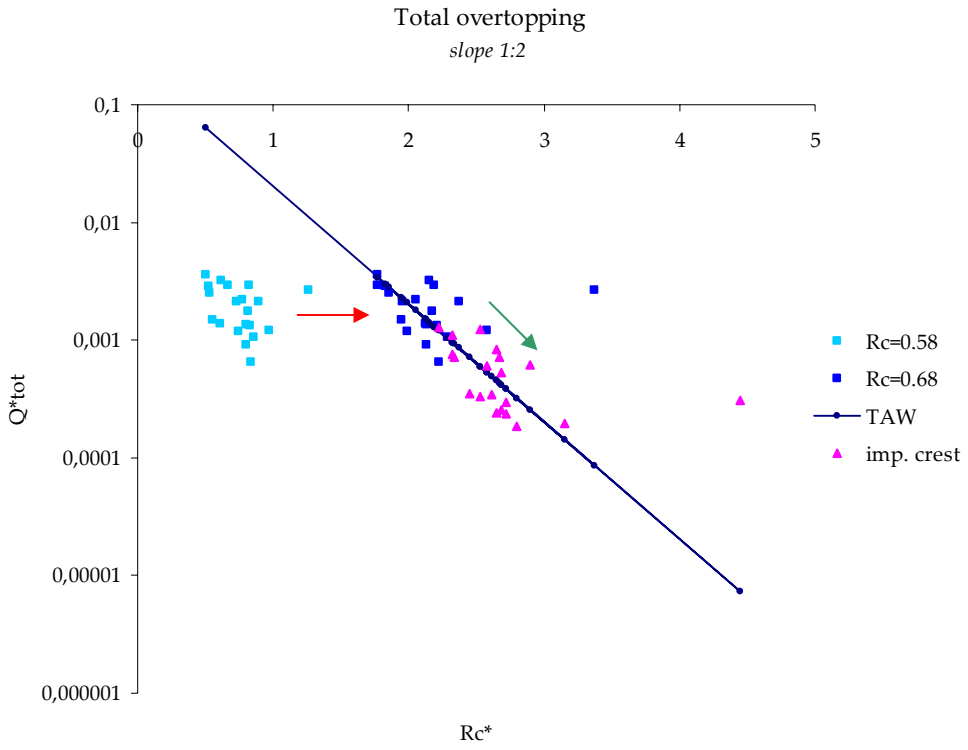

Fig. 4.2: Impact of different crest height definitions

4.2.3 Impact of the wave steepness/period and permeability of the crest

Since in this part of the analysis the influence of the wave steepness is investigated, data only from one slope (1:2) are analysed in the graphs. Similar graphs for the other slopes (1:1.5 and 1:3) can be found in the appendix.

For better understanding, the test findings are first presented separately for permeable and impermeable crest.

4.2.3.1 Permeable crest

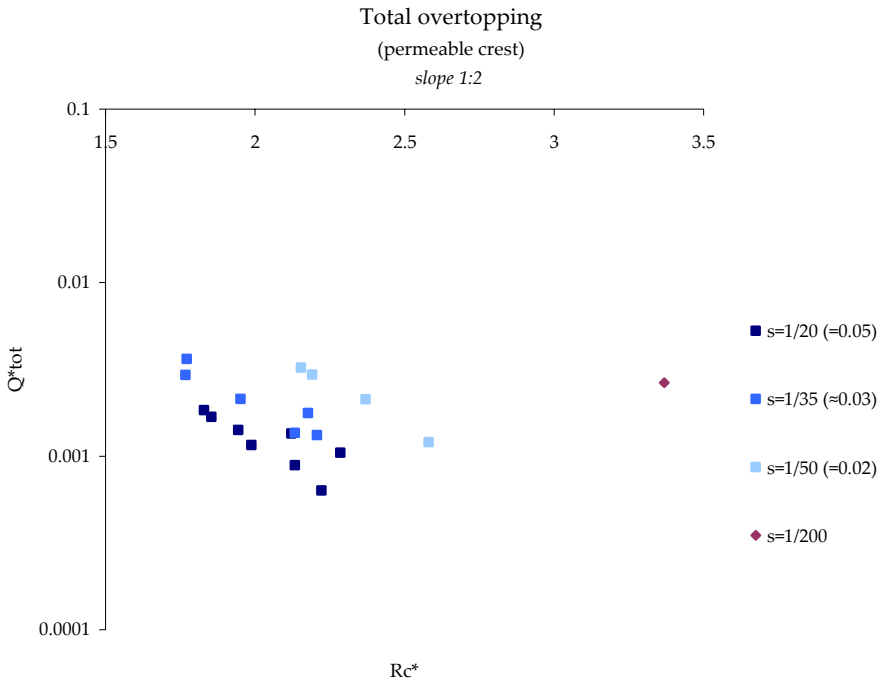

Fig. 4.3: Total overtopping, shorted by wave steepness (permeable crest)

From figure 4.3, it can be noticed that the data are grouped according to steepness/ period: for longer waves result in higher amount of overtopping. All the groups follow the same trend (parallel trendlines).

The relative position of the swell on the graph can be explained also from the difference of the spectrum. For this wave condition, the peak enhancement factor is γ= 9 while for the rest of the tests is 3.3. This difference leads a narrower spectrum which means more uniform wave conditions. Since the overtopping is caused by the bigger waves of the spectrum, it is expected that for swell conditions, more waves (of the total spectrum) will caused overtopping and thus the dimensionless overtopping Q_{tot}* will be higher.

4.2.3.2 Impermeable crest

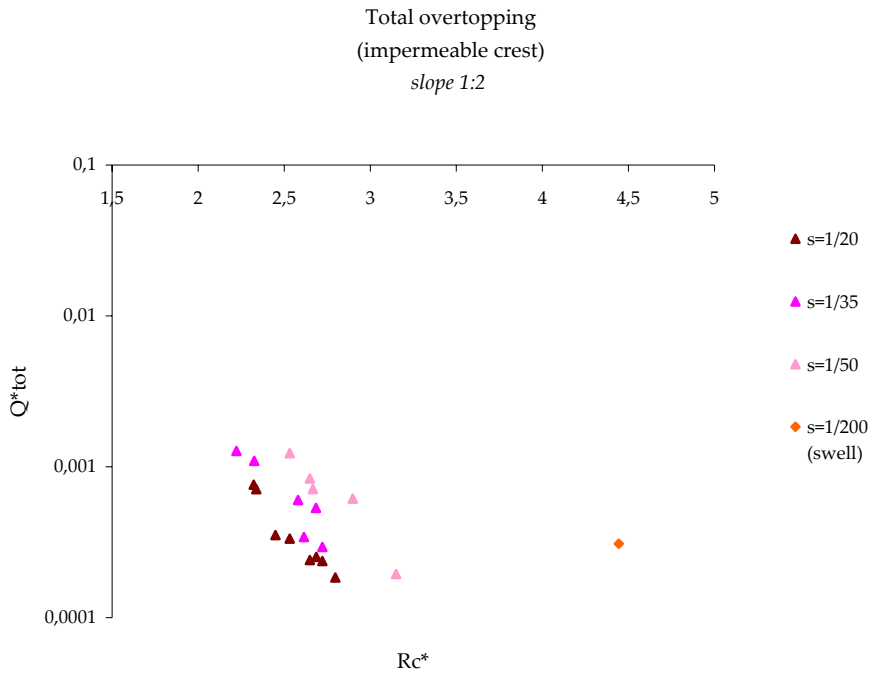

Fig. 4.4: Total overtopping, shorted by wave steepness (impermeable crest)

Apparently, exactly the same trend can be observed for impermeable crest: all the data are again shorted by the wave steepness in the same way as in the previous case. Swell's relative position on the graph is again the same for both situations.

4.2.3.3 Overall

The following figure presents the previously shown test data in one graph. In this graph, the important notice is that the trend of each steepness group is the same for permeable and impermeable crest: independently of the permeability of the crest, the data are grouped according to the wave steepness.

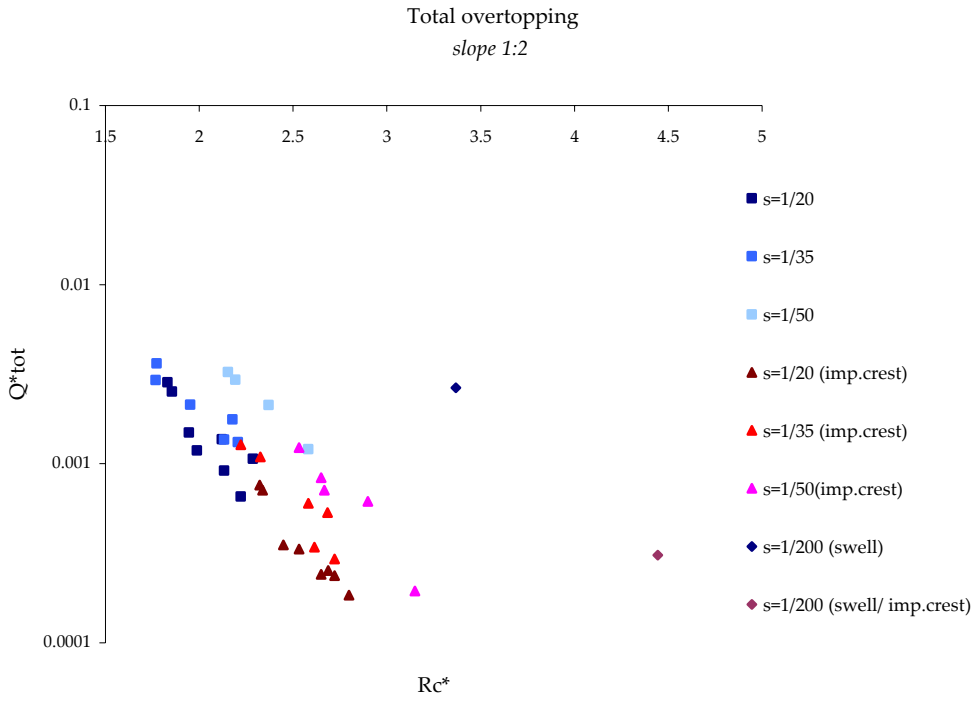

Fig. 4.5: Impact of the wave steepness on the total overtopping

Exactly the same trend can be observed for the other slopes also. Again all the observations are shorted according to wave steepness; shorter waves tend to break and thus to result in smaller amounts of overtopping.

Consequently, it becomes clear that the influence of the wave period is prominent in the whole process of overtopping. Moreover the existence of a scatter (caused by the wave steepness) in the above presented graphs means that the dimensionless parameters (proposed by TAW/EurOtop Manual) do not consider properly this influence of the wave period.

4.2.4 Influence of the slope

Since the impact of the permeability of the crest is discussed previously, for better understanding, in the part of the analysis only the findings of the original test model (permeable crest) will be examined.

Figure 4.6 presents the total overtopping measured for three different slopes: 1:1.5, 1:2 and 1:3. In the graph, the TAW formula is also denoted.

From this graph, it can be observed the data are grouped according to slope. Generally, a vertical shift of the data (parallel to y-axis, red arrow) can be observed implying a relation between total overtopping and slope: steeper slopes result in higher overtopping rates.

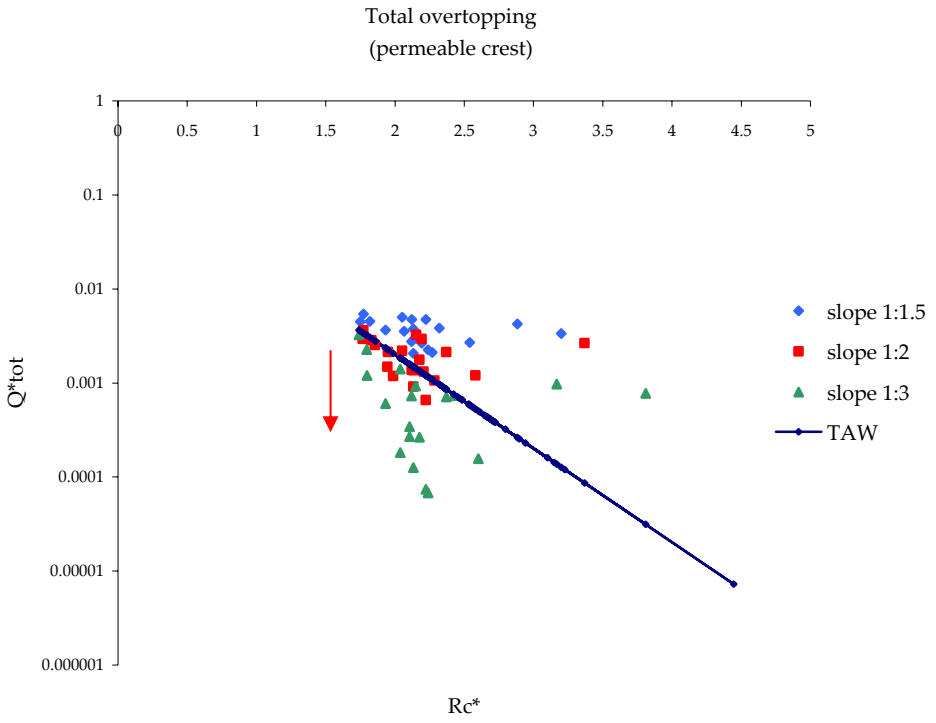

Fig. 4.6: Impact of the slope on total overtopping

Compared to the TAW method, it seems that the prediction formula has a tendency to overestimate the overtopping discharge for mild slopes (1:3 and milder) and to underestimate it for steeper slopes (1:1.5).

4.2.5 Comparison with existing formulae (TAW)

4.2.5.1 Limited formula

Figure 4.7 presents the whole data record of all measurements, both with permeable and impermeable crest. The data are shorted by slope and crest permeability. In the graph, the TAW formula, as proposed by TAW and EurOtop, is shown. As explained in subchapter 4.2.1, for ξ>2 (which is the case for all the tests performed in this research), the TAW suggests that overtopping reaches a maximum value which is irrelevant from ξ (equation 2.2-9). This limited version of TAW formula is used the following graph.

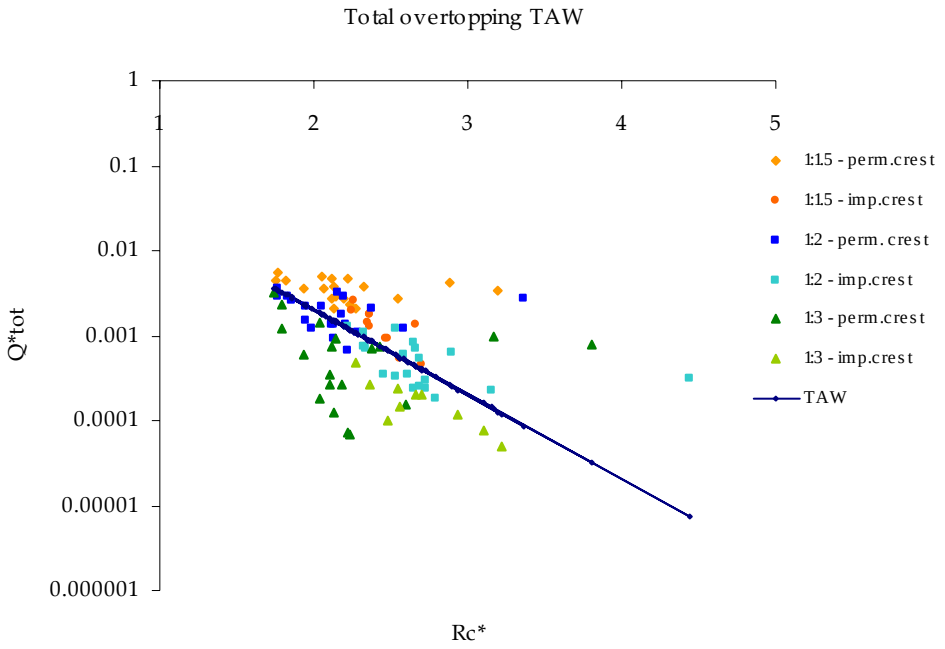

Fig. 4.7: Total overtopping, TAW formula (limited)

The formula applies quite well in terms of general trend but the spread (which is explained thoroughly in the previous subchapters) remains an issue of accuracy and reliability of the method.

4.2.5.2. Extended formula

Since from the previous analysis it was found that this spread is caused mainly by the wave steepness and secondarily by the slope angle, the introduction of a dimensionless parameter which will include them, theoretically would be a solution. For that reason, the extend TAW formula (equation 2.2-6) which introduce the breaker number ξ (and thus steepness and slope) can be used, even if ξ>2 in all the tests.

The result is presented in the following figure. Now apart from the theoretical prediction line, the horizontal x-axis is different: instead of dimensionless freeboard R_c^*, the following parameter is used:

$$R_c^* \cdot \frac{\sqrt{H_s / L}}{\tan a} = R_c^* / \xi$$

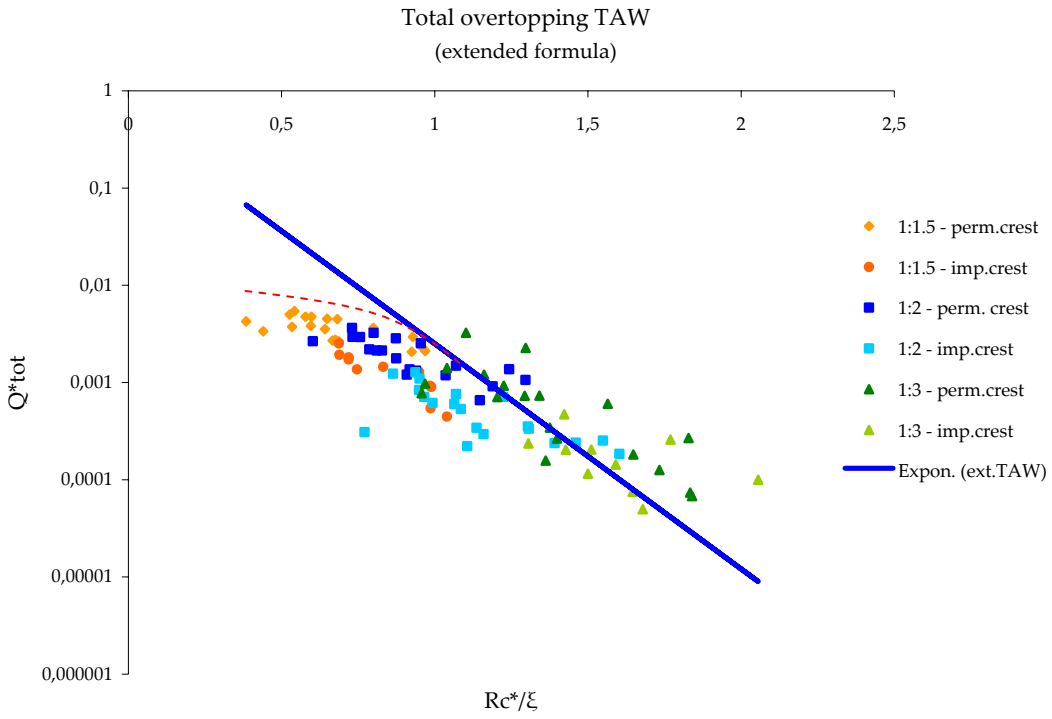

Fig. 4.8: Total overtopping, TAW formula (extended)

The new graph presents a better correlation between the results and the theory. The scatter is smaller and the measurements lay closer to the TAW line. Apparently with the introduction of ξ, a better description of the process is achieved. Even the data from tests with very long waves (swells) stay closer to the other experiments and to the theoretical prediction line.

From this graph it can also be observed that for smaller values of Rc*/ξ, the extended TAW line tends to overestimate the measurements. This implies that indeed there seem to be a maximum limit for the overtopping (red dashed line), a threshold (around 0.01 in this case). This consorts with the suggestion of TAW/EurOtop that for higher breaker numbers, there is a maximum.

In order to investigate the impact of the wave steepness on the extended TAW, graph 4.8 is re-plotted (figure 4.9) but with the measurements sorted by wave steepness. On the new graph, the regression lines of each steepness group are presented.

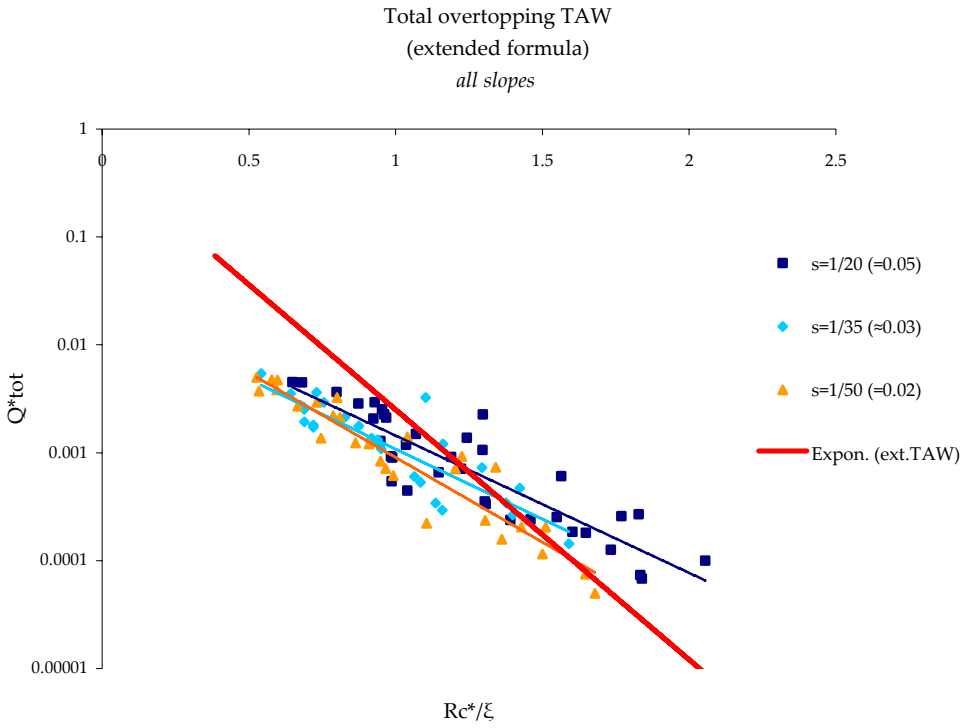

Fig. 4.9: Impact of wave steepness on Extended TAW formula

From figure 4.9, it can be observed that the measurements are again grouped according to steepness but the regression lines are identical and follow in general the trend of TAW. This implies that wave period/steepness is also well introduced by the parameter R_c^*/ξ.

The introduction of breaker parameter ξ changes the relative order of the data on the graph: now steeper waves are above the TAW line (underestimation of the experiment by the theoretical formula) and longer waves below the line (overestimation).

However, as already noted, the spread is smaller and the grouping not as clear as in the case of limited TAW formula.

4.2.5.3 Improved formula

This change of the relative position/order of the measurements on the graph (described just above) and the existence of a (smaller) spread implies that the introduction of ξ improved the correlation but its influence was slightly overestimated. For this reason, a possible reduction of this impact may result in even better correlation.

To change the impact breaker parameter ξ, it should be raised in a different power. Obviously, if this change is a reduction, a smaller power should be used. Thus, a power 0.5 is used (instead of 1).

Now the horizontal x-axis will change again and instead of $R_c^*\cdot\xi$, a new parameter will be used: $R_c^*\cdot\xi^{0.5}$ (= $R_c^*\cdot\sqrt{\xi}$).

The TAW formula is also plotted but in different form; the breaker parameter ξ is again raised to the power 0.5 and the coefficients of the formula were adjusted properly. The proposed equation is the following:

$$\frac{Q}{\sqrt{gH_{m0}^3}} = \frac{0.134}{\sqrt{\tan a}} \cdot \gamma_b \cdot \xi_0 \exp(-3.7 \frac{R_c}{H_{m0}} \frac{1}{\xi_0 \cdot \gamma_f \cdot \gamma_b \cdot \gamma_\beta \cdot \gamma_v}) \qquad \text{eq.4.2-1}$$

In fact, this equation is an intermediate situation between the extended and the limited TAW formulae. The limited formula coincides with the extended if in the later the breaking parameter ξ is raised to the power 0. The constants follow also this "rule": the above used values come from interpolation of the two "extreme" situations. Consequently, the TAW formula can be written in a more generic form:

$$\frac{Q}{\sqrt{gH_{m0}^3}} = (0.2 - 0.133 \cdot k) \cdot \left(\frac{\gamma_b \cdot \xi_0}{\sqrt{\tan a}} \right)^k \exp\left[-(2.6 + 2.15 \cdot k) \frac{R_c}{H_{m0}} \frac{1}{\gamma_f \cdot \gamma_b \cdot \gamma_\beta \cdot \gamma_v \cdot \xi_0^{\,k}} \right] \qquad \text{eq.4.2-2}$$

According to TAW/EurOtop, the value of ***k*** can take the following values: 1 (extended TAW formula for breaking waves) and 0 (limited TAW formula for non-breaking waves, maximum overtopping).

Since both conditions are analysed previously, an intermediate one is finally tested.

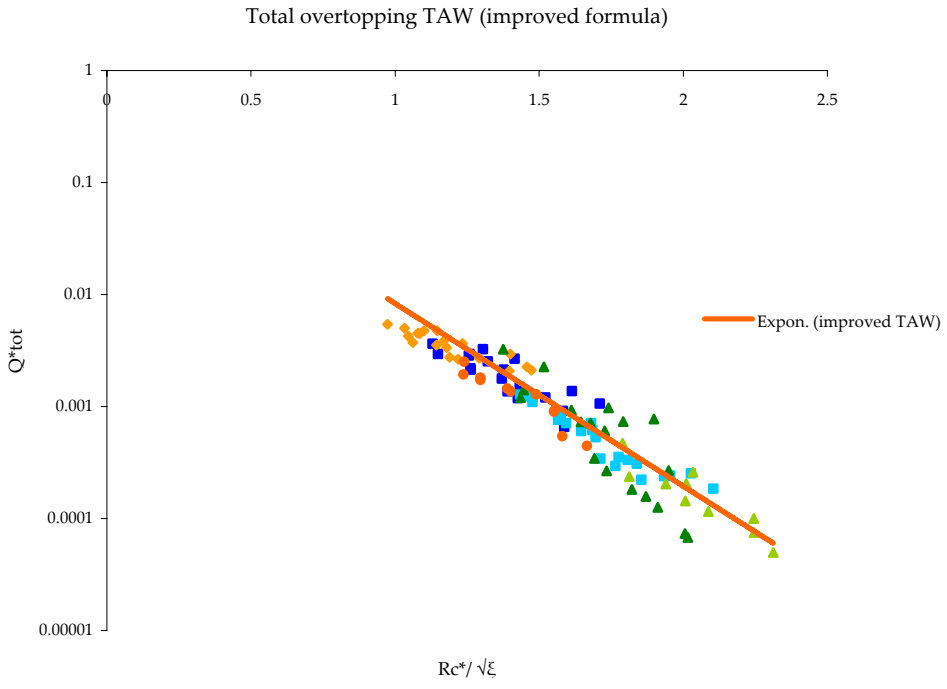

Fig. 4.10: Total overtopping, improved TAW formula

The impact of the reduction of breaker parameter ξ is apparent: the data follow exactly the same trend and the spread is almost neutralized. There is no obvious grouping as the data are positioned along the trendline.

Additionally, this trend of the test findings coincides exactly with the "improved" TAW line. The data are sorted along the prediction line and no tension for overestimation or underestimation can be detected.

In this graph, the data from all the tests performed in this research are presented: several wave heights and periods, three different slope angles, different crest heights/freeboards, different spectral characteristics (swells), even different structural aspects (permeable/impermeable crest). The characteristics of those tests are completely different in the each case. However, with the previously described adjustment of TAW method, all those data can be correlated and finally shorted along an applicable prediction formula (equation 4.2-2 for k=0.5).

As far as it concerns the distinction between breaking and non-breaking waves (with an upper limit on the later case) proposed by TAW/EurOtop, this form seems to be "independent" of wave breaking as it applies very well under a wide range of breaker numbers: the ξ value varies from 2 to more than 9.

4.2.6 Influence of the roughness factor γ_f

As already mentioned, one of the parameters of the TAW formulae is the roughness of the armour layer. It is introduced as a reduction factor γ_f in the dimensionless freeboard R_c^*. Values of γ_f for several armour units can be found in table 2.2 of chapter 2.2.1.

For the test model used in this research, since it is used one double layer of stones (two layers of the same material), the appropriate value is γ_f=0.4 (for *two layers of armour stone over permeable core*). However, since inside the core a tank was placed (see figure 3.6), the permeability of the core may be affected from the watertight walls of this tank. For this reason also, it is important to investigate the influence of the roughness factor on the final outcome.

According to Bruce et al [03], in case of armour stone, this value depends also on the slope of the armour layer and generally is smaller for milder slopes.

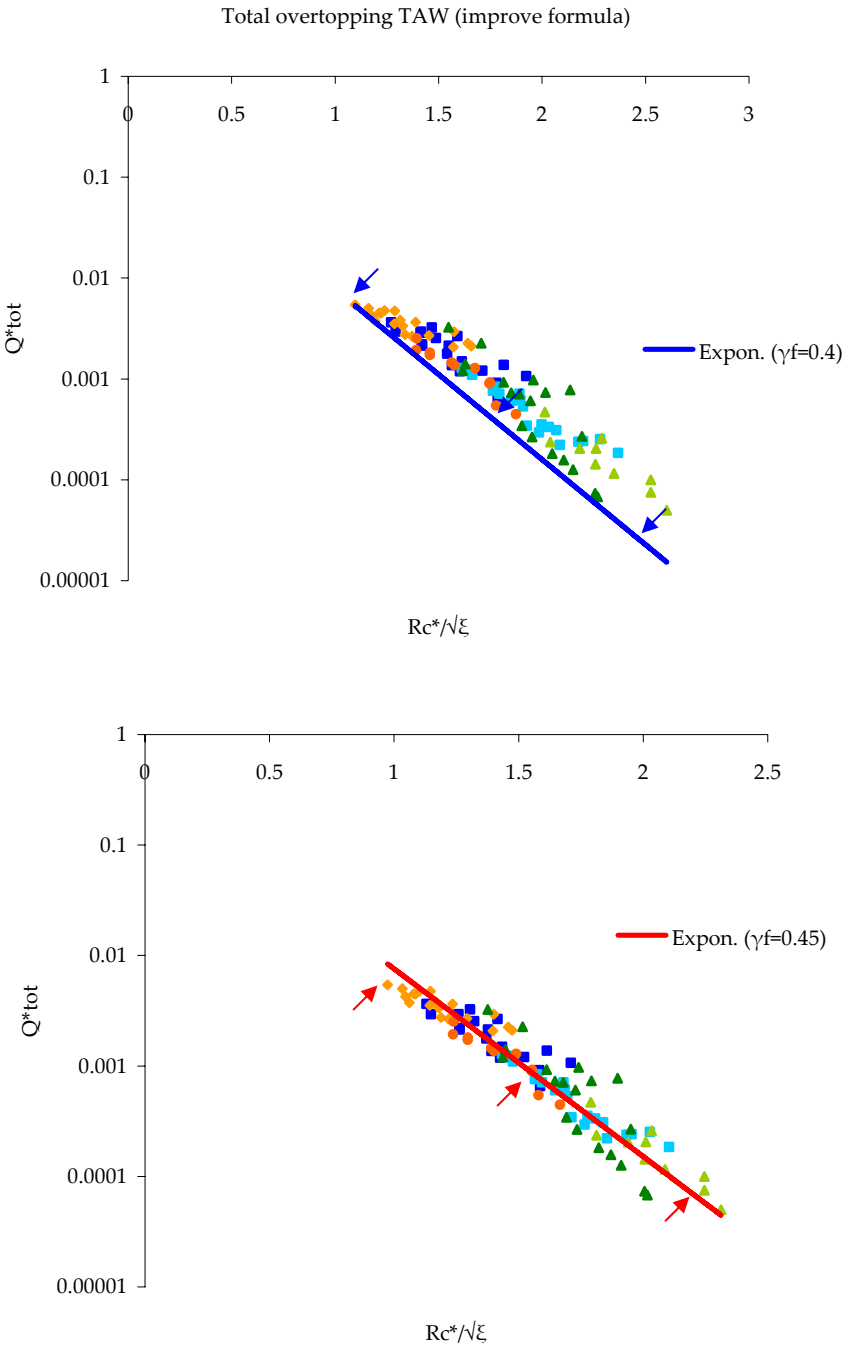

Fig. 4.11: Impact of the roughness factor

In figure 4.11, the impact of different roughness factors is shown: the (extended) TAW line tends to shift lower in the graph for smaller roughness values. This is totally expected because smaller roughness values reduce more the overtopping prediction.

For the findings of this research, it seems that a roughness factor γ_f=0.45 (which is slightly higher than the theoretically proper value for this case) fits better. This can be explained by the existence

of the impermeable wall placed inside the core which can affect the permeability of the core and consequently the roughness factor.

Generally, for safety reasons, a more conservative value (around 0.45-0.5) can be selected in order to cover the majority of the cases, especially if the dominant waves (or the design wave) are very steep (with s=1/20 or steeper).

4.2.7 Conclusions

The main conclusions that can be drawn from the above presented analysis for the total overtopping are the following:

- The ***determination of crest height*** is of critical importance. The suggestion of TAW/EurOtop that the (permeable) crest should not be taken into account is not correct. Instead, in case of totally permeable crest, a 0.5·Dn50 reduction of crest height is suggested.
- The ***slope angle*** affects the total overtopping (and thus should be inserted in the prediction formula). Generally, for steeper slope angles, overtopping increases.
- The ***limited TAW formula*** (for non breaking waves, ξ>2) does not consider properly the impact of wave steepness. Steeper waves are overestimated while longer waves are underestimated.
- The ***extended TAW formula*** for breaking waves (which uses ξ in the calculation) applies better but it overestimates the impact of wave steepness presenting an opposite attitude: overestimation of longer waves and underestimation of steep waves.
- Because of all these problems, an "intermediate" condition, an ***"improved" TAW formula*** is proposed instead, which applies very well to the test findings and seems able to predict accurately the total overtopping for a considerable range of hydraulic and structural conditions (equation 4.2-2).

$$\frac{Q}{\sqrt{gH_{m0}^3}} = (0.2 - 0.133 \cdot k) \cdot \left(\frac{\gamma_b \cdot \xi_0}{\sqrt{\tan a}} \right)^k \exp\left[-(2.6 - 2.15 \cdot k) \frac{R_c}{H_{m0}} \frac{1}{\gamma_f \cdot \gamma_b \cdot \gamma_\beta \cdot \gamma_v \cdot \xi_0^{\,k}} \right] \qquad \text{eq.4.2-2}$$

- The selection of ***roughness factor γf*** is very important in the final outcome of TAW prediction. The related research of Bruce et al (2009) [03] applies very well to this experimental set. If the improved TAW formula is used, a more conservative value of γf increased by 10-15% is suggested (for similar structural conditions).

4.3 Discharge directly behind the crest

4.3.1 General

As described in Chapter 2.3.1, there are two existing formulae which predict the overtopping discharge directly behind the crest: the first is developed by Steenaard [16] and the second by v.Kester [12].

The rationale behind those two methods is basically the same: both of them introduce a (different in each case) dimensionless parameter and based on that they "build" a formula (with several coefficients).

At first level, those two parameters are investigated and not the formulae themselves. If the parameter is found to apply in the test findings, then the form and the coefficients can be discussed.

4.3.1.1 Steenaard parameter

According to Steenaard, the governing parameter is:

$$Q^*_{tot,S} = \frac{Q_{tot}}{\sqrt{g \cdot B^3}}$$

This number implies that the most critical aspect is the crest width.

4.3.1.2 v.Kester parameter

v.Kester introduces the following dimensionless parameter to describe overtopping discharge directly behind the crest:

$$H^* = \frac{H_s \cdot L}{B \cdot R_c}$$

This number introduces 3 more variants: the wave height, the wave length and the crest freeboard and implies that they influence equally the process.

4.3.2 Result presentation

In this subchapter, the measured overtopping discharges behind the crest $Q_{b.c.}$ (point x=0) will be presented. In the next figure, the data are made dimensionless ($Q^*_{b.c.}$) and again are plotted as a function of the parameter $R_c^*/\xi^{0.5}$.

The improved TAW formula (eq.4.2-2 for k=0.5) is noted also on the graph and can always serve as a line of reference. In this way, these overtopping discharges can be related to the equivalent total overtopping.

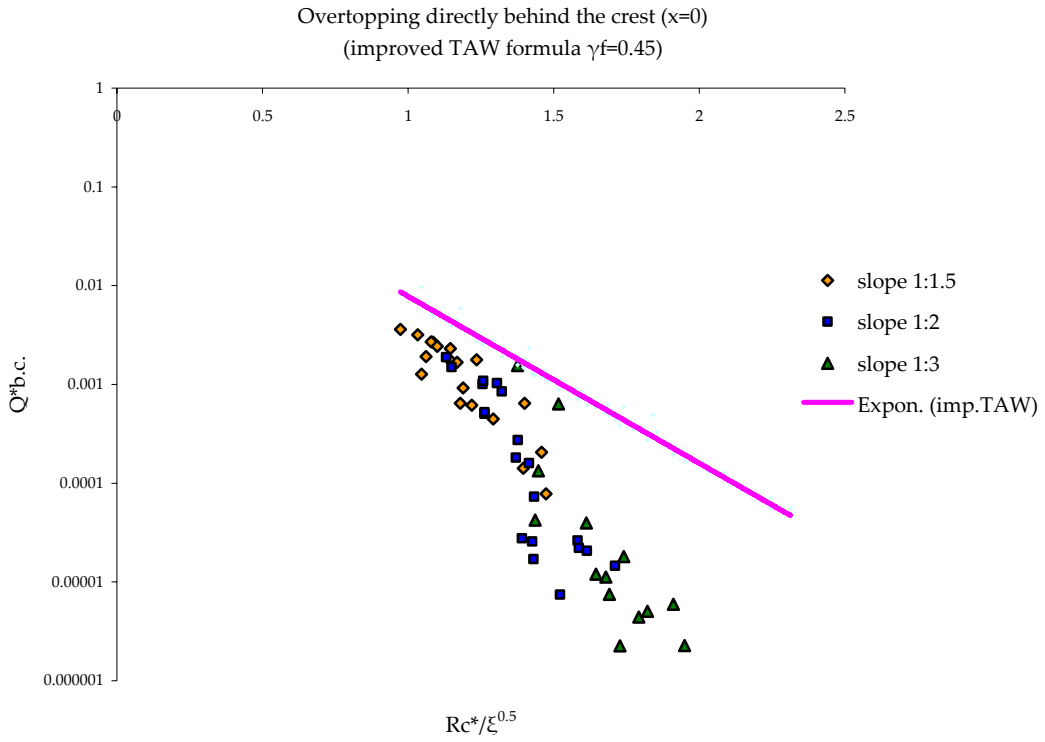

Fig. 4.12: Overtopping discharge directly behind the crest

From figure 4.12 it can be observed that the results generally follow the TAW trend. This implies that the overtopping-directly-behind-the-crest is dominated by the same influencing factors as total overtopping. Apparently, the TAW dimensionless parameters dictate this amount of water also.

If the reduction factor is reduced to γ_f=0.3 the TAW line fits better to the measurements (figure 4.13). This new value of γ_f is deduced only by curve fitting using the findings of this experiment; there is no physical explanation about the amount of reduction of roughness factor.

The reduction itself though is totally expected: a part of the total overtopping is infiltrated through the crest to the core of the structure and never reaches the landward end of the crest.

However, since roughness factor has a specific physical meaning, in order to avoid confusion, it is better instead of changing arbitrarily this factor, to introduce a new one. Thus it is proposed a new reduction factor γ_C which will describe the impact of the crest (width) when the overtopping discharge directly behind the crest is requested.

Based on the measurements of this research, and for crest width $B \approx 4 * D_{n50}$ (0.28m which is equivalent to 5.6m in real scale), the value of this crest width reduction factor is γ_C=0.7.

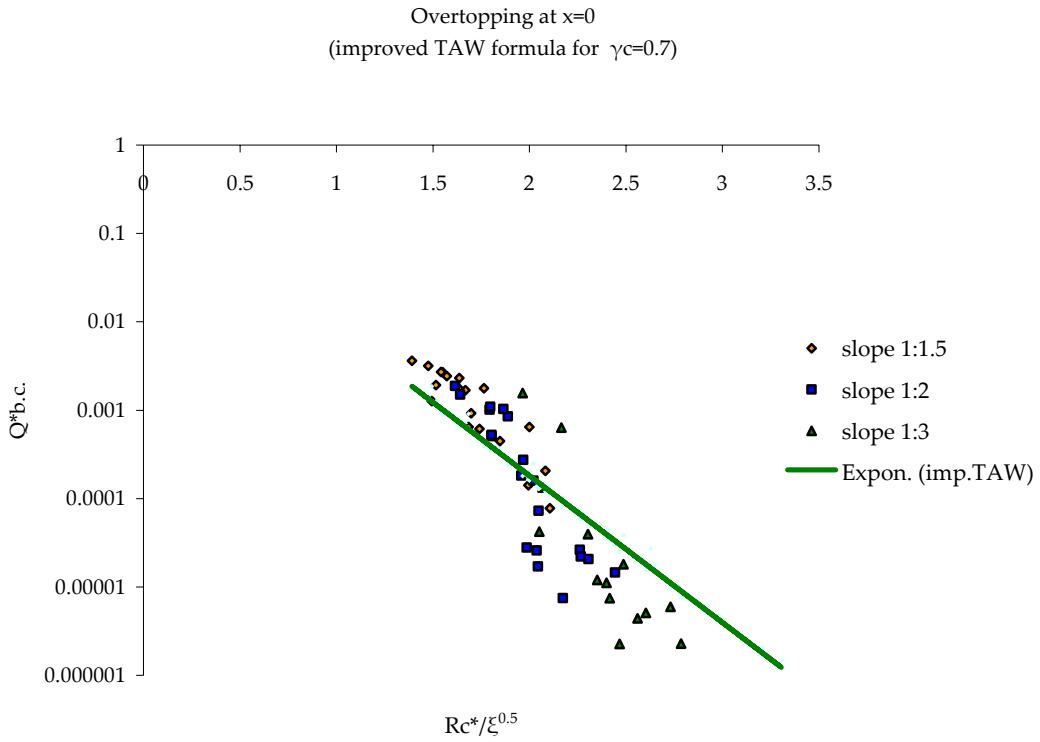

Fig. 4.13: Overtopping-directly-behind-the-crest

The spread in figure 4.13 is higher than the one detected in the case of total overtopping. This can be explained by the fact that the amounts of water collected at this point were much smaller and thus the results are more sensible to relative error. Especially the points which are placed lower in the graph correspond to very small overtopping discharges and so their deviation from the theoretical line should not be taken into serious consideration.

For slope angles steeper that 1:2, it is recommended the use of a slightly higher γ_c; values around 0.75-0.8 result in a more safe prediction.

Concluding, the overtopping-directly-behind-the-crest can be calculated with the improved TAW formula (equation 4.2-2) if an additional reduction factor is introduced:

$$\frac{Q}{\sqrt{gH_{m0}^3}} = (0.2 - 0.133 \cdot k) \cdot \left(\frac{\gamma_b \cdot \xi_0}{\sqrt{\tan a}} \right)^k \exp\left[-(2.6 - 2.15 \cdot k) \frac{R_c}{H_{m0}} \frac{1}{\gamma_f \cdot \gamma_b \cdot \gamma_\beta \cdot \gamma_v \cdot \xi_0^{\,k} \cdot \gamma_c} \right] \qquad \text{eq.4.3-1}$$

4.3.3 Comparison with existing formulae

Both methods do not calculate the discharge directly behind the crest but the ratio of the overtopping at that point over the total overtopping.

To compare the test measurements with the previously mentioned method, the data will be plotted against the dimensionless parameters introduced by each method.

4.3.3.1 Steenaard

For better understanding, the tests are sorted by wave steepness and the regression line for each steepness group is plotted.

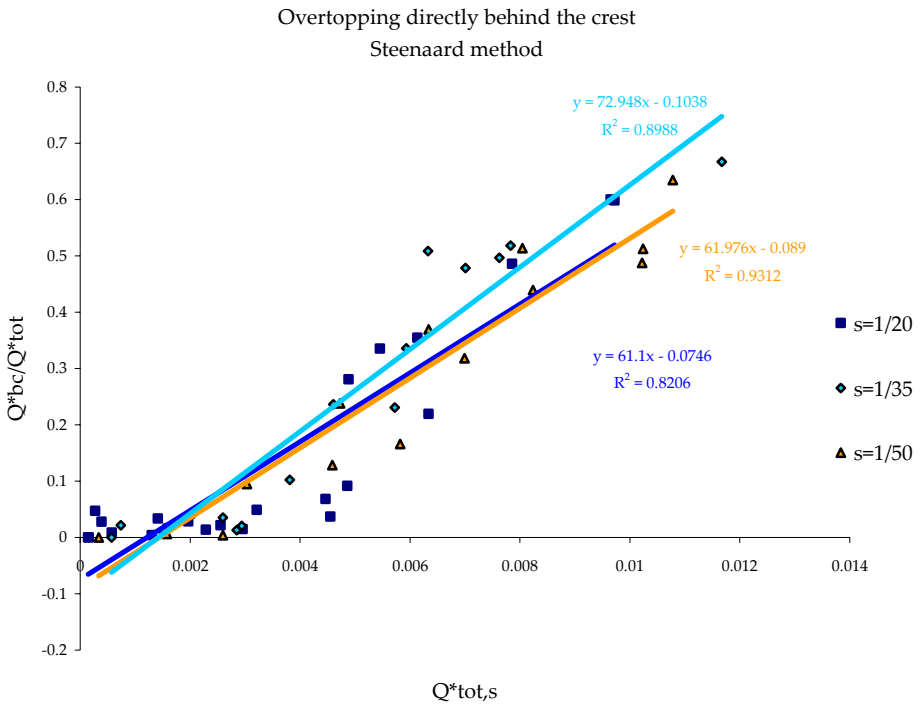

Fig. 4.14: Overtopping-directly-behind-the-crest (Steenaard's parameter)

From graph 4.14, it is can be easily observed that the three regression lines coincide (with very minor deviation). This means that using the Steenaard's parameter, the influence of wave steepness/period is trivial.

Analysing statistically the above graph, it can be noted that for longer waves, the scatter is smaller, there is a better convergence to the average trendline (higher correlation coefficients R^2). This can be explained by the fact that longer waves caused more overtopping and thus the measurements are expectedly more accurate.

For the test measurements of this research model, it can be deduced an average trendline using Steenaard's dimensionless $Q_{tot,S}^*$ parameter:

$$\frac{Q_{bc}}{Q_{tot}} = 64 \cdot Q_{tot,S}^{*} - 0.08 \qquad \text{eq.4.3-2}$$

The values of the constants may vary depending on the hydraulic and structural conditions of each case.

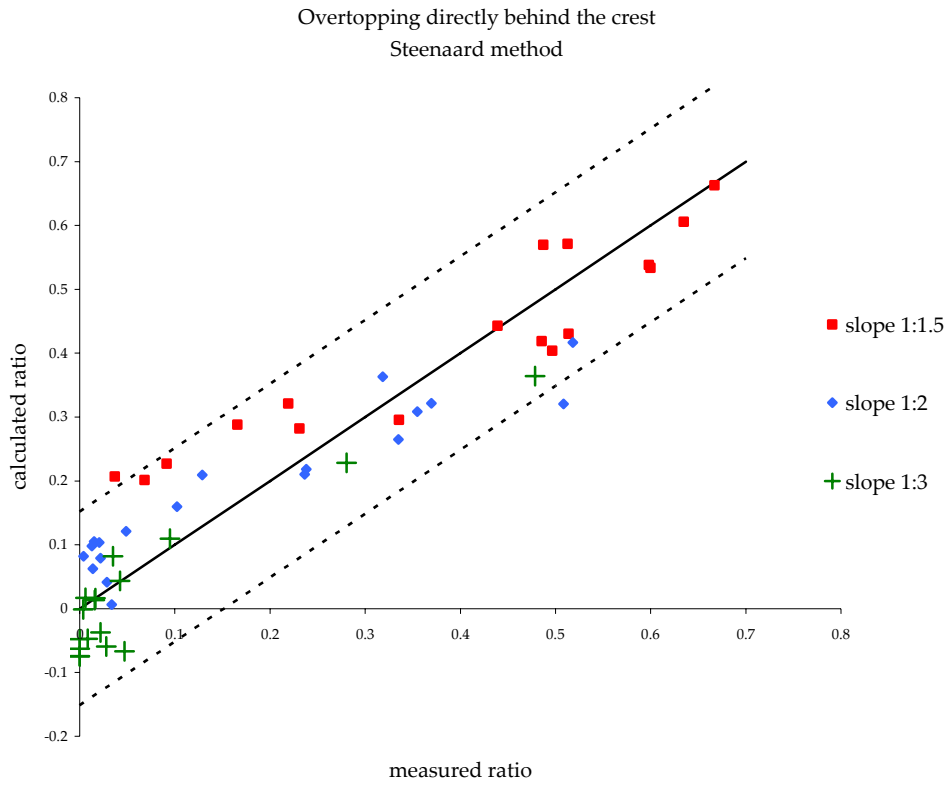

Fig. 4.15: Evaluation of prediction formula for overtopping-directly-behind-the-crest

Figure 4.15 presents an evaluation of the equation 4.3-1: the dashed lines are ±2σ (standard deviation). Performing a statistical error analysis, its accuracy can be determined. For this test series, the standard error is 2σ≈0.14. If the variables are considered to follow normal distribution, this means that 95.4% of the observations are between ±14% of the predicted value.

4.3.3.2 v.Kester

The measurements (ratio of overtopping behind the crest over total overtopping) now are plotted as a function of the dimensionless parameter H* introduced by v.Kester.

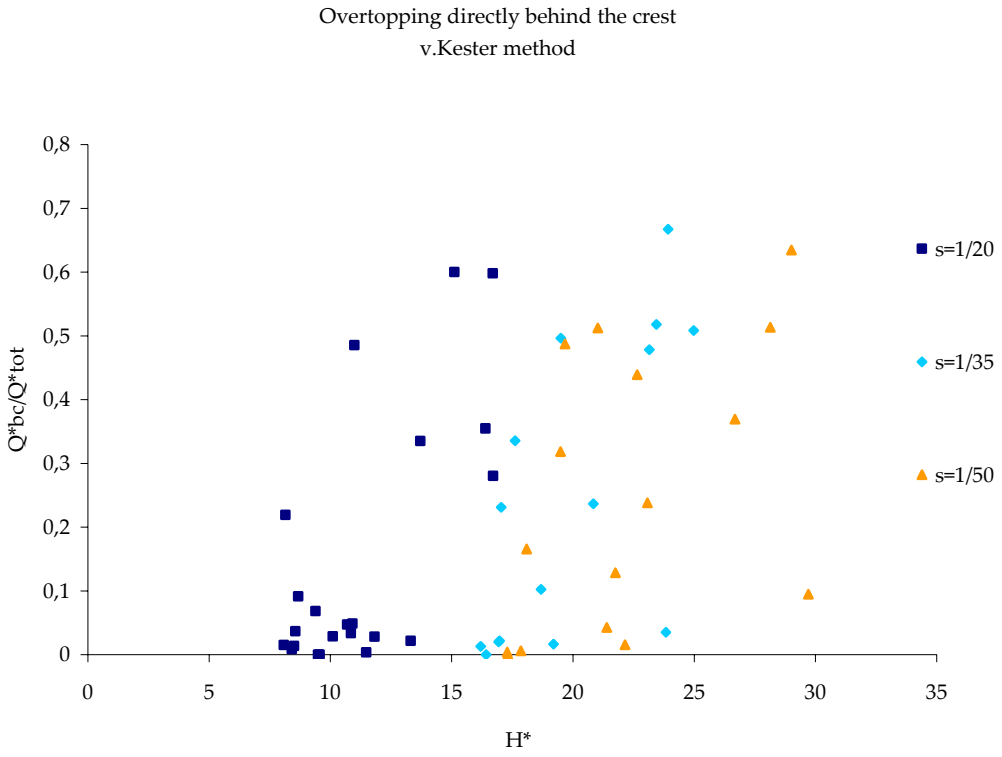

Fig. 4.16: Overtopping-directly-behind-the-crest (v.Kester parameter)

The data are again grouped according to wave period but no other dependency can be observed.

Apparently, for the findings of this research, this parameter does not apply; no correlation can be detected, the data are spread without creating any trend.

4.3.4 Conclusions

From the above presented analysis, the main conclusions that can be drawn are following:

- The ***discharge-directly-behind-the-crest*** follows the same trend as the total overtopping. This implies that it is governed by the same parameters.
- It can be predicted with reasonable accuracy using the ***improved TAW formula*** by introducing a new reduction factor γc (equation 4.3-1). For the conditions of this experimental research the value of γc=0.7.

$$\frac{Q}{\sqrt{gH_{m0}^3}} = (0.2 - 0.133 \cdot k) \cdot \left(\frac{\gamma_b \cdot \xi_0}{\sqrt{\tan a}} \right)^k \exp\left[-(2.6 - 2.15 \cdot k) \frac{R_c}{H_{m0}} \frac{1}{\gamma_f \cdot \gamma_b \cdot \gamma_\beta \cdot \gamma_v \cdot \xi_0^{\,k} \cdot \gamma_c} \right] \qquad \text{eq.4.3-1}$$

- ***Steenaard's*** parameter Q*tot,S seems also to describe adequately this overtopping discharge.
- ***v.Kester's*** parameter H* does not apply to the findings of this research.

4.4 Overtopping distribution behind the crest

4.4.1 General

For the overtopping distribution behind the crest (for rubble mound structures like the model of this research), there are developed to two methods: Juul Jensen's [11] and Besley's [02]. v.Kester [12] based on the second, proposed an different formula introducing more parameters. In his analysis, regular waves were tested.

Both the three methods are described in detail in the second Chapter (2.3.2). In this subchapter, just a brief review will be presented.

4.4.1.1 Juul Jensen

In this method, overtopping intensity $q(x)$ (m^3/s per meter width, per meter length) is used instead of overtopping discharge Q (m^3/s per meter width). According to the method, it is defined by the equation 2.3-5:

$$q(x) = q_0 \cdot 10^{-(x/\beta)} \qquad \text{eq.2.3-5}$$

Next, by integration, the discharge can be calculated:

$$Q = q_0 \cdot \beta / \ln 10 \qquad \text{eq.2.3-7}$$

According to this method, the main dominant parameter is the β which represents the distance for which the overspill intensity decreases by factor of 10.

4.4.1.2 Besley

Besley's method introduces a reduction factor which corresponds to the reduction (percentage) of total overtopping for certain point. Initially it was developed for the prediction of the overtopping discharge directly behind the crest. The proposed reduction factor is:

$$C_r = 3.06 \cdot \exp(-1.5 \cdot B / H_{m0}) \quad \text{with } C_r \le 1 \qquad \text{eq.2.3-3}$$

If instead of crest width B, a certain distance x is used, the reduction percentage can be found. The requested discharge is calculated multiplying the total overtopping with this factor.

4.4.1.3 v.Kester

v.Kester, based on the previous method, makes use of a reduction factor in the same way but he introduces more varying parameters on its formula. The reduction factor is calculated from equation 2.3-11.

$$C_r = \frac{Q^*_{over,x}}{Q^*_{over,0}} = e^{A\left(\frac{x}{H_s}\cdot\frac{1}{(H0T0)^n}\right)} \qquad \text{eq.2.3-11}$$

The main parameter of this factor is:

$$H0T0 = \frac{H_s}{R_c}\cdot T_s \cdot \sqrt{\frac{g}{R_c}} \qquad \text{eq.2.3-10}$$

In equation 2.3-11, the coefficient A and the power n depend on the permeability of the backfill.

The method uses the same idea as Besley but introduced 3 more primal parameters: the wave height, the wave period and the crest freeboard.

4.4.2 Result presentation

Since a correlation between the (improved) TAW formula and the test findings was found (with the use of reduction factor γ_c), the data collected for certain distances behind the crest will be presented again in the same way. The adjusted TAW formula (equation 4.3-1) is employed again and the data are plotted against $R_c^*/\sqrt{\xi}$.

For each point several values of γ_c were tested in order to find the one which fits better to the data and thus expresses the average trend in each graph.

For safety reasons, in order to cover all possible cases, higher values of the reduction factor can be selected. A 10% increase of γc represents a more conservative approach which is suggested in case of design.

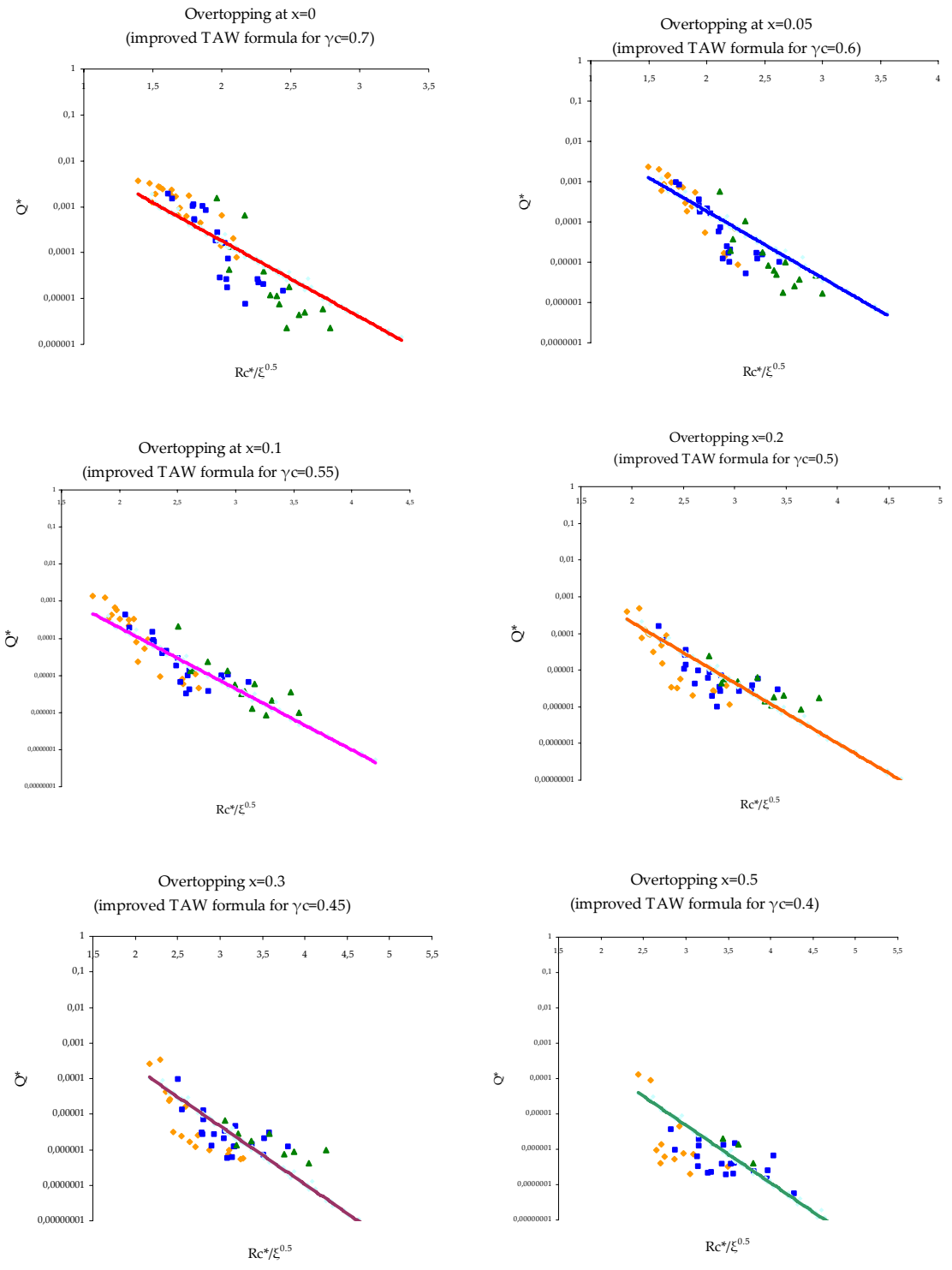

Fig. 4.17: Overtopping behind the crest

From the graphs of figure 4.17, it can be concluded that overtopping discharge tends to follow the TAW line (with the appropriate reduction factor γc at each point). The measured data do not

present considerable spread despite the fact that in those graphs, all the tests performed in this research are plotted.

The scatter that is detected is totally reasonable and is explained by the fact that very small quantities of water were collected at the further point. The amount of water collected in many of those cases was hardly measurable and so the corresponding discharges were almost trivial. Generally at the further points (x=0.2m and further), even a deviation in the order of 10 does not correspond to considerable error. For example, an average value of Q* for x=0.3 is in the order of magnitude of 10^{-6} which corresponds to overtopping discharge 0.015lt/s/m in real conditions (for an indicative wave height of 3m).

Apparently the whole process of overtopping distribution is dominated by the same factors and can be adequately predicted with the use of the adjusted TAW formula (equation 4.3-1 for k=0.5) by changing properly the reduction factor γc.

Consequently, in this way, the decline of the overtopping discharge is expressed with the change of the reduction factor γc. The variation of γc, based on the findings of this experiment, can be seen in the following figure.

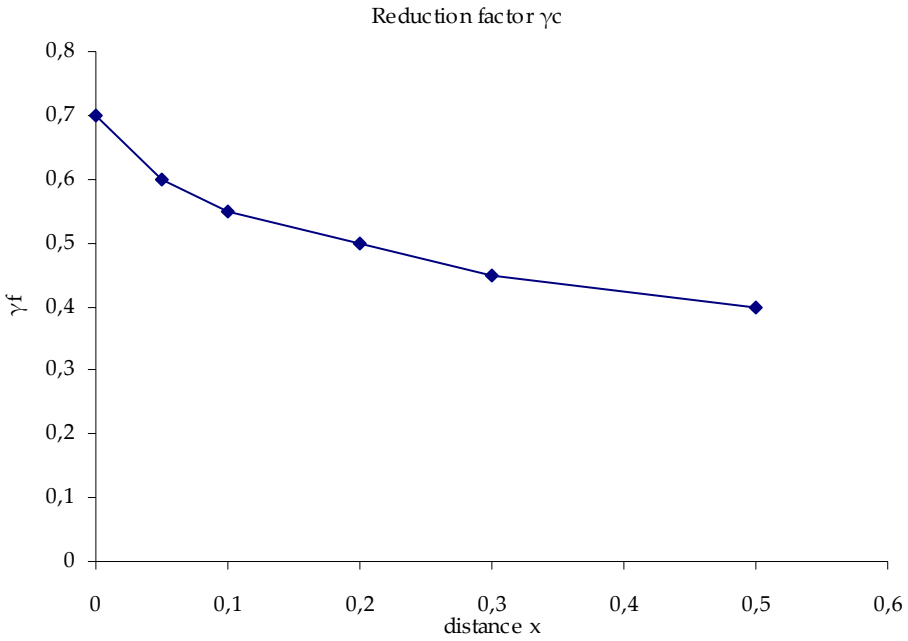

Fig. 4.18: Reduction factor γc

The decline of γc has an exponential shape. It seems also that there is a low limit (threshold) around 0.4 which is not (physically) reasonable: at some point the overtopping discharge becomes zero. However this happens because of the issue of the trivial amounts of water measured.

In order to create a formula to calculate the reduction factor (and thus the discharge at certain distance behind the crest) the proposed for design values of γc will be considered (10% higher values).

Additionally, since all the lengths in this research are in model scale (1:20), a dimensionless distance should be used in order to make applicable in real conditions the estimation of γc. For that reason, the γc values will be plotted against x/B (where B is the crest width, 0.28 in this model).

The crest width B is selected in this case because it is a physical dimension in the same direction as distance x (unlike crest freeboard R_c) and thus physically it is more related to it. In addition, it is constant for a given structure, unlike all hydraulic dimensions (wave height, length).

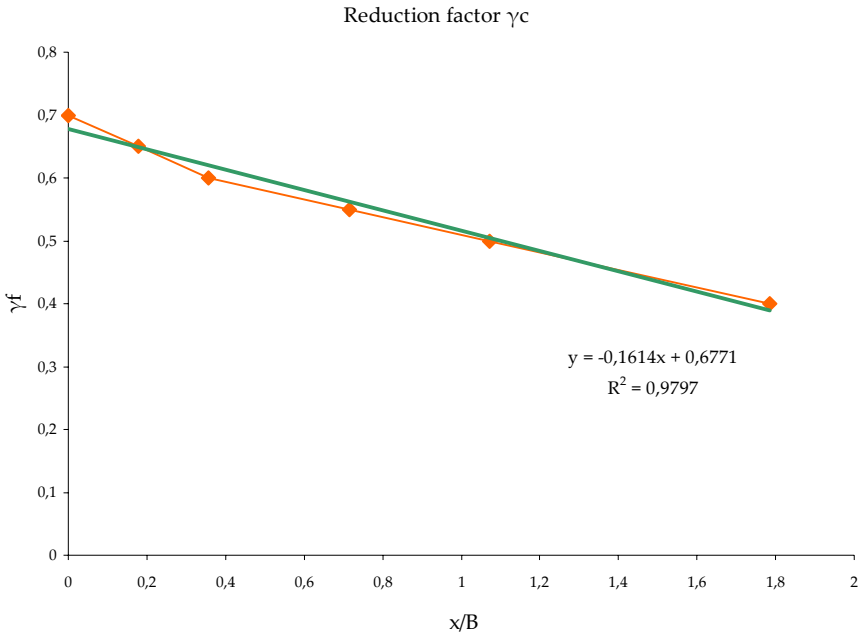

Fig. 4.19: Calculation of reduction factor γc

The decay of the reduction factor in this case is linear which is more reasonable since γc exists in the exponent of the overtopping formula (equation 4.3-1), and thus the decay of the overtopping will be exponential (which is expected).

From figure 4.19, it can be also noted that the regression line coincides exactly with the (estimated from the tests) γc values. This means that the equation of the regression line of figure 4.19 describes very well the decay of the reduction factor γ_c.

Thus the reduction factor γ_c for certain distance x behind the crest can be calculated with the use of the following formula:

$$\gamma_c = -0.164 \cdot \frac{x}{B} + 0.677 \qquad \text{eq.4.4-1}$$

Remark: the distance starts measuring from the point where the crest ends. This means that for x=0, the reduction factor for the overtopping-directly-behind-the-crest is calculated.

4.2.2.1 Evaluation of the method

In order to have an overview of the performed analysis and an evaluation of its outcome, the measured overtopping discharges will be compared with the corresponding theoretical predictions.

Figure 4.18 shows the dimensionless overtopping discharges at each point for the whole test record. These data are plotted against the corresponding calculated (dimensionless) overtopping discharges. For the later, the improved TAW formula (equation 4.3-1) is used for k=0.5. The reduction factor γc is calculated by equation 4.4-1.

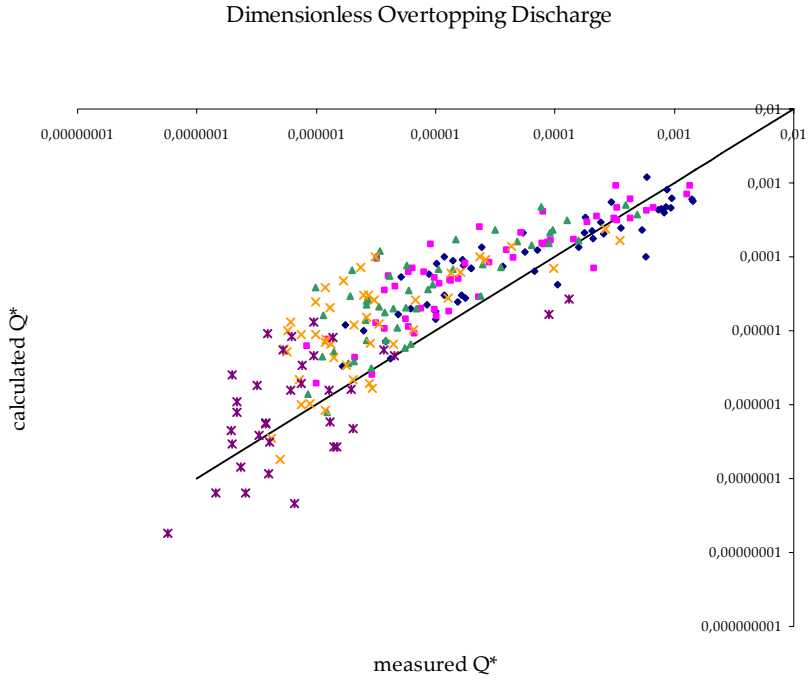

Fig. 4.20: Evaluation of the adjusted TAW formula

In the above graph, a spread can be detected mainly in for smaller overtopping values. The existence of this scatter is expected and it is explained in detail in the previous subchapter.

Another comment on this graph is that the most of the points are on the calculation side which means that the prediction formula slightly overestimates the majority of the cases. This is totally expected since conservative values of reduction factor γc are selected in order to be on the safe side in case of design. If the average values of γc are used, then the points move closer to the 1:1 line which means that the calculated values coincide with the measured.

Generally, from this figure, it can be concluded that the overtopping discharge for certain point behind the crest can be adequately predicted with the use of improved TAW formula with the introduction of the γc reduction factor.

4.4.3 Comparison with existing methods

4.4.3.1 Juul Jensen

Juul Jensen's method in order to predict the overtopping distribution behind the crest makes use of two main input parameters: the overtopping intensity directly behind the crest and the β value.

Concerning the first parameter, the method derives it from the total overtopping (equation 2.3-7). As it is shown in chapter 4.3, this is not correct as the overtopping-directly-behind-the-crest is not the same as the total. A consideration like this leads to considerable overestimation.

Thus, in this subchapter, the method will be investigated using the findings of this analysis. Thus the initial intensity q_0 will be calculated according to the method from equation 2.3-7 but using the Q_{bc} instead:

$$q_0 = Q_{b.c.} \cdot \ln 10 / \beta \qquad \text{eq.4.4-2}$$

The β number is used as it is defined in the method. According to the method, the ratio β/B* (for the definition of B* see 2.3.2.2) is constant and its value varies between 0.4-0.55 depending the ratio B/B* (crest width over B*). For this case, the lower β value is used.

The overtopping distribution at certain point behind the crest is calculated by integration of the corresponding intensity which is found from equation 2.3-5.

Since the amount of the test data is large and in order to avoid confusion, only some indicative distributions will be presented next. In that way, the predicted distribution can be compared with measured one. In the following graphs, the distribution predicted using the improved TAW formula with the proper adjustments is also plotted.

In the next figure, data from three tests with totally different characteristics are presented: first a steep wave (s=1/20=0.05) on 1:2 slope, next a longer wave (s=1/35≈0.03) on 1:1.5 slope and finally a swell on 1:3 slope.

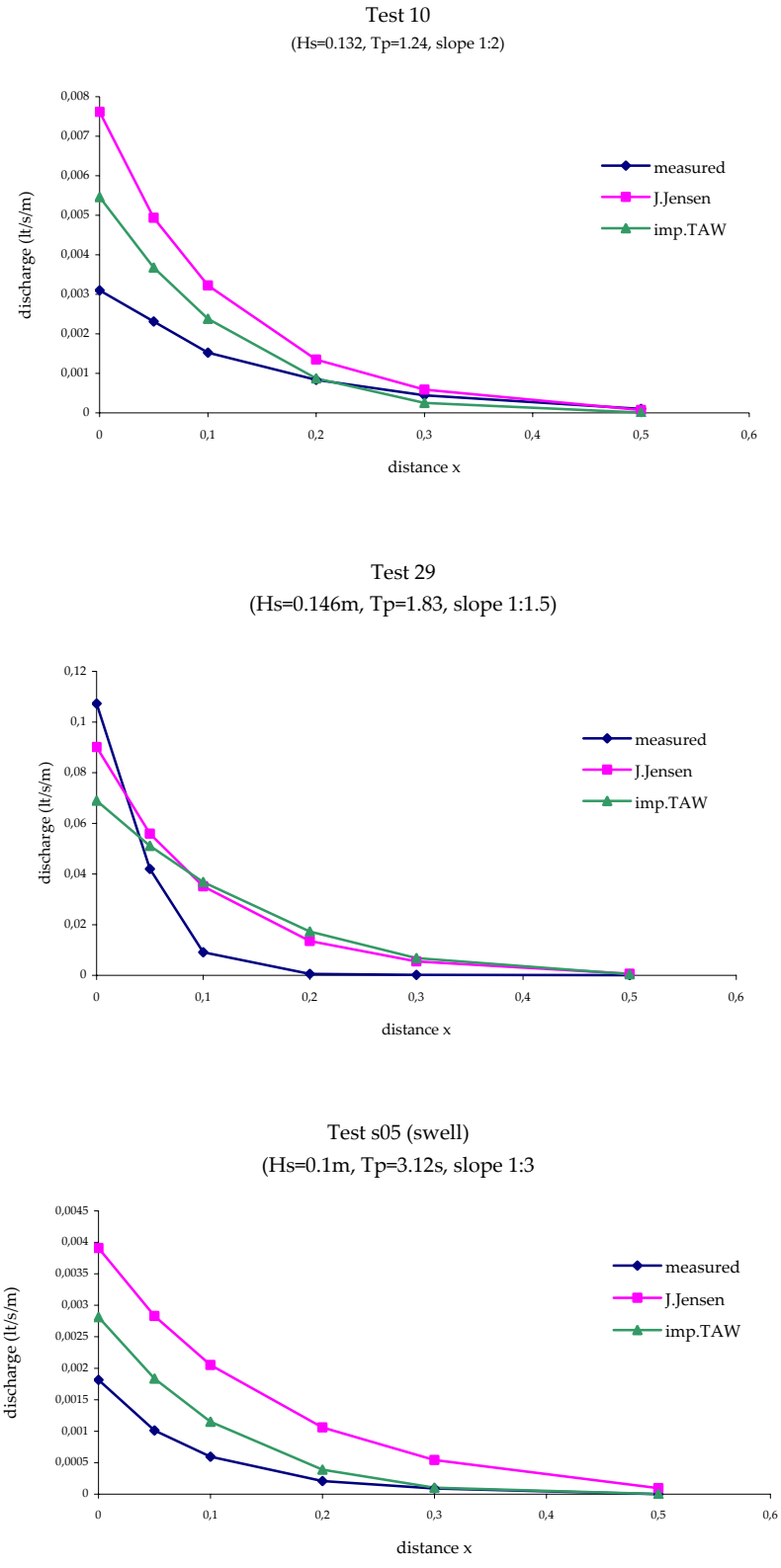

Fig. 4.21: Overtopping distribution (imp. TAW, Juul Jensen)

From the previous graphs, the first observation is that the Juul Jensen's method seems to work adequately: the shape of the measured distribution is generally the same with the predicted. There is a deviation but both values are in the same order of magnitude and their difference is not significant. Generally, this method tends to overestimate the discharge.

An important comment is that the consideration of improved TAW formula in the calculation of initial intensity q_0 is correct. If the total overtopping was used, the overestimation would be much higher resulting in different order of magnitude.

The distribution of this method and the corresponding prediction of the improved TAW coincide in general. The later seems to be closer to measurements and thus it can be considered more accurate.

The similarity of the two methods is reasonable if the initial dominating parameters are considered: the decay in Juul Jensen method is a function of β which derives from B*, a representative length closely related to crest width B. So, in fact, the primal parameter according to this method is the crest width.

The decay of improved TAW formula is determined by the reduction factor γc which again is a function of distance x over crest width B.

In the subchapter 4.3.3.1, where the Steenaard's method was analysed leading to positive results, the introduced dimensionless parameter $Q^*_{tot,s}$ was again a function only of the crest width.

Consequently, it seems that indeed that the crest width is a critical parameter in overtopping discharge at any point.

Next, an evaluation of Juul Jensen's method is presented. The graph is similar to figure 4.20, the predicted values are plotted against the measure. The line on the graph represents the perfect correlation between the two sets of data.

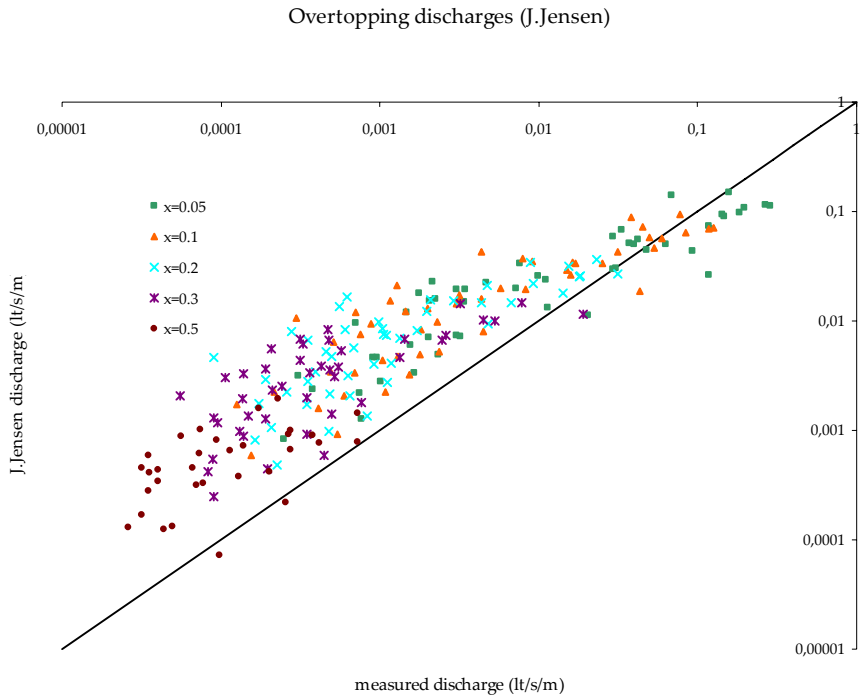

Fig. 4.22: Evaluation of Juul Jensen method

The prediction method seems to work quite adequately since the data follow in general the 1:1 line. The scatter is again higher in lower values which is expected and explained above.

4.4.3.2 Besley

In order to check the applicability of Besley's method [02], the test data are analysed according to the method: first the ratio of overtopping at certain point x Q(x) over the overtopping-directly-behind-the-crest $Q_{b.c.}$ is calculated and then this is plotted against a dimensionless distance x/Hs.

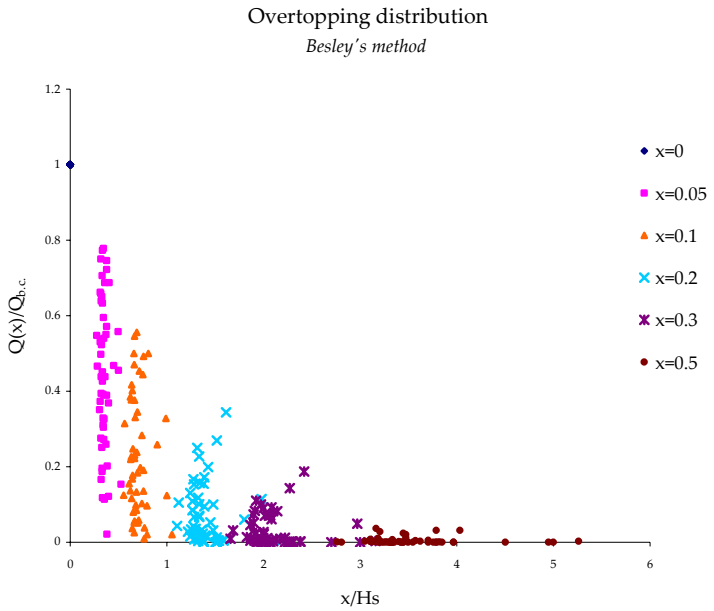

Fig. 4.23: Overtopping distribution according to Besley

According to the method, the data should follow an exponential trend. The data indeed follow such a trend individually but the spread in graph 4.23 is very large. No regression around a trendline can be detected and thus no correlation between the test data and Besley's predictions can be concluded.

A possible explanation of this deviation is that this method was originally developed just for estimating in an easy and simple way the overtopping-directly-behind-the-crest. Its purpose was not to predict the overtopping distribution.

4.4.3.3 v.Kester

v.Kester's method is analysed in the same way as Besley's. Again, the ratio of overtopping $Q(x)/Q_{b.c.}$ is calculated from test results (it is the same as previously) and next the dimensionless parameter H*T* of the method is found using the corresponding hydraulic conditions of each test.

The method makes distinction between permeable and impermeable backfill resulting in two different formulae. The only difference is the power to which the H*T* parameter is raised: for permeable backfill the value of the power is 3 and for impermeable is 6.

The values of these powers derived just by curve fitting of a specific experimental set and there is no physical explanation behind this choice. For that reason firstly the parameter H*T* (to the power 1) will be investigated in order to determine if there is any physical dependency between the parameter and the tests. Next, the parameter is raised to the power 3 since the backfill in this research was permeable.

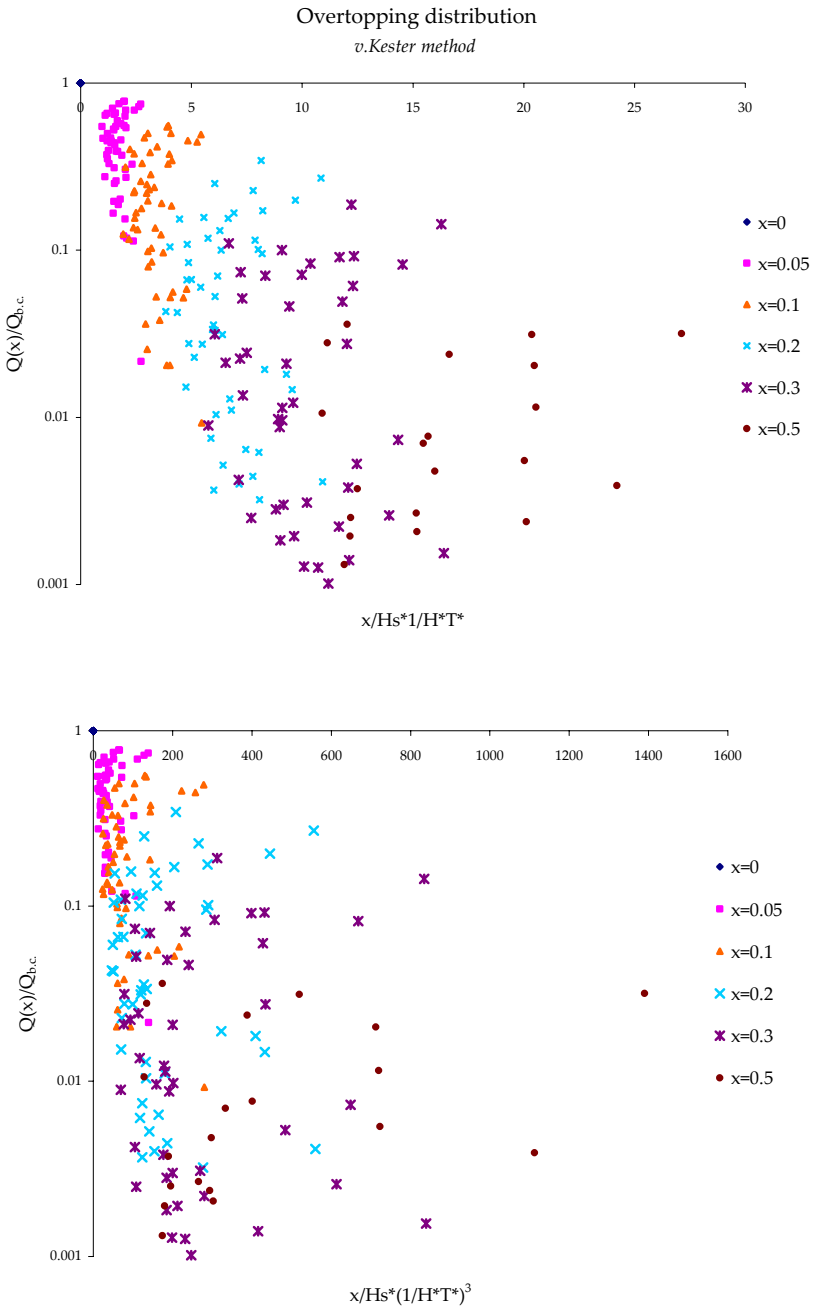

Fig. 4.24: Overtopping distribution according to v.Kester

From the above graphs, it is apparent that no correlation can be observed using the parameter that v.Kester proposed. There seems to be a very general (exponential) trend but the spread is too large to consider any dependency. The change of the power (from 1 to 3 which is suggested) seems to work indeed better but again the scatter in the graph is too large to draw any reliable conclusion.

The fact that there is no correlation of this method with the test results is not completely unexpected. The first reason that the measurements do not correspond to this method is the experimental set that was used. v.Kester ran separate tests to measure the total overtopping, the overtopping-directly-behind-the-crest and the overtopping at certain distance. This can be problematic because the test conditions may change from one test to another.

The other main reason of this deviation is that the whole method of v.Kester is based on regular waves while in this research, real sea-state conditions where tested (irregular waves). This difference is of critical importance since the whole process of overtopping distribution is considerably different in case of irregular waves.

In the first case (regular waves), practically only the overtopping per wave is measured; the sequence between 2 or 3 completely different waves can not be taken into account. For example, in the first case, if a wave with certain height and period "produces" X amount of overtopping, then it is concluded that all the waves with these characteristics will "produce" the same amount of overtopping.

In case of irregular waves, the same wave may produce much more overtopping at certain distance if it follows a larger one. This can happen in the first place just because of the interaction between the two consecutive waves: smaller waves can "jump" on top of larger waves (under certain hydrodynamic circumstances) transporting the water further on the backfill. Secondarily, this may be caused because the permeability of the core and backfill is not infinite. After two or three large waves which curry very large amounts of water, the surface may become instantly impermeable, "facilitating" the water to move again further on the backfill (since there is no infiltration).

Generally, in case of irregular waves, overtopping "evolves" spatially in a completely different way and thus the direct correlation of the two conditions is not safe and reliable and it may lead to significant differences.

For those reasons, v.Kester suggested that in case of irregular waves, instead of the significant wave height Hs which is equal to $H_{1/3}$, the $H_{1/1000}$ should be used. The transformation of $H_{1/1000}$ is achieved with use of a method developed by Battjes and Groenendijk [01]. The resulting graph is presented below.

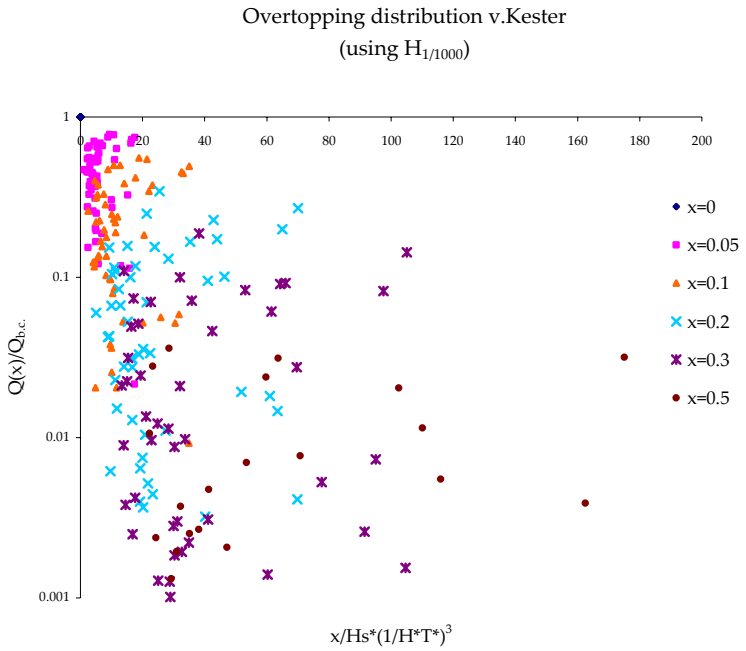

Fig. 4.25: Overtopping distribution using $H_{1/1000}$

Apparently, there is no significant difference with the use of different wave height. The spread still exists and again no correlation can be concluded. This means that v.Kester formula is not applicable to this model.

4.4.4 Conclusions

The main conclusions which are derived from the above analysis of the overtopping distribution behind the crest are the following:

- The distribution is dominated by the ***same parameters*** as the total overtopping and the overtopping-directly-behind-the-crest. TAW describes adequately the whole process.
- The overtopping discharge at certain distance can be calculated with the use of ***improved TAW formula*** (equation 4.3-1) using different reduction factors γc.

$$\frac{Q}{\sqrt{gH_{m0}^3}} = (0.2 - 0.133 \cdot k) \cdot \left(\frac{\gamma_b \cdot \xi_0}{\sqrt{\tan a}} \right)^k \exp\left[-(2.6 - 2.15 \cdot k) \frac{R_c}{H_{m0}} \frac{1}{\gamma_f \cdot \gamma_b \cdot \gamma_\beta \cdot \gamma_v \cdot \xi_0^{\,k} \cdot \gamma_c} \right] \qquad \text{eq.4.3-1}$$

- The decay is determined by the reduction factor γc which is calculated by the ***equation 4.4-1***. This formula gives conservative results and it is developed for design.

$$\gamma_c = -0.164 \cdot \frac{x}{B} + 0.677 \qquad \text{eq.4.4-1}$$

- The reduction factor γc is a function of ***crest width B***. Crest width is also the dominant parameter in Steenaard and Juul Jensen methods.
- ***Juul Jensen*** method describes adequately the physics of the process. If the overtopping-behind-the-crest calculated with improved TAW id used as an input (instead of the total overtopping), then it can also predict adequately the discharge at certain point.
- Juul Jensen tends to ***overestimate*** slightly the discharge compared to improved TAW formula. Generally, the two methods coincide.
- ***Besley*** and ***v.Kester*** methods do not apply to this model.

5. CONCLUSIONS & RECOMMENDATIONS

5.1. Conclusions

The basic idea which can be concluded from the whole research and which constitutes the final outcome of this thesis is that overtopping discharge can be predicted at any point with the use of an improved version of TAW formula:

$$\frac{Q}{\sqrt{gH_{m0}^3}} = (0.2 - 0.133 \cdot k) \cdot \left(\frac{\gamma_b \cdot \xi_0}{\sqrt{\tan a}} \right)^k \exp\left[-(2.6 - 2.15 \cdot k) \frac{R_c}{H_{m0}} \frac{1}{\gamma_f \cdot \gamma_b \cdot \gamma_\beta \cdot \gamma_v \cdot \xi_0^{\,k} \cdot \gamma_c} \right]$$

The proposed value of k is 0.5. The reduction factor γc is a function of distance x (x=0 is the landward end of the crest) and crest width B and can be calculated by the following formula:

$$\gamma_c = -0.164 \cdot \frac{x}{B} + 0.677$$

The detailed conclusions of the analysis are summarised in the end of each subchapter of Chapter 4. The most important of them are:

- The suggestion of TAW/EurOtop that the (permeable) crest should not be taken into account is not correct. Instead, in case of totally permeable crest, a $0.5 \cdot D_{n50}$ reduction of crest height is suggested.
- Steenaard's method (its parameter, not the original formula) seems to work and can be applied after adjustments.
- Juul Jensen's method (slightly adjusted) seems to apply also and predict within reasonable accuracy the distribution of overtopping.
- v.Kester's findings do not apply on this research.
- The shape of the decay is mainly characterised by crest width B.

5.2 Recommendations

The results of this research lead to some important recommendations which are presented below.

5.2.1 Validation of the method

In this experimental research, the design of the scale model and the selection of parameters were conducted in such a way in order to cover a wide range of possible cases and thus to develop an applicable prediction formula which would be valid under different circumstances and not only for special occasions. In addition, the model was designed in a manner that the whole overtopping process would be simulated as realistically as possible.

However, since the proposed outcome seems to improve a valid theoretical formula which has been developed after a significant amount of previous research, it is recommended to apply the findings of this thesis to other overtopping tests in order to validate its correctness.

A possible idea would be to analyse the findings of this experiment with Neural Network tool which is a prediction method based exclusively on physical modelling results. Neural Network collected a series of different experiments to create a database (CLASH database) which is used as a basis to predict overtopping. In that way, a correlation with other test results can be achieved leading to safer conclusions over the applicability of the suggested formula.

5.2.2 Influencing parameters

This recommendation comes as a follow-up of the previous. As mentioned above, in this research, many varying parameters were taken into account in order to cover many different cases. However, there are several other factors that were not considered in this model and may influence the prediction of overtopping distribution. Such parameters are:

- Oblique waves
- Wind action
- Berm
- Crest width
- Permeability (of structure and backfill)
- Wave spectrum type
- Armour (type and size)

Most of these parameters are analysed and introduced in TAW formula. Since the proposed method is based on TAW, it is recommended to investigate if the way that they are introduced in TAW applies also in the improved version. In that way, all the research on those issues may be introduced to this formula without analysing again everything from the beginning.

For the above listed factors, the parameters that have not been analysed yet properly and influence considerably the distribution of overtopping, is the permeability of the backfill and the crest width. Especially the later seems to have critical impact on distribution. According to

existing literature (including this research), it is one of the dominant factors. Thus, it is suggested a further (experimental) investigation on this issue.

5.2.3 Scale and model effects

In the entire research on overtopping, a major issue which concerns the accuracy of the final outcome is the scale and model effects. Scaling process results in scale models which simulate adequately the reality. However there are phenomena (viscous forces) which may affect the entire process, that are not considered properly on scaling process.

This the case for model effects also. In the analysis performed in this research, the main issue concerning the accuracy of the method was the small quantities of water measured at the further sectors. This consists of model effect and further research should be conducted to neutralise the impact of such effects.

6. REFERENCES

[01] BATTJES, J.; GROENENDIJK, H. [2000], "Wave height distributions on shallow foreshores"
Coastal Engineering, Vol 40, pp.161-182

[02] BESLEY, P. [1999], "Overtopping of seawalls: design and assessment manual"
R&D Technical Report No.W178, Environment Agency, Bristol

[03] BRUCE, T; V.D.MEER, J.W.; FRANCO, L; PEARSON, J.M. [2009] "Overtopping performance of different armour units for rubble mound breakwaters"
Coastal Engineering, vol.56, pp.166-179

[04] CIRIA;CUR;CETMEF [2007] "The Rock Manual. The use of rock in hydraulic engineering (2nd edition)"
C683, CIRIA, London

[05] D'ANGREMOND et al. [2008] "Breakwaters and Closure Dams, 2nd edition"
VSSD,Delft

[06] EUROTOP [2007], "Wave Overtopping of sea defences and related structures: Assessment manual"

[07] GODA, Y. [1985], "Random seas and design of maritime structures"
University of Tokio Press, ISBN 0-86008-369-1

[08] HOLTHUIJSEN, L.H. [2006] "Waves in Oceanic and Coastal Waters"
Delft University of Technology, UNESCO-IHE, Delft

[09] HOUGHTALEN, R.J.; OSMAN AKAN, A.; HWANG, N.H.C. [2010], "Fundamentals of Hydraulic Engineering Systems – 4th edition"
Prentice Hall, ISBN 978-0-13-601638-0

[10] HUGHES, S. [1993], "Physical models and laboratory techniques in coastal engineering"
World Scientific, ISBN 981-02-1540-1

[11] JUUL JENSEN, O. [1984], "A monograph on rubble mount breakwaters"
Danish Hydraulic Institute, Horsholm

[12] v.KESTER, D. [2009], "Spatial distribution of wave overtopping"
Delft University of Technology, Faculty of Civil Engineering and Geosiences, Delft

[13] LYKKE ANDERSEN, T.; BURCHARTH, H.F. [2006], "Hydraulic response on rubble mound breakwaters"
Aalborg University, Aalborg

[14] MOHAN, K.R.; MAGOON, O.; PIRRELLO, M. [2003], "Advances in coastal structure design"
ASCE Publication, ISBN 0-7844-0689-8

[15] OWEN, M. W. [1980)] "Design of seawalls allowing for wave overtopping"
HR Wallingford , 924 (report EX)

[16] STEENAARD, J. [2002], "Verdeling van overslaand water over een golfbreker"
Delft University of Technology, Faculty of Civil Engineering and Geosiences, Delft

[17] v. d. MEER, J.W. [1988b] "Rock slopes and gravel beaches under wave attack"
PhD thesis, Delft University of Technology, Delft

APPENDIX

A.1 Physical model

A.1.1 Model drawings

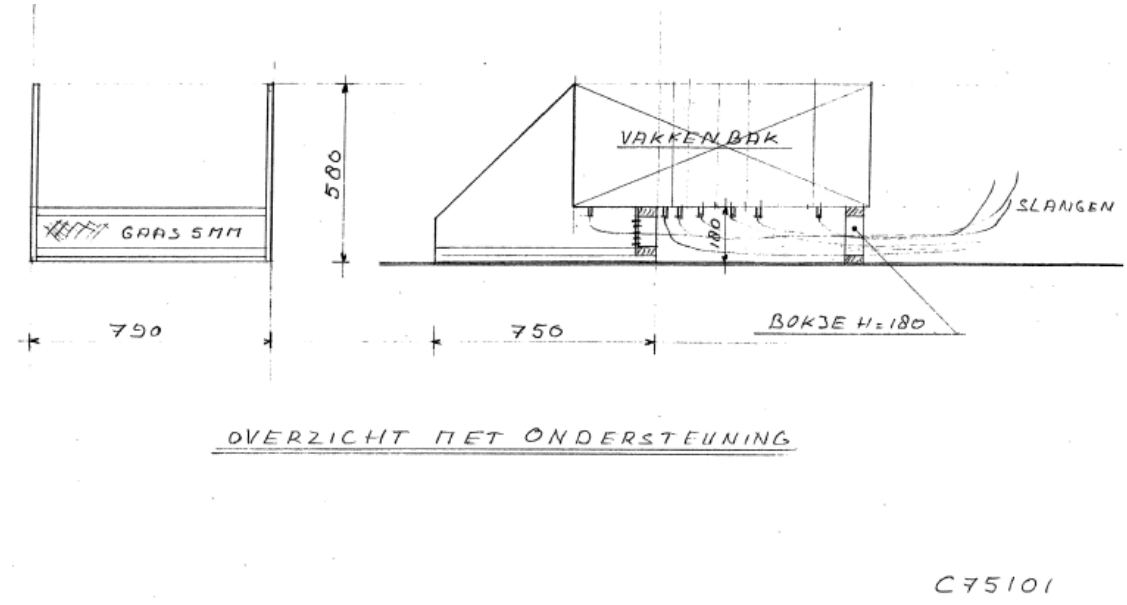

Fig. A.1: General view, height of the top of the splitting tank = 580 mm above the bottom of the flume.

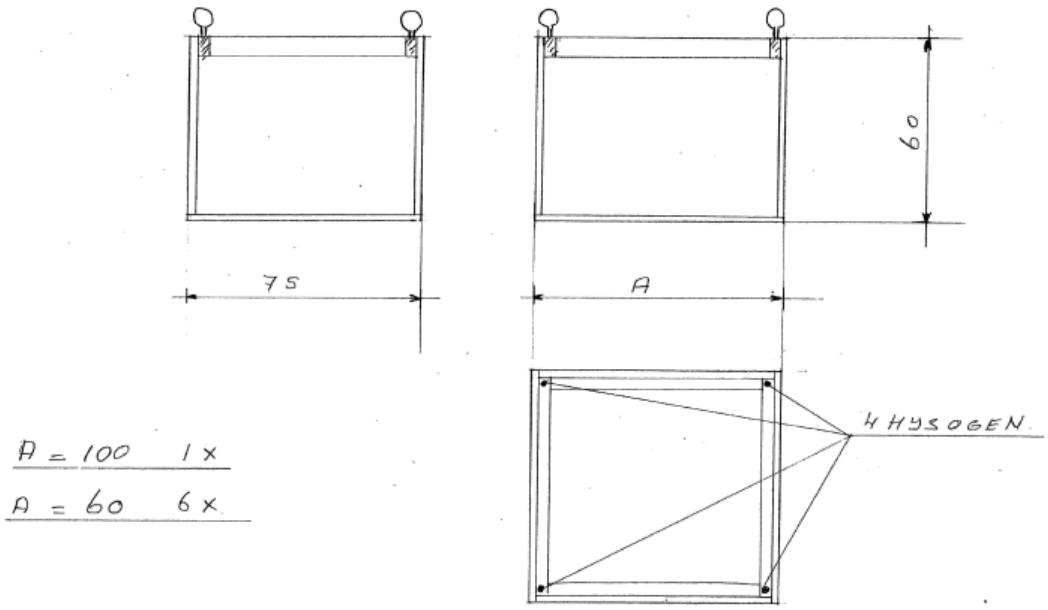

Fig. A.2: Collecting (floating) tanks

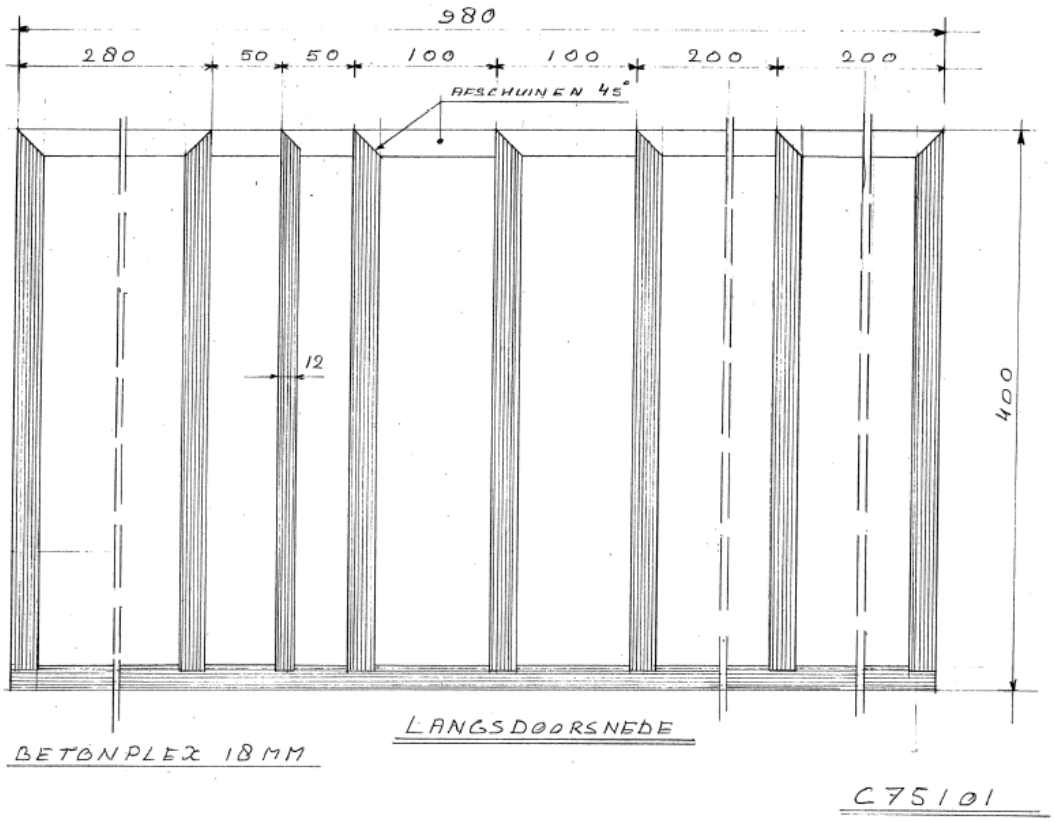

Fig. A.3: Splitting tank: cut in the length direction

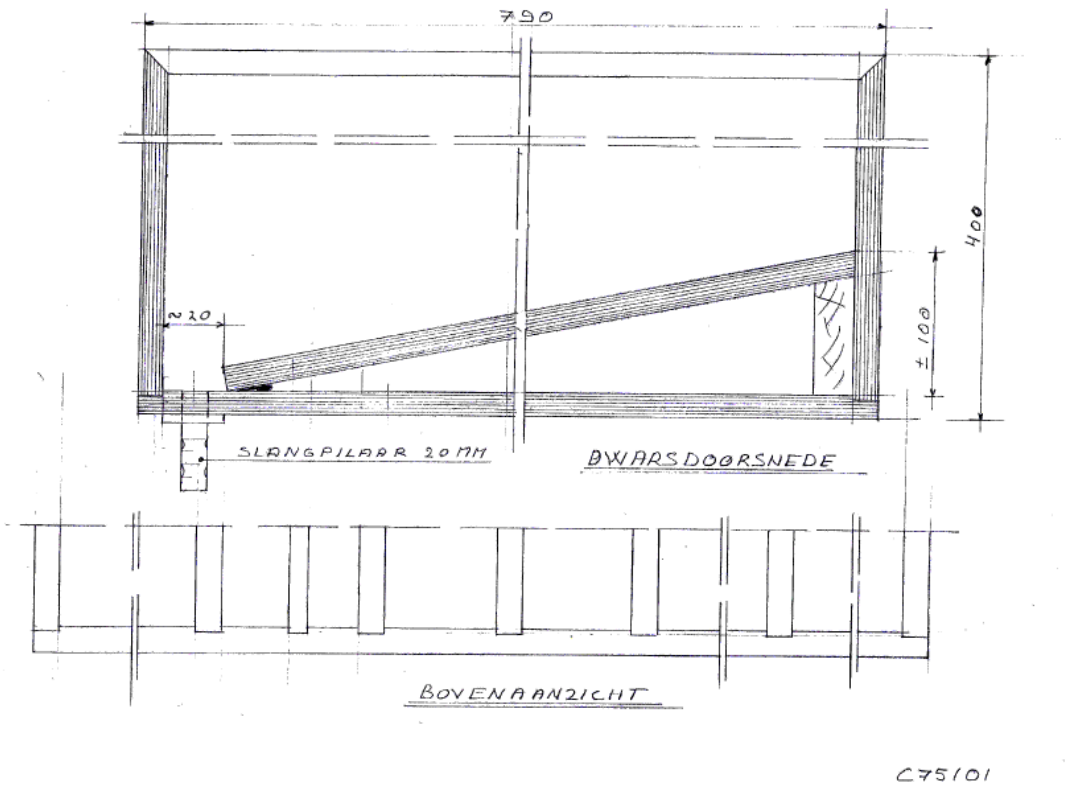

Fig. A.4: Splitting tank: cut in the width direction & view from above

A.1.2 Photos

A.3 Measurement data

A.3.1 Initial measurements

A.3.1.1 Slope 1:2

Volumes (lt)												
test	0	0,05	0,1	0,2	0,3	0,5	0,7	Total	duration (s)	Hs (cm)	Tp (sec)	Depth
t010	206,2	0,8	0,8	0,7	0,4	0,35	0,1	0,000206	1270	13,2	1,24	0,54
t004	184,4	0,8	0,6	0,65	0,3	0,2	0,01	0,000174	1340	14	1,32	0,52
t019b	184,7	2	1,4	1,5	0,4	0,12	0,03	0,000166	1430	15	1,39	0,52
t007	286,2	10,7	1,3	1,3	0,5	0,6	0,3	0,000255	1475	14,4	1,38	0,54
t013b	292,7	2,2	1,8	1,65	0,55	0,25	0,05	0,000240	1560	16,1	1,54	0,52
t019	125,1	2	0,85	0,75	0,35	0,35	0,05	0,000112	1440	14,4	1,47	0,52
t013	386	158	26,2	8,1	1,55	0,55	0,05	0,000465	1560	15,1	1,51	0,54
t011	454,5	187,2	42,8	17,3	1,85	0,6	0,15	0,000534	1650	15,3	1,64	0,54
t017	344,2	4,1	1,4	1,15	0,35	0,1	0,05	0,000248	1770	15	1,8	0,52
t014b	378,6	177,1	165,8	32	13,3	3,25	0,25	0,000708	1360	18,1	1,99	0,52
t005	321,2	1,7	1,5	0,35	0,35	0,2	0,1	0,000229	1780	14,5	1,79	0,52
t020b	512,9	103,1	31,1	20,3	2,25	1,75	0,4	0,000444	1890	16,4	1,91	0,52
t008	406,5	219,6	118,6	61,9	14,4	21,6	0,85	0,000715	1475	15,8	1,93	0,54
t020	424,1	33,3	10,3	3,15	1,05	0,45	0,1	0,000312	1890	14,7	1,91	0,52
t018	557,5	105,6	39,5	17,6	7,4	3,6	0,65	0,000424	2160	15,6	2,06	0,52
t012b	508,8	189,7	39	8,1	0,65	0,25	0,05	0,000476	1960	13	1,94	0,54
t003	257,5	0,3	0,15	0,15	0,15	0,25	0,05	0,000165	1960	12,4	2	0,52
t006	498,2	54,5	11,5	5,25	1,4	0,55	0,35	0,000331	2160	13,5	2,15	0,52
t021b	580,8	228,4	66,9	37,4	6,95	0,75	0,1	0,000514	2240	14,6	2,29	0,52
s002	329,9	17,8	2,8	0,3	0,05	0,03	0,001	0,000244	1800	9,5	3,45	0,52
z010	38,9	0,54	0,31	0,31	0,18	0,11	0,06	0,000039	1300	13,4	1,27	0,54
z004	31,7	0,67	0,516	0,503	0,172	0,239	0	0,000031	1350	14,3	1,32	0,52
z019b	46,6	1,31	1,16	0,98	0,23	0	0	0,000044	1420	15,1	1,41	0,52
z007	75	1	0,63	0,56	0	0	0	0,000062	1550	14,7	1,44	0,54
z013	154,6	5,14	3,8	3,59	1,25	0,45	0,21	0,000135	1570	15,4	1,5	0,54
z013b	75	2,11	1,97	2,25	0,82	0,46	0	0,000066	1570	*15,8*	1,54	0,52
z019	46,5	0,86	0,76	0,87	0,33	0,24	0,09	0,000042	1480	14,7	1,5	0,52
z011	180,2	3,02	3,97	3,5	1,28	0,49	0,44	0,000145	1660	15,5	1,71	0,54
z017	84	2,51	1,8	2,03	0,52	0,38	0,153	0,000064	1780	15,3	1,8	0,52
z005	68,7	1,79	1,49	1,3	0,41	0,23	0	0,000052	1780	14,7	1,8	0,52
z008	256,3	13,6	11,8	14,7	4,18	5,1	0,31	0,000260	1470	16,2	1,91	0,54

z020b	157,7	6	4,24	4,6	1,38	0,45	0,097	0,000115	1895	15,5	1,91	0,52
z014b	223,1	10,5	10,9	14,5	4,4	2,08	0,34	0,000244	1360	17,2	2,03	0,52
z020	134,9	3,43	2,88	2,52	0,67	0,13	0,72	0,000096	1890	14,9	1,91	0,52
z012b	162,4	4,5	3,14	1,97	0,5	0,38	0,19	0,000111	1956	13,5	2,03	0,54
z018	218,4	10,17	10,2	17	5,41	4,22	1,04	0,000154	2165	15,1	2,17	0,52
z003	46	1,38	0,86	0,41	0,28	0,3	0	0,000031	1960	12,7	2,03	0,52
z006	145,4	6,84	6,72	7	2,94	1,57	0,33	0,000099	2160	13,8	2,17	0,52
z021b	363,5	21,6	18,9	20,6	8,17	4,75	0,51	0,000242	2260	15,8	2,33	0,52
sz002	37	0,14	0,07	0,1	0,12	0,18	0	0,000026	1800	9	3,46	0,52

A.3.1.2 Slope 1:1.5

test	0	0,05	0,1	0,2	0,3	0,5	0,7	Total	duration (s)	Hs (cm)	Tp (sec)	Depth
t043	387,7	25,1	1,75	1,05	0,4	0,15	0	0,000377	1380	15	1,34	0,52
t028	383,3	26	10,6	1,3	0,6	0,1	0	0,000382	1380	14,3	1,32	0,52
t040	356,1	12,1	0,75	0,6	0,1	0,1	0	0,000350	1320	14,1	1,32	0,52
t031	378,9	249,1	90,3	17,5	0,65	0,05	0,05	0,000631	1460	14,5	1,38	0,54
t037	457,1	321,8	212,7	127,5	16,3	6,35	0,35	0,000898	1590	16	1,54	0,54
t035	461,3	327,5	189,5	145,2	18,5	5,9	0,05	0,000854	1680	15,4	1,65	0,54
t041	484,1	196,7	41,7	5,35	0,45	0,25	0,2	0,000506	1800	15,1	1,83	0,52
t029	514	94	47,3	12,35	0,5	0,2	0	0,000464	1800	14,6	1,83	0,52
t044b	561,1	311,2	144,1	83	15,2	0	0	0,000676	2060	15,5	1,9	0,52
t032	388,7	266,3	218,6	209,4	27	29,5	28,1	0,001065	1370	15,8	1,95	0,54
t036	556,5	358	148,6	71,9	6,8	0,3	0	0,000714	2000	13,2	2	0,54
t036b	465,9	279,8	120,6	40,1	2,4	0,05	0	0,000664	1710	12,6	1,98	0,54
t027	454,5	79,3	9,1	1,45	0,2	0,2	0	0,000378	1800	12,6	2,03	0,52
t030	597,3	262,7	113	67,5	20,2	3,25	1,25	0,000614	2170	13,8	2,17	0,52
t045	524,8	329	217,1	226,1	39,7	74,8	25,4	0,000966	1860	15,6	2,31	0,52
t042	573,3	332,8	138,5	94,1	26,7	13,3	0,3	0,000679	2170	15	2,32	0,52
s004	387,9	50,1	30,5	11,4	0	0	0	0,000333	1800	10	3,45	0,52
s003	580,3	131,1	51,6	48,9	14,8	0	0	0,000492	2100	11,1	3,75	0,52
p043	0	247,3	44,6	3	0,6	0	0	0,000270	1370	14,9	1,34	0,52
p040	0	198,4	7,5	1,5	0,6	0	0	0,000194	1340	14	1,31	0,52
p041	0	359,8	164,4	271,5	1,32	0	0	0,000553	1800	15,2	1,83	0,52
p044	0	273,8	221,8	226,8	20,2	25,5	12,1	0,000707	1380	17,2	2	0,52
p044b	0	400	220,5	107	36	27,4	9,95	0,000470	2130	15,4	1,91	0,52
z031	161,4	5,9	5,7	5,81	1,87	0,95	0,68	0,000157	1450	14,6	1,43	0,54
z2037	340,5	11	12,2	12,9	4,06	0	0	0,000238	2000	15,2	1,46	0,54
z031	167,1	4,8	4,58	5,12	1,56	0,71	0,07	0,000160	1440	14,5	1,44	0,54
z037	121,2	3,2	2,77	3,03	1,39	0	0	0,000105	1570	15,6	1,54	0,52
z3037	107,8	3,7	4,07	4,23	1,48	0,72	0,13	0,000080	1920	14,8	1,5	0,52

z2035	322,5	14,3	11,1	12,4	3,99	0,25	0	0,000271	1680	15,3	1,66	0,54
z032	378,7	104,9	63,6	61,8	15	6,1	1	0,000387	2040	16	1,96	0,54
z038	291,1	40,1	16,9	11,01	1,81	0	0	0,000376	1200	16,9	2,03	0,52
z2038	301,1	46,8	21,7	17,6	5,01	1,74	0,18	0,000394	1250	16,9	2,03	0,52
z2032	527,3	113,2	65,8	76,8	13,86	0	0	0,000500	1993	15,9	1,97	0,54
z2036	314,8	11	7,65	4,34	0,95	0,2	0	0,000212	2000	13,5	1,97	0,54

A.3.1.3 Slope 1:3

test	0	0,05	0,1	0,2	0,3	0,5	0,7	Total	duration (s)	Hs (cm)	Tp (sec)	Depth
t052	12,3	0	0	0	0	0	0	0,000013	1220	14,4	1,38	0,52
t064	12,8	0	0	0	0	0	0	0,000012	1390	14,3	1,38	0,52
t067	24,3	0,25	0,25	0,35	0,15	0,2	0	0,000023	1390	15	1,43	0,52
t055	120	0,1	0,1	0,25	0	0	0	0,000105	1440	14,5	1,41	0,54
t061	41,8	0,3	0,4	0,3	0,1	0,1	0	0,000035	1520	15,7	1,47	0,52
t059	410,4	133,4	20,8	4,6	0,75	0,35	0,1	0,000437	1630	15,6	1,64	0,54
t065	89,8	0,7	0,3	0,5	0,3	0,2	0	0,000064	1800	15,2	1,79	0,52
t062	262,7	5,1	1,45	2	0,7	0,3	0	0,000284	1200	17,8	1,96	0,52
t053	67,6	0	0	0	0	0	0	0,000047	1800	14,7	1,79	0,52
t056	521,7	300,3	113	58,1	5,26	1,39	0,63	0,000658	1900	16,1	1,9	0,54
t068	152,9	0,75	0,6	0,9	0,3	0	0	0,000134	1450	15,1	1,91	0,52
t066	272,5	6,65	1,45	2,1	1,05	0,85	0	0,000167	2130	14,9	2,03	0,52
t060	173,7	0,45	0,4	0,2	0	0	0	0,000110	1985	13,2	1,97	0,52
t051	30,6	0	0	0	0	0	0	0,000021	1800	12,3	2,01	0,52
t069	450,6	34,2	7,5	3,5	1	0,5	0,5	0,000274	2270	15,7	2,33	0,52
t054	187,2	1,35	0,8	0,55	0,3	0	0	0,000110	2160	13,5	2,17	0,52
s005	161,3	1,35	0,7	0,65	0,2	0,15	0	0,000098	2100	10,1	3,12	0,52
s006	56,8	0	0	0	0	0	0	0,000059	1200	8,4	3,46	0,52
p067	0	7	0,3	0,3	0,2	0,1	0	0,000007	1430	15,1	1,43	0,52
p062	0	107,8	10,1	2,5	0,55	0,1	0	0,000126	1200	17	1,97	0,52
p066	0	110,3	10	3,75	0,75	0,75	0,15	0,000074	2120	14,9	2,03	0,52
z055	19,7	0,1	0,11	0,1	0	0	0	0,000017	1450	14,5	1,38	0,54
z062	48,6	1,7	1,39	1,79	0,6	0	0	0,000056	1200	16,9	1,65	0,52
z056	137,1	2,99	2,45	2,85	0,72	0,12	0,15	0,000092	1980	15,8	1,91	0,54
z068	29	0,9	0,7	1,11	0,56	0	0	0,000028	1460	15,6	1,91	0,52
z059	48,8	0,45	0,3	0,3	0,15	0	0	0,000031	2010	13,3	1,96	0,54
z066	56,5	2,32	1,87	2,48	0,96	0	0	0,000037	2160	15	2,17	0,52
z060	16,2	0,25	0,19	0,35	0,22	0	0	0,000011	1980	12,9	2,03	0,52
z051	9,6	0,06	0,05	0,09	0	0	0	0,000007	1800	12,4	2,03	0,52
z069	78,9	0,25	1,52	1,96	1,01	0	0	0,000046	2270	15,7	2,32	0,52
z054	29,9	1,03	0,81	0,78	0,29	0	0	0,000018	2260	13,6	2,17	0,52